W. A. Davis

NATIONAL ACADEMIES OF SCIENCE AND ENGINEERING

NATIONAL RESEARCH COUNCIL

of the

UNITED STATES OF AMERICA

UNITED STATES NATIONAL COMMITTEE

International Union of Radio Science

National Radio Science Meeting

6-9 November 1978

Sponsored by USNC/URSI
in cooperation with
Institute of Electrical and Electronics Engineers

University of Colorado at Boulder
Boulder, Colorado
U.S.A.

Price $5.00

National Radio Science Meeting
6-9 November 1978
Condensed Technical Program

SUNDAY, 5 NOVEMBER

2000		
USNC/URSI Meeting		UMC 159

MONDAY, 6 NOVEMBER

0900-1200		
B-1	Scattering - I	UMC West Ballroom
B-2	Antenna Theory	UMC Forum Room
C-1	Signal Processing	UMC 156
D-1	Power and Energy Measurements at FIR and Submillimeter Wavelengths	UMC 159
F-1	Atmospheric Effects Above 10 GHz	UMC East Ballroom
1330-1700		
Combined Session		UMC Center Ballroom
1715		
Commission A Business Meeting		UMC 158
Commission C Business Meeting		UMC 156
Commission D Business Meeting		UMC 159
1830-2030		
Reception		UMC West Ballroom and Glenn Miller Lounge

TUESDAY, 7 NOVEMBER

0830-1200		
A-1	Measurements and Standards Needs at Millimeter, Sub-Millimeter, and Far Infra-Red Frequencies	UMC 158
B-3	New Concepts in Electromagnetics	UMC West Ballroom
C-2	Computer Networks	UMC 156
F-2	Radiooceanography - SEASAT 1	UMC East Ballroom
G-1	Ionospheric Heating Experimental Results	UMC Forum Room
J-1	Radar Astronomy	UMC 157
1330-1700		
A-2	Nondestructive Electromagnetic Probing and Testing	UMC 158
B-4	Earth Effects and Sommerfeld Integral	UMC West Ballroom
C-3	Satellite Communications	UMC 156
F-3	Radiooceanography - Radar Observations	UMC East Ballroom
G-2	Ionospheric Behavior and Propagation	UMC Forum Room
J-2	Panel Discussion on Techniques of Very Long Baseline Interferometers	UMC 157
1715-1800		
Commission F Business Meeting		UMC East Ballroom

United States National Committee

INTERNATIONAL UNION OF RADIO SCIENCE

PROGRAM AND ABSTRACTS

National Radio Science Meeting
6-9 November 1978

Sponsored by USNC/URSI in cooperation
with IEEE groups and societies:

Antennas and Propagation
Circuits and Systems
Communications
Electromagnetic Compatibility
Geoscience Electronics
Information Theory
Instrumentation and Measurement
Microwave Theory and Techniques
Nuclear and Plasma Sciences
Quantum Electronics and Applications

Hosted by:

National Oceanic and Atmospheric Administration
National Bureau of Standards
Institute for Telecommunication Sciences
National Telecommunications and Information Administration
University of Colorado at Boulder
and
The Denver-Boulder Chapter, IEEE/APS

NOTE:

Programs and Abstracts of the USNC/URSI Meetings are available from:

USNC/URSI
National Academy of Sciences
2101 Constitution Avenue, N.W.
Washington, D.C. 20418

at $2 for meetings prior to 1970, $3 for 1971-75 meetings, and $5 for 1976-78 meetings.

The full papers are not published in any collected format; requests for them should be addressed to the authors who may have them published on their own initiative. Please note that these meetings are national and they are not organized by international URSI, nor are the programs available from the international Secretariat.

MEMBERSHIP

United States National Committee
INTERNATIONAL UNION OF RADIO SCIENCE

Chairman:
Dr. John V. Evans, Lincoln Laboratory, M.I.T.**
Vice Chairman:
Dr. C. Gordon Little, Environmental Research Labs, NOAA#**
Secretary:
Dr. James R. Wait, Environmental Research Labs, NOAA#**
Editor and Secretary Designate:
Dr. Thomas B.A. Senior, University of Michigan
Immediate Past Chairman:
Dr. Francis S. Johnson, University of Texas, Dallas**

Members Representing Societies, Groups and Institutes:

American Astronomical Society	Prof. Gart Westerhout
American Geophysical Union	Dr. Christopher T. Russel
American Meteorological Society	Dr. David Atlas
Institute of Electrical & Electronic Engineering	Dr. Ernst Weber+#
IEEE Antennas & Propagation Society	Dr. Robert C. Hansen
IEEE Circuits & Systems Society	Dr. Mohammed S. Ghausi
IEEE Communications Society	Mr. Amos Joel
IEEE Information Theory Group	Dr. Jack K. Wolf
IEEE Microwave Theory & Techniques	Dr. Ken J. Button
IEEE Quantum Electronics Society	Dr. Robert A. Bartolini
Optical Society of America	Dr. Michael K. Barnoski

Liaison Representatives from Government Agencies:

National Science Foundation	Dr. W. Klemperper
Department of Commerce	vacant
National Aeronautics & Space Administration	Dr. Erwin R. Schmerling
Federal Communications Commission	Mr. Harry Fine
Department of Defense	Mr. Emil Paroulek
Dept. of the Army	Mr. Allan W. Anderson
Dept. of the Navy	Dr. Alan H. Schooley
Dept. of the Air Force	Mr. Allan C. Schell

Members-At-Large:

Mr. D.E. Barrick
Mr. L.S. Taylor
Mr. A.W. Guy

Chairmen of the USNC-URSI Commissions:

Commission A	Dr. Raymond C. Baird
Commission B	Dr. Thomas A. Senior
Commission C	Dr. William F. Utlaut
Commission D	Dr. Kenneth J. Button
Commission E	Mr. George H. Hagn
Commission F	Dr. A.H. LaGrone
Commission G	Dr. Thomas E. VanZandt
Commission H	Dr. Frederick W. Crawford
Commission J	Dr. K.I. Kellermann

Vice Chairmen of the USNC-URSI Commissions:

Commission B	G.A. Deschamps#
Commission C	M. Schwartz
Commission E	A.D. Spaulding
Commission F	R.K. Crane
Commission G	J. Aarons
Commission J	A.T. Moffet

Officers of URSI resident in the United States:
(including Honorary Presidents)

Vice President	Prof. William E. Gordon+/**

Chairmen and Vice Chairmen of
Commissions of URSI resident
in the United States:

Chairman of Commission A	Dr. Helmut M. Altschuler
Chairman of Commission J	Prof. Gart Westerhout
Vice Chairman of Commission B	Prof. Leopold B. Felsen#
Vice Chairman of Commission E	Mr. George H. Hagn
Vice Chairman of Commission F	Prof. Alan T. Waterman, Jr.
Vice Chairman of Commission H	Dr. Frederick W. Crawford

Foreign Secretary of the U.S. National Academy of Sciences	Dr. George S. Hammond+
Chairman, Office of Physical Sciences-NRC	Dr. D. Allan Bromley
NRC Staff Officer	Richard Y. Dow
Honorary Members:	Dr. Harold H. Beverage Prof. Arthur H. Waynick#

\+ NAS Member
\# NAE Member
** Member of USNC-URSI Executive Committee

DESCRIPTION OF

INTERNATIONAL UNION OF RADIO SCIENCE

The International Union of Radio Science is one of 17 world scientific unions organized under the International Council of Scientific Unions (ICSU). It is commonly designated as URSI (from its French name, Union Radio Scientifique Internationale). Its aims are (1) to promote the scientific study of radio communications, (2) to aid and organize radio research requiring cooperation on an international scale and to encourage the discussion and publication of the results, (3) to facilitate agreement upon common methods of measurement and the standardization of measuring instruments, and (4) to stimulate and to coordinate studies of the scientific aspects of telecommunications using electromagnetic waves, guided and unguided. The International Union itself is an organizational framework to aid in promoting these objectives. The actual technical work is largely done by the National Committees in the various countries.

The officers of the International Union are:

President:	J. Voge (France)
Immediate Past President:	Sir Granville Beynon (UK)
Vice Presidents:	W.N. Christiansen (Australia) W.E. Gordon (USA) V.V. Migulin (USSR) F.L.H.M. Stumpers (Netherlands)
Secretary General:	C.M. Minnis (Belgium)
Honorary Presidents:	B. Decaux (France) W. Dieminger (West Germany) J.A. Ratcliffe (UK) R.L. Smith-Rose (UK)

The Secretary's office and the headquarters of the organization are located at 7 Place Emile Danco, 1180 Brussels, Belgium. The Union is supported by contributions (dues) from 35 member countries. Additional funds for symposia and other scientific activities of the Union are provided by ICSU from contributions received for this purpose from UNESCO.

The International Union, as of the XVIII General Assembly held in Helsinki, Finland, August, 1978, has nine bodies called Commissions for centralizing studies in the principal technical fields. The names of the Commissions and the chairmen follow.

A. Electromagnetic Metrology
Altschuler (USA)

B. Fields and Waves
van Bladel (Belgium)

C. Signals and Systems
Picinbono (France)

D. Physical Electronics
Smolinski (Poland)

E. Interference Environment
Likhter (USSR)

F. Wave Phenomena in Nonionized Media
Eklund (Sweden)

G. Ionospheric Radio
King (United Kingdom)

H. Waves in Plasmas
Gendrin (France)

J. Radio Astronomy
Westerhout (USA)

Every three years, the International Union holds a meeting called the General Assembly. The next General Assembly, the XX, will be held in Washington, D.C., in August, 1981. The Secretariat prepares and distributes the Proceedings of these General Assemblies. The International Union arranges international symposia on specific subjects pertaining to the work of one Commission or to several Commissions. The International Union also cooperates with other Unions in international symposia on subjects of joint interest.

Radio is unique among the fields of scientific work in having a specific adaptability to large-scale international research programs, for many of the phenomena that must be studied are worldwide in extent and yet are in a measure subject to control by experimenters. Exploration of space and the extension of scientific observations to the space environment is dependent on radio for its research. One of its branches, radio astronomy, involves cosmos-wide phenomena. URSI has in all this a distinct field of usefulness in furnishing a meeting ground for the numerous workers in the manifold aspects of radio research; its meetings and committee activities furnish valuable means of promoting research through exchange of ideas.

NATIONAL RADIO SCIENCE MEETING COMMITTEE MEMBERS:

Steering Committee:

S.W. Maley, Steering Committee Chairman
T.B.A. Senior, Technical Program Committee Chairman
R.H. Ott, Assistant Chairman, Technical Program Committee
H.A. Patterson, Registration & Facilities Committee Chairman
P.L. Jensen, Publications Chairwoman

S.W. Maley
R.C. Baird
H.E. Bussey
D.C. Chang
R.Y. Dow
W.L. Flock
R.L. Gallawa
D.A. Hill
P.L. Jensen
C.T. Johnk
E.F. Kuester
C.G. Little
R.H. Ott
H.A. Patterson
T.B.A. Senior
A.D. Spaulding
W.F. Utlaut
T.E. VanZandt
P.F. Wacker
J.R. Wait

Technical Program Committee:

T.B.A. Senior, Chairman
R.H. Ott
J. Aarons
R.C. Baird
C.M. Butler
K.J. Button
R.K. Crane
K. Davies
G.A. Deschamps
K.M. Evenson
R.W. Fredricks
H. Kobayashi
H. Liebe
A.T. Moffet
M. Nesenberg
R. Phelan
A.D. Spaulding
W.F. Utlaut
M. Kindgren, Secretary to the Committee

MONDAY MORNING, 6 NOV., 0900-1200

SCATTERING - I

Commission B, Session 1, UMC West Ballroom
Chairman: Y. Rahmat - Samii, Jet Propulsion Laboratory, Pasadena, CA 91103

B1-1 0900 **ON THE USE OF ASYMPTOTIC APPROXIMATIONS IN ELECTROMAGNETIC THEORY:** K. M. Mitzner, Aircraft Group, Northrop Corporation, Hawthorne, CA 90250

As Erdélyi and Wyman have pointed out (Arch. Rat. Mech. Anal., 14, 217-260 (1963)), there is no one unique general asymptotic expansion for a function and thus there cannot be a universal method of constructing general asymptotic expansions. It is, however, possible to select an asymptotic expansion which is especially well-suited for a given class of problems in the sense that it is general enough to yield good results but not so general that it introduces unnecessary complications. This paper discusses some of the principles and concepts which can be used to select such expansions for electromagnetics problems.

For a body with various critical points, it has proved desirable to calculate the contribution from each critical point by using an expansion around that point. This procedure, which can be justified mathematically by using neutralizers, yields approximations which are valid both when critical points almost coalesce and when they are widely separated. Often it is useful to define an ordering among related approximation techniques. As a simple example, we consider the line integral which describes the far-field physical optics scattering when a cylinder is illuminated by a plane wave. We define a first order approximation which assumes linear phase variation near a critical point and which yields a series in inverse powers of frequency, a second order approximation which assumes quadratic phase variation and which yields a series with a Fesnel integral as the first term and subsequent terms involving Hermite polynomials, a third order approximation which assumes cubic phase variation and leads to the "incomplete Airy functions" of Felsen and Marcuvitz, (Radiation and Scattering of Waves, Prentice Hall, 1973, Sect. 4.6 b) and so on.

From this viewpoint, a second order approximation is necessary whenever there is an ordinary specular point (one at which curvature does not vanish) but, once the second order approximation has been selected, no special attention is required for the case in which a specular point approaches an end point. Furthermore, it can be seen that there is no significant advantage to using a third order or higher approximation unless the curvature vanishes somewhere along the line of integration or is small at an endpoint.
The idea of ordering has proved even more useful in treating the surface integrals of three-dimensional physical optics. It was used as the basis for deriving a formula for scattering from an edge scattering center which lies near a specular point.

B1-2 0920 PHYSICAL OPTICS BACKSCATTER FROM A BODY OF REVOLUTION: K. M. Mitzner and H. C. Heath, Aircraft Group, Northrop Corporation, Hawthorne, CA 90250

A simple technique is presented for accurate calculation of the off-axis physical optics backscatter from a perfectly conducting body of revolution. The surface of the body is treated as the limit of a set of circular rings of infinitesimal thickness, and the physical optics surface integral is evaluated by integrating first around each ring and then along the axis of the body.
The scattering from a ring can be calculated analytically if the entire ring is geometrically illuminated. If the ring is partially shadowed, its scattering contribution can be calculated numerically or by a mixed analytical-numerical technique in which it is never necessary to do a numerical integration over more than 1/8 of the ring.
The integration along the axis is performed numerically. The computations simplify greatly for axial incidence.

B1-3 0935 EFFECT OF SURFACE RAY TORSION ON DIFFRACTION BY A SMOOTH OBJECT: S. Safavi-Naini and R. Mittra, Department of Electrical Engineering, University of Illinois, Urbana, IL 61801

In a recent paper (R. Mittra, S. Safavi-Naini, Radio Sci., 1979, to appear), the authors reported an asymptotic expansion for the far field radiated by a magnetic dipole of density $\vec{M}$ on a conducting circular cylinder of radius a, in which the effect of nonzero torsion of the surface rays was taken into account. In the present paper, we have attempted to isolate the effect of the torsion of rays and to represent it explicitly as an additive correcting term to the GTD solution for torsionless rays. The final result, after some algebraic manipulation, can be written as:

$$E_{n_2} = E^{GTD}_{n_2} + [(\vec{M}\cdot\hat{\sigma}_1)(\frac{\tau\rho_\sigma}{2}) - (\vec{M}\cdot\hat{\beta}_1)\frac{(\tau\rho_\sigma)^2}{2}]\cdot G(\sigma,\beta)\cdot\frac{e^{-jkR}}{R}$$

$$E_{\beta_2} = E^{GTD}_{\beta_2} - (\tau\rho_\sigma)(\vec{M}\cdot\hat{\beta}_1)\cdot H(\sigma,\beta)\cdot\frac{e^{-jkR}}{R}\quad,\quad \beta\neq\frac{\pi}{2}$$

where G and H are transition functions governing the propagation of fields along the surface rays and are given in (R. Mittra, S. Safavi-Naini, Radio Sci., 1979, to appear). The other quantities σ, $\hat{\sigma}$, β, $\hat{\beta}$, $\hat{n}_2$, R are shown in the figure. τ is the torsion and ρ_σ is the radius of curvature of the ray. We observe that the additional correcting terms to the GTD results are proportional to τ and are absent when $\tau = 0$, as would be expected.

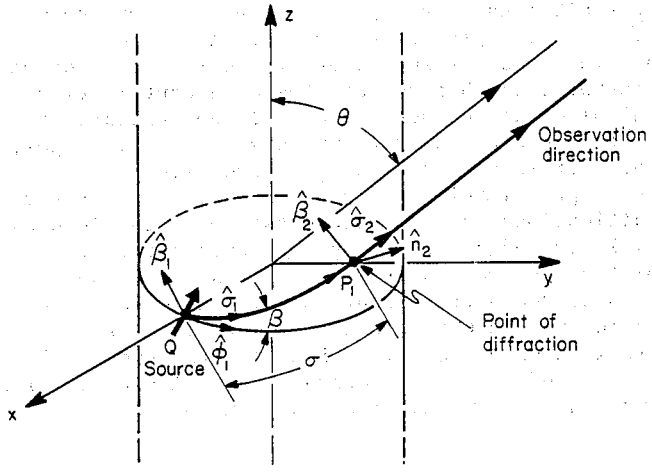

B1-4
0955

HIGH FREQUENCY SCATTERING FROM SMOOTH SURFACES WITH EDGES — A SPECTRAL DOMAIN APPROACH:

W.L. Ko and R. Mittra, Department of Electrical Engineering, University of Illinois, Urbana, Illinois 61801

The conventional approach to high frequency scattering from objects with sharp edges is to employ GTD in conjunction with one of the several available uniform theories that modify Keller formulas at the geometrical-optical transition regions where the Keller coefficients become infinite. In this procedure, the total diffracted field is comprised of the specularly reflected GO field from the smooth part of the object and the edge-diffracted fields from the sharp edges. Both of these contributions are derived by invoking the principle of the local field, and in particular, the edge-diffracted fields are constructed by using the GTD diffraction coefficients for the semi-infinite half planes or infinite wedges that approximate the local geometry of the edge in the neighborhood of the trip.

In this paper the above problem of scattering by smooth surfaces with edges is examined from the point of view of the spectral domain (STD) approach wherein the scattered far field is expressed in terms of the transform of the induced surface current. For a cylindrical shell, for instance, the induced surface current can be decomposed into two principal constituent parts each of which can be identified with certain geometrical features of the scatterer. The first of these, viz., the physical optics contribution, can be readily associated in the usual manner with the smooth portion of the scatterer. The second part, which is identified as being the contribution of the curved edge, is derived in the STD method by employing a novel approach which departs from the principle of the local field for edge diffraction. The need for such a departure from the conventional GTD methods, which associate the edge contribution with semi-infinite half planes, is clearly demonstrated in the paper. It is shown that for curved surfaces with eges, the half-plane currents need to be modified using Fock-functions and appropriately truncated as well. The effect of these modifications on the representation of the induced current is illustrated by comparing the scattered fields derived from the spectral and the GTD approaches. These numerical results demonstrate that the STD method corrects the deficiencies in the GTD results and obviates the need for the uniform theories as well. Finally, the numerical results are verified using the boundary condition test which is conveniently applied within the STD framework.

B1-5 1045 A NEW LOOK AT THE EDGE DIFFRACTION PROBLEM — *OR* — DO WE *REALLY* NEED UNIFORM THEORIES: R. Mittra and W. L. Ko, University of Illinois, Urbana, Illinois 61801.

Historically, uniform theories of edge diffraction were introduced to repair the GTD formulas in the transition regions (shadow boundaries), where the Keller coefficients predict infinite fields. At least two distinctly different forms of these uniform formulas, viz., UAT and UTD, are available in the literature. The construction of both of these formulas is based on certain hypotheses that are inspired from the structure of the exact solution of the *semi-infinite* half-plane problem. In this paper, we employ the spectral domain concepts (as contrasted to the ray approach) to derive a new representation for the scattered fields from *finite* bodies with edges. The following conclusions are derived on the basis of a thorough examination of the spectral domain results for several test problems, e.g., diffraction by a finite strip and a rectangular cylinder: (a) the expression makes direct use of the Keller diffraction coefficient, but is simpler than either the UAT or UTD formulas; (b) it yields finite and accurate scattered fields for all observation angles, including the transition regions at the shadow boundaries, without requiring *a posteriori* corrections via uniform theories; and, (c) the formula identifies an important missing term in the GTD expressions for the scattered field. The exclusion of this term is shown to produce *discontinuous* scattered fields at certain angles *away* from the transition regions of the GO field even when uniform theories are used. The spectral domain representation for the scattered field also lends itself to convenient and systematic generalization to curved surfaces with edges, whereas GTD formulas are found to introduce additional and substantial errors for certain observation angles away from the shadow boundaries. In summary, the formula based on the spectral domain approach requires no *a posteriori* correction at shadow boundaries and yet it is simpler, as well as more accurate, than the uniform GTD formulas. It is also shown to be applicable to more general surfaces.

B1-6
1105

THE RESOLUTION OF AN APERTURE FOR COHERENT IMAGING, RADAR, AND HOLOGRAPHIC APPLICATIONS:

W. Ross Stone, Megatek Corporation,
1055 Shafter Street, San Diego, CA 92106

There are many instances in which a field is recorded over a finite aperture and this data is then used to reconstruct information about the source of the field: This is one class of inverse scattering problems. This is also a basic process in radio frequency "imaging" systems, such as radar, holographic, and radio telescope systems. The process of recording the field over a finite aperture introduces a fundamental limitation on the reconstruction, often expressed in terms of the lateral resolution limit of the aperture. The classical value for this limit is $K\lambda z/D$, where λ is the wavelength, z is the perpendicular distance between the source of the field (or the scatterer or the object being imaged) and the aperture, and D is the size of the aperture. The value of K depends on the resolution criterion chosen (e.g., $K = 1.22$ for the Rayleigh criterion). In this paper it is shown that the lateral resolution for such a coherent imaging system is given, in the Fresnel approximation, by $\Delta\phi/2\pi$ times the above expression, where $\Delta\phi$ is the accuracy with which the phase of the field can be measured across the aperture. Because phase measurements at radio frequencies can typically be made to accuracies small compared to 2π radians, this often implies that a resolution which is a power of 10 or more smaller than the classical value can be obtained. It is further shown that $\Delta\phi$ is related in a simple way to the signal-to-noise ratio of the measurement. Similar results are also derived for the longitudinal, or depth, resolution. These results are illustrated by simple computer generated examples.

B1-7
1120

IMAGING OF LINEAR SOURCE DISTRIBUTIONS:

E. K. Miller and D. L. Lager, Electronics Engineering Department, Lawrence Livermore Laboratory, Livermore, California 94550

One version of the inverse problem is that of determining the source distribution which produces a given field. When the sources lie on a perfectly conducting object, and the fields can be obtained arbitrarily close to it, then the inversion is trivial. Of more practical interest is the situation where the fields are observable only at a large distance from the object. In this case, it might be expected that only those sources that produce far field radiation will be directly derivable. Using the far fields to locate the radiating sources is an exercise that may be regarded as imaging, and is the subject of this discussion.

Previous work by the authors has demonstrated that Prony's method can be used to image a linear array of discrete sources from its far field, and to synthesize discrete source distributions which produce the fields of continuous ones. Here we examine the possibility of using the same procedure to image the source distribution of a straight-wire from its far field. The effects of varying the wire's length, radius and excitation are discussed. As previously found, a resolution limit of $\sim$ two sources per wave length seems to hold. Sources are consistently obtained which seem to be due to radiation from the wire's ends and excitation point when operated as an antenna. Other sources are also found which may be interpreted as originating from traveling wave radiation. The implications of these findings with respect to imaging simple objects are discussed.

B1-8 1140 A WAVE EQUATION FOR RADIATING SOURCE DISTRIBUTIONS:

Norbert N. Bojarski, 16 Pine Valley Lane, Newport Beach, CA 92660

Bleistein and Cohen (1977) have shown that any source distribution, giving rise to fields that satisfy the inhomogeneous Helmholtz wave equation (for acoustics, electromagnetics, etc.), can be separated into radiating and non-radiating portions; and that the radiating source distribution can be determined completely and uniquely in a well-conditioned manner from knowledge of the radiated fields on any closed surface exterior to the support of the source distribution.

An alternative formulation of this separation is developed in a form suitable for deriving a wave equation which governs the radiating portion of the source distribution.

The implications of this wave equation on Inverse Scattering theory (and quantum mechanics) are discussed.

ANTENNA THEORY
Monday Morning, 6 Nov., UMC Forum Room
Chairman: L. W. Pearson, University of Kentucky, Lexington, KY 40506

B2-1
0900

A LOG-PERIODIC INTEGRATED MICROWAVE ANTENNA.

H.Pues, J.Vandensande, A.Van de Capelle, K.U.Leuven, Dept. of Electrical Engineering, Div. M.I.L., B 3030 Heverlee, Belgium.

The theory of frequency independent structures is already well known in the antenna field of engineering and has found many applications. We have examined in an experimental way the possibility of applying the principles of this theory to microwave integrated antennas (H.Pues, J.Vandensande : "Study of Broadband Integrated Microwave Antennas", Internal Report K.U.Leuven). As a conclusion of this study we can postulate that it is possible to build planar printed circuit antennas with a nearly unlimited bandwidth. For example, a log-periodic antenna with circular teeth has been built on a PTFE substrate of 1/16" thickness. Because the structure was self-complementary the radiation resistance equals 188 ohm. The antenna was matched to 50 ohm with a tapered line which was etched on the backside of the structure. The frequency band of operation is 2 to 12GHz, but can be easily increased to lower frequencies by increasing the dimensions of the antenna. The radiation pattern in the E-plane (which was nearly identical to that in the H-plane) is shown in the figure at two frequencies. The pattern is bidirectional with the main lobes perpendicular to the structure.

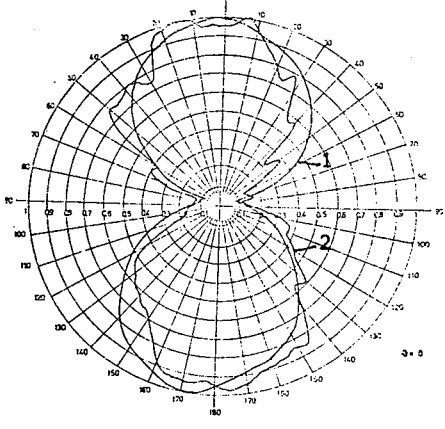

Radiation pattern in the E-plane.

1 : f = 2 GHz
2 : f = 9 GHz

B2-2
0920

Analysis of an Arbitrarily Oriented Thin-Wire Antenna in the Presence of A Conducting Sphere

Chalmers M. Butler and T. Keshavamurthy,
Department of Electrical Engineering, University of Mississippi, University, MS 38677

For a thin-wire antenna in the presence of a conducting sphere, one can modify the usual integro-differential equation for an isolated wire to account for the scattering from the sphere. The electric field scattered from the sphere by an elementary electric dipole is computed in terms of spherical, vector wave functions and this field is incorporated into the wire equation. The generalized equation is solved by standard numerical techniques and current distributions on the wire are computed for several cases of interest. From knowledge of the solutions for wire current obtained, input admittance to the antenna as well as far-field radiation patterns are computed. In addition, measurements have been performed to determine the input admittance to a monopole above a ground plane with a brass hemisphere located near the monopole. Experimental and theoretical values of input admittance are compared and found to be in good agreement.

B2-3
0935

Analysis of Man-Pack Radio Antenna above Ground:
T. K. Wu and C. M. Butler, Electrical Engineering Department, University of Mississippi, University, Mississippi 38677

In this paper, the interaction of a thin-wire antenna with a human body above a perfectly conducting ground is investigated via the solution of the wire integral equation with a numerical Green's function. The human body is modeled by a homogeneous lossy dielectric body of revolution, as depicted in the figure, with dielectric constant and conductivity equal to those of sea water. The numerical Green's function for the lossy dielectric body of revolution has been calculated previously, both by a Surface Integral Equation (SIE) and an Approximate Integral Equation (AIE). In this paper the effect of the ground is accounted for by image theory. An integro-differential equation is formulated and is solved numerically to determine the current on the wire antenna, and subsequently the body currents are also computed. The antenna input impedance and far-field pattern are next determined. Results are given for the antenna input impedance and far-field patterns in order to assess the effects of the presence of a human body above ground.

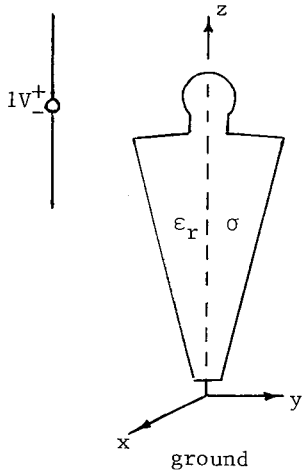

B2-4
0950

NETWORK MODELING OF MULTIELEMENT RADIATING STRUCTURES:

G. Goubau and N. Puri, Rutgers University, New Brunswick, NJ; and F. Schwering, U.S. Army Communications R&D Command, Fort Monmouth, NJ

The theory discussed in this paper applies to radiating structures consisting of an assembly of conductive elements which are interconnected by concentrated current paths.

A simple example is a monopole antenna with a top capacitator. In this case, there are two "structure elements": the vertical conductor and the top capacitor, which are electrically connected by the current at the junction of these elements. Structures such as the multielement monopole antennas described in Ref. 1+ consist of a number of structure elements with one, two or more current interconnections. If the current flow is interrupted at one of the junctions, the antenna properties are drastically changed since the coupling between the elements is primarily produced by the junction currents.

If an element with one interconnection is thought to be separated and suspended in space, with a current enforced through the connection terminal (an assumption, which, of course, is not physically realizable), there exists a current distribution which satisfies the boundary condition at the surface of the element. This current distribution is termed "dominant" current distribution since the currents due to radiation coupling between the elements are relatively small. The scalar potential produced by the dominant current distribution at the terminal and the impressed current can be used to define an impedance which is determined by the distribution function of the dominant current. An element with n interconnections has n dominant current distribution, one for each terminal. The relationship between the scalar potentials at the terminals, and the n impressed currents can be formulated by a n x n impedance matrix which has the same symmetry properties as those of ordinary n-port networks. The entire antenna structure can be modeled as an assembly of "leaky" n-port networks whereby the leakage represents the radiation coupling between the elements and can be represented by coupling elements.

The theory is expected to be useful to the study of multielement antennas and their representation by lumped element circuits.

+ Proc. Workshop on Electr. Small Antennas, G. Goubau and F. Schwering, Editors, pp. 63-67, Oct. 1976, Fort Monmouth, NJ

B2-5
1010 ANALYTICAL AND NUMERICAL TECHNIQUES FOR EVALUATING AN ELECTRICALLY-SHORT DIPOLE WITH A NONLINEAR LOAD: Motohisa Kanda, Electromagnetic Fields Division, National Bureau of Standards, Boulder, Colorado 80303

An electrically-short dipole with a nonlinear dipole load is analyzed theoretically using both analytical and numerical techniques. The analytical solution is given in terms of the Anger function of imaginary order and imaginary argument, and is derived from the nonlinear differential equation for the Thevenin equivalent circuit of the dipole and load. (The detailed mathematical steps for solving the equation have been performed by P. F. Wacker). The numercial technique used was to solve nodal equations using a time-stepping finite difference equation method. The nonlinear load is treated using a conventional iteration technique.

The nonlinear load considered in this paper is a beam lead Schottky barrier diode. Both analytical and numerical techniques are used and their solutions agree very well. The transition from the square-law to linear detection region was observed as the induced voltage was varied. Comparison of the transfer functions of the electrically-short dipole with the diode indicates that the decrease in the transfer functions at frequencies below 10 kHz was explained well through the time-domain sinusoidal waveforms obtained from the time-stepping finite difference equation technique.

One of the advantages of using an analytical solution in terms of the Anger function of imaginary order and imaginary magnitude is that the solution to the differential equation governing the circuit is given in closed form, and is very easy to evaluate. However, it may be very difficult, or even impossible to find closed-form solutions to more complicated models (e.g., circuits including a nonlinear capacitance, a linear inductance, as well as a nonlinear and linear reistances and a linear capacitance). In such cases, a time-stepping finite difference equation technique along with an iteration method provides accurate time-domain solutions for more general nodal equations.

B2-6
1045

GENERAL FORMULA FOR VOLTAGE INDUCED IN A RECEIVING ANTENNA: D.M. Kerns, EM Fields Division, National Bureau of Standards, Boulder, Colorado 80303

We derive a generalized version of the formula for open-circuit modal (or conventional) voltage V_{oc} at the terminals of a receiving antenna, viz.,

$$V_{oc} = \int_V \underline{J}_e^a \cdot \underline{E}\, dV.$$

Here $\underline{E}$ is the arbitrary exciting electric field that would exist in the absence of the antenna, and $\underline{J}_e^a$ is a current-density vector precisely defined below. The most nearly comparable formula seems to be that given by Weeks (see W.L. Weeks, Electromagnetic Theory for Engineering Applications, John Wiley, 1964, where further references are given). Our generalization consists in the explicit admission of magnetic and magnetoelectric media and in the removal of the reciprocity requirement. Indeed, the distribution of material media making up an antenna is described by the constitutive equations

$$\underline{D} = \underline{\underline{\varepsilon}} \cdot \underline{E} + \underline{\underline{\tau}} \cdot \underline{H}, \quad \underline{B} = \underline{\underline{\nu}} \cdot \underline{E} + \underline{\underline{\mu}} \cdot \underline{H}.$$

Here the tensors $\underline{\underline{\varepsilon}}$ and $\underline{\underline{\mu}}$ have their usual roles; $\underline{\underline{\tau}}$ and $\underline{\underline{\nu}}$ describe magnetoelectric properties. The tensor parameters will, of course, depend upon position within the region V of the antenna considered; outside this region the parameters must reduce nominally to vacuum values. In addition to the given system described by the above equations, we must consider the adjoint system, described by the equations for the adjoint medium,

$$\underline{D} = \tilde{\underline{\underline{\varepsilon}}} \cdot \underline{E} - \tilde{\underline{\underline{\nu}}} \cdot \underline{H}, \quad \underline{B} = - \tilde{\underline{\underline{\tau}}} \cdot \underline{E} + \tilde{\underline{\underline{\mu}}} \cdot \underline{H},$$

where the tilde denotes the transposed tensor and the $\underline{\underline{\varepsilon}}$, $\underline{\underline{\mu}}$, $\underline{\underline{\tau}}$, and $\underline{\underline{\nu}}$ themselves are the parameters of the given system. The derivation depends upon a generalized Lorentz reciprocity relation

$$\nabla \cdot (\underline{E}' \times \underline{H}'' - \underline{E}'' \times \underline{H}') = \underline{E}'' \cdot \underline{J}_o' - \underline{E}' \cdot \underline{J}_o'',$$

holding for any two electromagnetic fields $\underline{E}', \underline{H}'$ and $\underline{E}'', \underline{H}''$ (of the same frequency) generated by sources $\underline{J}_o'$ and $\underline{J}_o''$ in the given and in the adjoint system respectively. In particular we let $\underline{J}_o''$ be the enforced current density that produces unit modal (or conventional) input current exciting the isolated adjoint antenna in its transmitting mode. Then, finally, we define $\underline{J}_e^a = \underline{J}_o'' - i\omega \underline{P}^a + \nabla \times \underline{M}^a$, where $\underline{P}^a$ and $\underline{M}^a$ are respectively the electric and magnetic polarization densities so induced in the adjoint antenna.

B2-7
1115

THE USE OF THE RADAR EQUATION FOR THE DETERMINATION OF INPUT CONDUCTANCES: Larry Rispin and David C. Chang, Electromagnetics Laboratory, University of Colorado, Boulder, CO 80309

The input conductance of a transmitting antenna is often difficult to determine when it is dominated by a very large susceptance term. Representative examples would include short linear antennas and antennas excited by small apertures, etc. Conventional methods, both analytical and numerical ones, usually require excessive numbers of higher order terms in order to attain a reasonably accurate expression for the conductance term. For instance, the conductance value of a short dipole of electric length $kh \ll 1$, is typically $(kh)^3$-order smaller than the capacitive term. In this work we show that by using the commonly known "radar equation," which is itself based upon the reciprocity theorem, the input conductance G_a may be determined from a knowledge of the receiving properties of the same antenna:

$$G_a = \eta\left(\frac{k}{4\pi}\right)^2 \int_0^{2\pi} d\phi_i \int_0^{\pi} d\theta_i \left[\sin\theta_i \left| I_{sc}(\theta_i,\phi_i)\right|^2\right]$$

where $I_{sc}(\theta_i,\phi_i)$ is the receiving current at the short circuited input terminals of the antenna due to a uniform plane wave incident at the angles θ_i and ϕ_i in the spherical co-ordinate system. $\eta = 120\pi$ and $k = \omega\sqrt{\mu_o \varepsilon_o}$. Clearly, the formula avoids the aforementioned difficulties encountered by the conventional techniques since only the leading term is needed in $|I_{sc}|$. Input conductances thus obtained agree well with values determined from conventional methods for various antennas including short dipoles, hollow thin cylinders excited by an internal evanescent mode, as well as that of a small loop antenna. In addition to conductance calculation, the relationship can also be used as an independent check for numerical programs computing the impedance matrix based upon moment methods. Such a check is particularly useful when the antenna structure is more involved.

B2-8
1135 AN ACCURATE NUMERICAL INVESTIGATION OF THE STEPPED-RADIUS ANTENNA:

A. W. Glisson and D. R. Wilton, Department of Electrical Engineering, University of Mississippi, University, MS 38677

In recent years a considerable controversy has arisen concerning the application of a charge "jump condition" when thin-wire theory is employed in numerical solutions for the current and charge on a stepped-radius antenna and, in general, on any structure containing junctions of wires of dissimilar radius. The two important questions to be answered in this regard are: (1) Is it necessary to incorporate any charge condition when thin-wire theory is used and, if so, (2) what is the correct condition to enforce? In this work an attempt is made to answer these questions by first obtaining an accurate numerical solution for the stepped-radius antenna. From the resulting charge distribution a numerical charge jump condition is computed. Results computed using thin-wire approximations are also compared.

An accurate numerical determination of the current and charge on the stepped-radius antenna is obtained by treating the wire as a body of revolution. The detailed behavior of the current and charge in the junction region is thus included. For antennas with large length to radius ratios, such a solution requires the use of a very large dynamic range of subdomain sizes on the wire. The capability of the procedure employed to handle a wide variation in subdomain size has been verified for linear antennas. Furthermore, the variation of the computed current and charge in the vicinity of the junction is found to be in excellent agreement with the approximate variation predicted by edge conditions. A procedure is next developed to compute a numerical charge jump condition at the radius discontinuity. The numerical condition is found to agree with the analytically derived Wu-King condition (T. T. Wu and R. W. P. King, IEEE Trans. Ant. Prop., AP-24, 42-45, 1976) for a wide range of wire radii, ratios of radii, and locations of the radius discontinuity. The question of incorporation of such conditions into thin-wire theory codes is discussed and numerical examples are presented.

Further investigations are in progress to determine if the same charge jump condition is valid for wires with bends, for scatterers, and for multiple wire junctions.

B2-9 1145 OPTIMAL DIRECTIVITY OF RADIATING SYSTEMS

T. S. Angell and R. E. Kleinman, Department of Mathematics, University of Delaware, Newark, Delaware 19711

The problem of selecting a surface current on a conformal antenna which will maximize radiated power in a preassigned sector of two or three dimensional space is discussed. Various a priori constraints, reflecting practical limitations, are imposed on the possible surface currents.
The problem is formulated as an optimal boundary control problem for the exterior Helmholtz equation in two and three dimensions.
A convergent Galerkin method for approximating the optimal surface current is presented, together with specific examples of unidirectional and bidirectional optimal antenna patterns.

SIGNAL PROCESSING
Monday Morning, 6 Nov., UMC 156
Chairman: R. E. Nathanson, Technology Service Corp., 8555 16th St., Silver Spring, MD 20910

C1-1 0900 REAL-TIME SIGNAL PROCESSING ON THE SURFACE CONTOUR RADAR: James E. Kenney, Naval Research Laboratory, Washington, DC 20375 and Edward J. Walsh, NASA Wallops Flight Center, Wallops Island, VA 23337

The Naval Research Laboratory and the NASA Wallops Flight Center have developed an airborne 8.6 mm bistatic radar designed to measure the directional wave spectra of the ocean. The system produces a real-time false-color coded display of the surface elevations within a swath beneath the aircraft whose width is equal to half the aircraft altitude. The radar uses an oscillating mirror to sinusoidally scan a pencil beam (0.85° x 1.2°) to interrogate the surface below the aircraft at a rate as high as 10 Hertz within a ± 15° sector perpendicular to the aircraft flight direction. Range tracking and system management are accomplished in software using a HP 21MX minicomputer as the central processor. Once the desired radar range resolution (1, 2, 4 or 10 ns), desired vertical extent to interrogate, and nominal aircraft altitude have been fed into the computer it computes a set of 51 range scan patterns, one of each 0.6° aircraft roll angle between ± 15° as determined by the aircraft inertial navigation system (INS). It is the predetermined scan patterns which permit the interaction between the radar hardware and the computer to be reduced to once per lateral sweep of the beam (one raster line on the elevation display) leaving enough time for the computer to make geometrical corrections to the radar range measurements to turn them into elevations in real-time.

C1-2 0925 PROBABILISTIC THEORY OF A STAGGERED PRF MTI SYSTEM:

James K. Hsiao, Naval Research Laboratory, Washington, D. C. 20375

In a conventional MTI system, the pulse repetition frequency (PRF) usually is maintained constant. Returns of target with a doppler frequency being an integer multiple of this PRF would be treated as clutter and filtered out. This blind velocity phenomenon can be alleviated by use of a staggered PRF system. Difficulty with such a system is how to choose a set of appropriate interpulse durations such that the desired performance can be achieved. There is no analytic solution to this problem. In this paper, a different approach to this problem is proposed. The PRF's may be treated as a random variable with a certain distribution. The MTI performance hence becomes probabilistic. Since the performance of an MTI system is the sum of the contributions of each individual pulse, which is statistically independent, this performance parameter can be approximated by a normal distribution on account of central limit theory. Mean and variance are estimated from the given PRF distribution. As an example, this paper presents the probability distribution of the MTI improvement factor and the lowest null of the filter response. The PRF distributions are assumed to be either uniform or normal. To verify the validity of this approach, the computed probability distributions are compared with the results computed directly from a large sample, each having a PRF chosen randomly from the given distribution. Limits and characteristics of these probabilistic distributions are also discussed.

C1-3 0950 SPECTRUM WIDTH ESTIMATES FOR WEATHER ECHOES:

D.S. Zrnic', The National Severe Storms Laboratory, NOAA, 1313 Halley Circle, Norman, OK 73069

Doppler spectrum width relates to wind shear and turbulence and thus is an important parameter that characterizes severe weather phenomena. The need to scan large volumes of space quickly and obtain real time estimates introduces stringent requirements on the signal processing. The Fourier transform and the autocovariance methods are candidate techniques. In particular, the autocovariance estimator as implemented on the National Severe Storms Laboratory's radar is discussed. Statistics of an improved and asymptotically unbiased (for Gaussian spectra) estimator of width is presented. Spurious effects on the complex video signal such as DC offsets and imbalances are assessed. Performance of the improved estimator on weather data is shown,

C1-4
1045

A STUDY OF TARGET IDENTIFICATION USING POLES:

E. K. Miller, Electronics Engineering Department, Lawrence Livermore Laboratory, Livermore, California 94550

The identification of a target from its radar return has been a long-sought goal. One approach to this problem is to somehow derive information about the target's scattering characteristics over a wide bandwidth which includes the resonance region. Such information could be obtained for example, by illuminating the target with an impulsive field or a set of discrete frequencies. The idea is that, however it is obtained, it should be feasible to estimate from this information a set of features or parameters which provide as nearly as possible a unique "signature" for each target. Of course, the problem becomes more manageable the fewer the targets there are in the set of interest. Note too, that while imagining could represent one way to identify a target, other characterizations could be equally valid and useful. Besides, imaging would generally require a much higher frequency range than suggested above.

The approach we consider here is the use of pole sets. Recent work has demonstrated that the poles of electromagnetically excited objects can be extracted from either frequency-domain or time-domain observables using Prony's method. These poles have particular potential for target identification because they are independent of the excitation (angle of incidence, polarization, etc.). It is therefore of interest to evaluate ways in which pole sets might be used for target indentification.

For purposes of this study, sets of poles were specified to generate transient waveforms to which varying levels of noise were added. Various schemes were then applied to the waveforms for estimating to which pole set each one belonged. These included a correlation technique; a linear predictor; computation of the residues; and direct extraction of the poles. Monte Carlo computer experiments were conducted to develop expected false-alarm rates and correlation matrices. The results obtained from this study are summarized, and lead to the tentative conclusion that greater computation effort is generally rewarded with increased probability of correct identification.

C1-5
1110

IMAGING OF LINEAR SOURCE DISTRIBUTIONS:*

E. K. Miller and D. L. Lager, Electronics Engineering Department, Lawrence Livermore Laboratory, Livermore, California 94550

One version of the inverse problem is that of determining the source distribution which produces a given field. When the sources lie on a perfectly conducting object, and the fields can be obtained arbitrarily close to it, then the inversion is trivial. Of more practical interest is the situation where the fields are observable only at a large distance from the object. In this case, it might be expected that only those sources that produce far field radiation will be directly derivable. Using the far fields to locate the radiating sources is an exercise that may be regarded as imaging, and is the subject of this discussion.

Previous work by the authors has demonstrated that Prony's method can be used to image a linear array of discrete sources from its far field, and to synthesize discrete source distributions which produce the fields of continuous ones. Here we examine the possibility of using the same procedure to image the source distribution of a straight-wire from its far field. The effects of varying the wire's length, radius and excitation are discussed. As previously found, a resolution limit of $\sim$ two sources per wave length seems to hold. Sources are consistently obtained which seem to be due to radiation from the wire's ends and excitation point when operated as an antenna. Other sources are also found which may be interpreted as originating from traveling wave radiation. The implications of these findings with respect to imaging simple objects are discussed.

*This work was performed under the auspices of the U.S. Department of Energy by the Lawrence Livermore Laboratory under contract number W-7405-ENG-48.

C1-6
1135

LINEAR PREDICTOR ANALYSIS

E.M. Kannaugh, D.L. Moffatt and K.A. Shubert
The Ohio State University ElectroScience Laboratory
Department of Electrical Engineering
Columbus, Ohio 43212

The basic idea to be exploited is that whether the echo signal as a function if time is approximated by a sum of exponentials or not, the ramp response, f(t), of a target satisfies the difference equation

$$\sum_{n=1}^{N} a_n \, f(t_m - n\Delta t) = \varepsilon_m$$

where N is smaller than twice the number of harmonics in f(t), ε_m is the error, and the sum of the squared error is small compared to the sum of the squared NM data points. Finding the set of coefficients, a_n, subject to the sum of their squares being unity and such that the sum of the squared error is minimized is a standard procedure of linear algebra. First the rectangular data matrix, D_{NM}, is formed from the NM sample values. The square NxN matrix, A, is computed by multiplying the transpose of D_{NM} times D_{NM}. The desired set of normalized coefficients is then the eigenvector associated with the minimum eigenvalue of A. This minimum eigenvalue is then equal to the minimum squared error. Because a homogeneous difference equation is sought, this method differs from standard linear difference equation procedures and allows different techniques to be utilized. Results of this method for several aircraft models, including a procedure for using data from several aspect angles, will be presented and related to the general identification problem.

Commission D Session 1

POWER AND ENERGY MEASUREMENTS AT FIR AND SUBMILLIMETER WAVELENGTHS

Monday Morning, 6 Nov., UMC 159

Chairman: R. J. Phelan, Jr., National Bureau of Standards, Boulder, CO 80303

D1-1
0900 PHOTOMETRY AND SPECTRAL CALIBRATION TECHNIQUES OF SUBMILLIMETER INCOHERENT DETECTION: K. Shivanandan, Naval Research Laboratory, Washington, D.C. 20375

This paper will present standard techniques used in the photometry and spectral calibrations of photoconductors and bolometers at cryogenic temperatures in the 100 to 1000 micrometer spectral band. Some measurements under high and low background conditions will be reviewed, and problem areas for space applications will be discussed.

D1-2 0920 ABSOLUTE CALIBRATION OF INCOHERENT SUBMILLIMETER RADIATION: P. L. Richards, Department of Physics University of California and Materials and Molecular Research Division, Lawrence Berkeley Laboratory Berkeley, California 94720

We have developed absorbing elements for composite submillimeter wave bolometric detectors which are well adapted to absolute power measurements. The absorbing element consists of a transparent dielectric substrate (typically sapphire) which is coated on the reverse side by a thin metallic film (such as bismuth or nichrome). The surface resistance of the metal film is selected so that electromagnetic waves are not reflected at the dielectric-film interface. This requires $R_{\square}$ = 200 Ohms per square for sapphire with refractive index n = 3. The absorptivity of this structure has been shown experimentally to be essentially independent of frequency from 5 to 250cm^{-1}. Absolute optical absorptivity measurements at submillimeter wavelengths gave 53 ± 5% compared with a theoretical absorptivity of 50%. When used as the absorbing element of composite bolometric detectors, these structures can make absolute measurements at power levels as small as 10^{-15}W. They should also be readily adaptable to high power measurements.

In the course of measurements of the spectrum of the cosmic background radiation we have developed techniques for absolute measurements of incoherent radiation over the frequency range from 5 to 50cm^{-1}. The accuracy of these measurements is typically a few per cent. The primary difficulties encountered in the measurement of incoherent submillimeter power arise from the fact that wavelengths are comparable to typical aperture sizes. It is therefore necessary to compute diffraction corrections for many measurements. If measurements are carried out over wide spectral bands, the number of electromagnetic modes involved can vary from one to many thousands. The mode structure of the propagating radiation must be evaluated as carefully as with experiments with coherent radiation. The systems used and some of the pitfalls encountered will be described.

D1-3
0940 POWER MEASUREMENTS WITHIN A TUNEABLE FIR HETERODYNE DEVELOPMENT PROGRAMME: PRESENT LIMITATIONS FUTURE NEEDS. P.F. Clancy, European Space Agency, Noordwijk, Netherlands.

The problems associated with the measurement of power levels encountered in a development programme of submillimetre heterodyne hardware are described. The special problems posed by the high tuneability (~20%) of the system are discussed. The development status of the key hardware items are briefly indicated. The techniques used for the estimation of performances of the backward wave oscillators, Josephson junction and Schottky diode mixers are explained. Although the Josephson junctions require only low levels (μW) of local oscillator power, a key feature of the room temperature Schottky diode system is the necessity of providing tens of mW's of local oscillator power to ensure minimum system noise temperatures. Measurements of the backward wave oscillator output powers over the whole tuning range are described. A flow microcalorimetric substitution technique with water as the working fluid has been used. Estimates of the accuracy of this technique indicate accuracy within ~3 dB. The present test set-up is considered unreliable below 5 mW. Currently developed BWO's (up to 400 GHz) deliver up to 50 mW output power. Tubes being developed and operating into the 500-600 GHz range are expected to deliver less than 10 mW so improvements in measurement techniques are required.
The Schottky diode mixers developed within this programme are briefly described. The use of the Schottky diode DC bias current as a monitor of the local oscillator (BWO) output power is described. Divergences between the power levels indicated using the microcalorimetric method and the diode bias current are discussed in the light of probable causes. Limitations of the technique associated with the difficulty of maintaining good matching into the calorimeter over the full tuning range are discussed.
The Josephson junction conversion losses measurement required an absolute local oscillator (laser) power level measurement. This was done at 455 GHz using a Golay cell calibrated against a thermopile radiometer at 790 GHz. The overall accuracy of this was estimated at ± 30%.
Consideration of the on-going development programme future needs will include at the least a capability for measuring absolute power over a range 1 μW to 100 mW in the frequency range 300 GHz to 1500 GHz with an accuracy approaching 20%.

D1-4
1020

ABSOLUTE POWER MEASUREMENTS FROM 100 TO 1200 μm USING COMMON LABORATORY DETECTORS*: F. B. Foote and D. T. Hodges, Electronics Research Laboratory, The Aerospace Corporation, P.O. Box 92957, Los Angeles, CA. 90009

Historically, power and energy measurements in the FIR/SUBmm spectral region have been difficult and uncertain, and only recently has a concerted effort been made to develop and refine techniques to accurately determine power levels. This paper describes efforts to calibrate in the FIR a common power meter designed for shorter wavelengths, the Scientech 362. The paper also discusses the responsivities of the $LiTaO_3$ pyroelectric detector and the GaAs photoconductive detector in this region.

*This work was supported under Department of Energy Contract

D1-5
1040

PULSE RESPONSE OF GOLAY CELL AND COMPARISON WITH OTHER NEAR-MILLIMETER WAVE DETECTORS: George J. Simonis, Bruce A. Weber, and W.A. Hulon
US Army Electronics Research & Development Command
Harry Diamond Laboratories, 2800 Powder Mill Road,
Adelphi, MD 20783

The Golay cell detector has seen frequent use in the near-millimeter wave (NMMW) spectral region because of its high responsivity, broad-band performance, room temperature operation, compact dimensions, and satisfactory noise equivalent power. It is conventionally used to detect modulated cw signals but has also found use with low duty cycle short pulse signals such as pulsed optically pumped NMMW oscillators. However, little information is available on its pulsed performance. Its low-frequency response precludes using it for the direct observation of fast time-dependent pulse shapes. Nevertheless, its peak voltage is an indication of the pulse energy over an appreciable range of pulse parameters due to its thermal-pneumatic basis of operation.

The pulsed performance of the Golay cell was examined by using near-infrared light emitting diodes and laser diodes because of the relative ease with which pulses and beam parameters could be adjusted with these devices and also because of the availability of fast sensitive absolutely calibrated large-area detectors in the 1 μm region. We examined the responsivity of an Oriel Model 7500 Golay cell as a function of input energy, pulse duration, repetition frequency, and location of the signal on the detector surface. We made an absolute calibration at 904 nm finding a responsivity of 60 V/μJ. Such a calibration is known to change with time due to aging of the detector. We conducted some time-dependent studies of the detector responsivity. The Golay cell was also compared with several other NMMW detectors at 0.5 mm and 1.2 mm.

D1-6
1100 WORK AT NPL ON LASER POWER MEASUREMENTS AT SUBMILLIMETER WAVELENGTHS: T. G. Blaney, National Physical Labortory, Teddington, England

Disc thermopile radiometers, with either black paint or metal film absorbers have been used at NPL for several years for the measurement of submillimeter wavelength radiation at milliwatt levels, propagating in free space. The performance of these devices, and the needs and prospects for the future will be discussed.

D1-7
1120 AN UNTUNED CAVITY RADIOMETER: H.A. Gebbie, Physics Dept., Imperial College, London; D. Llewlyn Jones, Appleton Laboratory, Slough, Berks, England

An untuned cavity of size and shape to give a high mode density is the basis of a new absolute radiometer for millimetre and submillimetre radiation. An emitter of any size or shape can be coupled to the cavity with a readily definable insertion loss and feedback characteristic. Its power can then be determined relative to a thermal source within the cavity. The temperature of this source is measured by a thermometer. Its surface area and emissivity are determined in terms of a directly measurable aperture in the cavity. Since all the radiation is contained no explicit diffraction corrections are involved and power can be measured absolutely in terms of temperature and length standards. The realisation of this for several types of sources will be described.

ATMOSPHERIC EFFECTS ABOVE 10 GHz
Monday Morning, 6 Nov., UMC East Ballroom
Chairman: D. Hodge, ElectroScience Lab, Ohio State University, Columbus, OH

F1-1
0900 A CATALOG OF PROGAGATION MODELS
J. T. Collins
National Telecommunications amd Information Administration, Institute for Telecommunication Sciences, Boulder, Colorado 80303

A recent program undertaken by NTIA/ITS has been the preparation of a catalog of computer program abstracts that are used in predicting the preformance of radio systems. A preliminary catalog has been published emphasizing the 10-100 GHz portion of the spectrum. Additional catalogs are currently being prepared. This is expected to be a continuing, long-term effort that produces a directory of models that are useful in predicting various aspects of radio propagation. Data bases that are frequently used in these various models will also be included.
Current efforts will be reviewed as well as future plans to cover the entire radio spectrum.

F1-2
0920 CONTINUOUS RADIOMETRIC MEASUREMENTS OF INTEGRATED WATER VAPOR: F. O. Guiraud, D. C. Hogg, J. Howard, A. B. Duncan and B. H. Goldman, National Oceanic and Atmospheric Administration, Environmental Research Laboratories, Wave Propagation Laboratory, Boulder, CO 80303

A two-channel microwave radiometer (20.6 and 31.6 GHz) which continuously senses total integrated water vapor (precipitable water) and cloud liquid water has been operated by NOAA/ERL/WPL at Boulder, CO from January-June 1978 and at the National Weather Service Forecast Office at Denver since July 1978. A single antenna with the same beamwidths at the two frequencies is employed. Comparisons between the data measured by the radiometers and NWS radiosondes made on a routine daily basis, are very good. In addition to these comparisons, examples of individual analog measurements of total water vapor and cloud liquid will be presented.

F1-3
0940

CALCULATION OF ATMOSPHERIC O_2 ZEEMAN PATTERNS AT EHF

H. J. Liebe, Institute for Telecommunication Sciences, National Telecom. & Inf. Adm., DoC, Boulder, CO 80302 and
G. G. Gimmestad*, Michigan Technical University, Keweenaw Research Center, Houghton, MI 49931

The oxygen microwave lines split into many components under the influence of the earth's magnetic field (H=2 to 8×10^{-5}T). The components are spread max. ±2 MHz around the unperturbed line centers, which becomes noticeable at altitudes, h>40 km. A consequence of the Zeeman splitting is an anisotropic, polarization-dependent (π, $\sigma^{\pm}$) complex refractivity N (W. Lenoir, J. Geophys. R. 73, 361-376, 1968).
Radio path modeling in the frequency bands, ν=50 to 70 and 118.8±0.1 GHz requires the correct refractivity $N(\nu, H, h)$ of air for the height range, h ≈40 to 110 km. A straightforward, consistent calculation scheme is discussed that supplements the spectroscopic data base given for O_2 lines by the authors in Radio Science 13, 245-251, 1978. Various results of height-dependent O_2 Zeeman pattern behavior are given, of which two examples are depicted below. Each Zeeman component was treated as an individual pressure- and Doppler-broadened line and a fast computer algorithm for the Voigt profile was employed. The approach to "zero" O_2 line intensity with increasing altitude depends upon various assumptions related to the Zeeman effect.

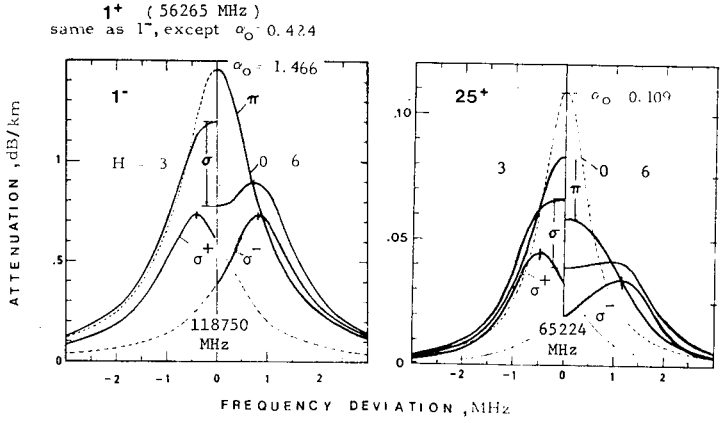

Examples of O_2-MS Zeeman patterns for 1^- and 25^+ lines at h=55 km (p=42.5 Pa and T=260.8 K; U.S. Std. Atm. 76) for two magnetic field strengths, H=3 (left half), H=6 (right half) x 10^{-5}T, and the unsplit line, H=0.

*formerly ITS/NTIA

F1-4
1000

PASSIVE MICROWAVE REMOTE SENSING OF SNOWPACKS: J. A. Kong, L. Tsang, B. Djermakoye and R. Shin, Department of Electrical Engineering and Computer Science and Research Laboratory of Electronics, Massachusetts Institute of Technology, Cambridge, MA 02139 and J. C. Shiue, NASA, Goddard Space Flight Center, Greenbelt, MD 20771

Two theoretical models are developed for the interpretation of passive microwave remote sensing data for snowpacks. Volume scattering effects of snow are accounted for with (1) the model of a homogeneous medium containing discrete spherical scatterers and (2) the model of a random medium with laminar as well as three-dimensional structures. Radiative transfer theory is applied to both models. The theory is used to interpret experimental data obtained from various snow experiments. It is observed that as the snow depth increases, the brightness temperature increases when the subsurface is an aluminum plate and decreases when the subsurface is soil. Variations in brightness temperatures due to diurnal changes have been measured as functions of frequency and view angle. The spectrum behavior of the brightness temperature exhibits opposite trend and the angular dependence is quite complicated. We find that some snowpacks can be characterized by the discrete scatterer model and some snowpacks are better described with the random medium model because they are more laminar in structure. The three-dimensional random medium model provides a more accurate description for general cases but the theoretical results can only be obtained with numerical methods and computationally require lots of computer time. The spectral and angular dependences of the brightness temperatures for both experimental data and theoretical results are illustrated and compared. The brightness temperatures as a function of snow depths are also interpreted and discussed.

F1-5
1040

MICROWAVE RADIOMETRIC DETECTION OF RAIN CELLS USING TOMOGRAPHY

W.A. Shaari and D.B. Hodge
The Ohio State University ElectroScience Laboratory
Department of Electrical Engineering
Columbus, Ohio 43212

Microwave radiometers have been used in detection of rain cells. Unlike radars, radiometers do not provide range information. Employing two microwave radiometers, a technique is used which will provide not only range information but also a two-dimensional display of the distribution of the rain cells and the intensity of rain within a region of interest. This technique is based on the Radon transform for the reconstruction of functions from their integrals over hyperplanes. This approach is well established. The principles of radiometry are briefly reviewed. Then the Radon transform is discussed in detail and a succinct account of various reconstruction methods is given. A reconstruction algorithm, the convolution method, is directly derived from the inverse-Radon transform. Total path attenuation values seen by the two radiometers are computer simulated and used as input data to such an algorithm. Finally, the results obtained for the cases of one, two and three rain cells are discussed.

F1-6
1100 DEPOLARIZATION OF 19 AND 28 GHz EARTH SPACE SIGNALS BY ATMOSPHERIC HYDROMETEORS: H. W. Arnold and D. C. Cox, Bell Laboratories, Crawford Hill Laboratory, Holmdel, NJ 07733

Characteristics of the depolarization of earth-space signals produced by atmospheric hydrometeors are of interest to satellite communications engineers and atmospheric physicists. For the engineer, depolarization is a source of crosstalk that needs to be minimized in dual polarized satellite communications systems. Depolarization measurements can provide physicists with information on the orientation of hydrometeors in the upper atmosphere. Measurements of amplitudes and phases of co- and cross-polarized signals from the polarization-switched 19 GHz COMSTAR Beacon have been used to determine the orientation of non-spherical raindrops and ice crystals in a plane perpendicular to the propagation path. Depolarization statistics for several incident polarizations will be accumulated. Ice particle orientation changes which produce abrupt changes in depolarization will be illustrated. Abrupt changes in the electric field between clouds and ground resulting from lightning discharges often accompany the depolarization changes.

F1-7
1120 FROZEN HYDROMETEOR ATTENUATION AND DEPOLARIZATION AT 11.7 GHz, 19.04 GHz, AND 28.56 GHz: R. E. Marshall, C. W. Bostian, W. L. Stutzman, E. A. Manus, and P. H. Wiley, Electrical Engineering Department, VPI&SU, Blacksburg, Virginia, 24061.

During the winter of 1977-1978 attenuation and depolarization data were collected using the CTS 11.7 GHz and the COMSTAR D2 19.04 GHz and 28.56 GHz beacons during several winter storms. Frozen rain, wet snow, dry snow, and frost were experienced by all three systems. Ground temperature was recorded at ten minute intervals. Antenna effects were temporarily separated from propagation effects several times during each storm when the antennas were cleaned. Feed effects, reflector effects, and spar effects were separated by careful antenna cleanings on the mornings following storms.
Occurences of severe fades with and without isolation deterioration were observed due to frozen hydrometeor build-up on the antennas. Instances of isolation enhancement just before snowstorms were observed on all systems before most storms. Fades with and without isolation deterioration were recorded with clean antennas in the presence of clouds with no ground precipitation. Sudden changes in isolation related to ground temperature variations were recorded. Instances of propagation effects rising above antenna effects were also observed.

F1-8
1140

CUMULATIVE FADE STATISTICS ASSOCIATED WITH THE COMSTAR BEACON SIGNAL AT 28.56 GHz FOR WALLOPS ISLAND, VIRGINIA:

J. Goldhirsh, Applied Physics Laboratory, The Johns Hopkins University, Laurel, MD 20810

From 1 April 1977 to 31 March 1978, the COMSTAR beacon signal at 28.56 GHz has been received continuously at Wallops Island, Virginia. During periods of rain the signal is monitored down to approximately 30 dB below the free space level and these data are digitized and recorded on tape for later reduction and analysis. Ancillary measurements are also obtained with radar, disdrometers, and raingages.
In this paper are presented the cumulative fade statistics for the year period and the results indicate the following:
[1] The cumulative rain attenuation distribution is shown with good approximation to be log normal over most of the fade range considered. [2] The most intense attenuations occurred during June and August with August representing the worst month. For example, of the 25 dB or greater fades that took place during the year, 31% of these occurred in August.
[3] The 8 hour slot of time for which fades were significantly greater than during other periods was from about 1600 to 2400 local time. This represents the period of maximum convection caused by ground heating characteristic of the summer months.
Using the concept of effective path length and the measured rain rate cumulative distribution, the fade distribution at 19.04 GHz is predicted. This predicted distribution results in attenuation ratios of the 28.56 to 19.04 GHz fades which are in agreement with measured results.

COMBINED SESSION
UMC Central Ballroom
Chairman: C. G. Little, Wave Propagation Lab, NOAA/ERL, Boulder, CO 80302

CS1-1
1330 PRELIMINARY ASSESSMENT OF THE ENVIRONMENTAL IMPACTS OF THE SATELLITE POWER SYSTEM (SPS)

S.L. Halverson and D.M. Rote, Argonne National Laboratory, Argonne, IL 60439
C.M. Rush, Institute for Telecommunication Sciences, Boulder, CO 80303
K. Davis, Battelle, Pacific Northwest Laboratory, Richland, WA 99352
M. White, Lawrence Berkley Laboratory, Berkley, CA 94720
D.F. Cahill, Environmental Protection Agency, Research Triangle Park, NC 27711

The Department of Energy is considering several options for the generation of electrical power to meet the future energy needs of the United States. One proposed option, the Satellite Power System (SPS), involves the collection of Solar Energy by a system of orbiting satellites, converting the energy to microwave energy and transmitting via extremely directive transmitting antennas to large receiving antennas (rectennas) located on the earth. (Laser power transmitting and receiving systems are presently being considered as an optional alternative.) All of the conceptual designs provide for the generation of 5-10 GWe at each rectenna. The impact of the SPS Microwave Power Transmission System (MPTS) as well as impacts related to other elements of the total SPS on the environment are being determined by several ongoing research efforts being funded by DOE. The goal of these programs is to advance the state of knowledge by the year 1980 to the point where an assessment can be made of the probability and severity of the impacts of the SPS. Assessments will be made of the effects on the health and safety of the public, and occupationally involved personnel, and on the ecology; the upper and lower atmosphere including climatological impacts; and on communications systems including electromagnetic compatibility, the effects of microwave heating of the ionosphere and magnetosphere, and the effects of F-layer depletion by launch vehicle and transport vehicle effluents. If the assessment indicates that the impacts are acceptable or that feasible mitigating strategies can be implemented and if other related assessments (the impact on society and a competitive comparison of the SPS with other energy alternatives) are favorable, a decision may be made to implement the development of the SPS related technologies. This paper identifies postulated effects and summarizes the ongoing research efforts to determine whether or not these effects will occur.

CS1-2
1405 PLANNING FOR THE FUTURE INTELSAT SYSTEM: H. L. Van Trees, Communications Satellite Corporation, Washington, D.C.

The objectives of the future INTELSAT System Planning Study include the development and analysis of alternative system and spacecraft concepts for the post-1985 period and the identification of key technologies necessary to implement these concepts.

The traffic in the INTELSAT system is projected to increase to 300,000 channels by year-end 1993. New system concepts and technologies are required to provide the necessary capacity efficiently. Several system concepts and spacecraft designs are described. The effect of intersatellite links, TDMA, small antennas, new frequency allocations, and intersatellite traffic distribution are discussed.

CS1-3
1440

Overview and Preliminary Results from Seasat-1

John R. Apel

Pacific Marine Environmental Laboratory
Environmental Research Laboratories
National Oceanic and Atmospheric Administration
Seattle, Washington

ABSTRACT

Seasat-1 was successfully launched by NASA on 26 June 1978, after several years of planning and implementation. Its missions are to measure surface waves, winds, temperatures, currents, and ice cover using microwave, visible and infrared sensors. The measurement program is largely experimental although several non-research users expect to incorporate the data into operational activities. Preliminary indications are that: (a) the synthetic aperature radar successfully images oceanic and terrestrial features with a resolution approaching 25 m, and phenomena that significantly modulate the short-length ocean wave spectrum will be imaged by the SAR; (b) the short pulse altimeter (ALT), wind scatterometer (SASS), and scanning multifrequency microwave radiometer (SMMR) all meet or exceed their engineering performance criteria; (c) the visible and infrared radiometer (VIRR) functions as intended. With minor exceptions, the mission to date has been technologically successful. Examples of Seasat-1 data will be presented and a preliminary assessment of the results will be made. Plans for assessing the geophysical performance of the system will be outlined.

CS1-4
1530

VOIR: PROSPECTS FOR RADAR MAPPING OF VENUS FROM ORBIT:

R. S. Saunders, Jet Propulsion Laboraotry, Pasadena, CA 91103

Venus is the only terrestrial planet that cannot be mapped using optical techniques. Since it is the planet most like the Earth, the scientific value of obtaining a map of the surface is extremely high. For the past decade the science requirements and the means for achieving them by an orbital imaging radar system have been under study. In the past year the feasibility of mapping Venus using a modified version of the Seasat synthetic aperture radar instrument has beed studied in detail. The current plan calls for a 120 day mission to produce a complete map of the planet at 300 meter resolution and to map a few percent of the planet's surface at 50 meter resolution. The swath width for the mapping resolution is 50km from a 300km near-polar circular orbit. Approximately 20% overlap is planned. The incidence angle is 50^{o} with a capability of imaging in the range 25^{o} to 55^{o}. The tentative frequency is 1275 MHz. It may be possible to obtain stereo coverage by varying the incidence angle. Other experiments would be performed during the mission, primarily global altimetry and determination of the gravity field.

CS1-5
1605

ELECTROMAGNETICS AND DIFFERENTIAL FORMS:

Georges A. Deschamps, Electromagnetics Laboratory, Department of Electrical Engineering, University of Illinois, Urbana, Illinois 61801, U.S.A.

By a systematic use of differential forms, the equations of electromagnetics can be given convenient and concise expressions. The exterior differential calculus that was developed in the early part of the century by E. Cartan contributed greatly to a rebirth of differential geometry. It can also be applied to many branches of physics and particularly to electromagnetics. It is simpler and more general than the conventional vector calculus: a single operator "d" replaces curl, grad, div; fewer formulas must be committed to memory; the transition from differential to integral formulations results from a single theorem (Stokes) valid for any dimension.

The equations of electromagnetics separate into two sets, each being completely independent of a metric (or notion of distance). This means that the structure of these equations is the same in all (smoothly related) systems of coordinates. This "covariance" property, which is not always recognized or sufficiently emphasized, is very convenient when using curvilinear coordinates. The relation between the two sets of equations, however, is expressed by the material operators (ε,μ) that do require a metric or the use of special reference frames. Quantities appearing in each set of equations are expressed by differential forms having the same dimensions (resp. that of coulombs and webers). Electric charges are exact mulitples of the electronic charge e. Dirac has shown (1931) that this implies magnetic charges (if they exist) that are also quantized, being exact multiples of $1/2g$, where $g = 137\ e$. Using e and g as units for the two sets of electromagnetic quantities makes $\varepsilon = \mu^{-1}$ equal, in vacuum, to the fine structure constant $\alpha = 1/137$.

Some of the concepts and rules of operation of exterior calculus will be presented in an attempt to show that this approach could be introduced at an elementary level. At a higher level, many properties related to differential exterior calculus could also be profitably exploited to deduce more efficiently old and new results and to reach a deeper understanding of these results. In particular, the relation between a four-dimensional space-time formulation appropriate to relativity, and the three-dimensional formulation, closer to applications, will be displayed in a flow diagram. This diagram could also be of some help (even without differential forms!) in teaching the intricate relations that exist between the various electromagnetics quantities.

CS1-6
1640 IMPRESSIONS OF THE XIXth GENERAL ASSEMBLY OF URSI, 28 JULY-8 AUGUST, HELSINKI, FINLAND:

J. V. Evans, Lincoln Laboratory, M.I.T., Lexington, Massachusetts 02173

The XIXth General Assembly of URSI attracted a larger attendance than any in recent history, and had a much stronger scientific content. In addition to the usual scientific meetings of commissions, open symposia were organized on Time and Frequency, Biological Effects, Optical Communications, Radio Waves and the Ionosphere and Wave Instabilities in Plasmas. The paper provides one individual's impressions of the General Assembly and the future direction URSI appears likely to take.

TUESDAY MORNING, 7 NOV., 0830-1200

MEASUREMENTS AND STANDARDS NEEDS AT MILLIMETER, SUB-MILLIMETER, AND FAR INFRA-RED FREQUENCIES

Commission A, Session 1, UMC 158

Moderator: P. S. Hudson, National Bureau of Standards, Boulder, CO 80303

A1 0900 PANEL DISCUSSION

Members: R. Harris, System Planning Corp.; T. Kemerly, Air Force Avionics Lab, WRAFB; R. Von Wagoner, Naval Research Lab; H. Gerlach, Harry Diamond Lab; K. Button, MIT Magnet Lab; T. Mukaihata, Hughes Aircraft Co.; A. Lance, RF and Microwave Metrology, TRW; and J. Taub, AIL Technology

Commission B Session 3

NEW CONCEPTS IN ELECTROMAGNETICS
Tuesday Morning, 7 Nov., UMC West Ballroom
Chairman: P. L. E. Uslenghi, University of Illinois, Chicago Circle Campus, Chicago, IL 60680
Organizer: C. E. Baum, AF Weapons Lab, Kirtland AFB, NM

B3-1 0830 INTRODUCTION: C.E. Baum, AF Weapons Lab, Kirtland, AFB, NM

Topic A: TOPOLOGICAL CONCEPTS AND ASSOCIATED MATRICES

B3-2 0840 TOPOLOGICAL CONCEPTS FOR ORDERING ELECTROMAGNETIC INTERACTION WITH COMPLEX SYSTEMS

Carl E. Baum, Air Force Weapons Laboratory
Kirtland AFB, New Mexico 87117

In analyzing the response of a complex system to an electromagnetic stimulus such as the nuclear electromagnetic pulse (EMP) one needs methods of analysis which take advantage of special properties of the system which can simplify the problem. An important set of such properties are those which can be referred to as topological; these are the conductor topologies of the system.

Electromagnetic topology begins with the common use of graph theory to describe the topology of lumped-element electrical networks. The Kirchhoff laws for voltage and current are written in terms of the graph elements as nodes and branches. Transmission-line topology also uses graph theory but with elements as junctions and tubes. Junctions are multiport networks; tubes are multiwire (plus reference) transmission lines. The equation governing the entire transmission-line network of junctions and tubes with lumped and distributed sources, impedances, etc., is referred to as the BLT equation; it uses scattering matrix concepts.

Complex systems can be thought of as electromagnetic scattering problems (including antenna problems), and for such problems one can analogously define an electromagnetic topology or scatterer topology. This kind of topology is based on volumes surrounded by closed surfaces as appropriate to electromagnetic theorems concerning energy, reciprocity, and uniqueness. For our purposes it is useful to have these surfaces coincide with approximately perfectly conducting surfaces of the system which may, however, have various penetrations (apertures, conductive penetrations, etc.) through them. This electromagnetic topology is further refined as a hierarchical topology involving principal volumes and surfaces which are contained one within another in a "nesting" concept, these being further divided into elementary volumes and sur-

faces. Based on the various divisions introduced into the hierarchical scatterer topology the wave-wave interconnection matrix and the associated scattering matrix can be partitioned to give corresponding supermatrices. These supermatrices have a special tridiagonal form allowing approximate solutions for cases of good shielding by the principal surfaces. They also have additional levels of block sparseness, i.e., a very ordered sparseness. This also leads to special results for the inverse of certain supermatrices. The scatterer topology (or topological diagram) with surfaces and volumes has a second representation, the interaction sequence diagram which takes the form of a graph (or better, a hierarchical graph). A third representation is the (partitioned) wave-wave interconnection supermatrix.

B3-3
0910 SELECTED TOPICS IN TRANSMISSION LINE NETWORK THEORY: F.M. Tesche, Science Applications, Inc., and T.K. Liu, LuTech, Inc.

The need for electromagnetic pulse (EMP) and electromagnetic compatability (EMC) analysis of large systems has caused renewed interest in the area of transmission line network theory. One common analytical approach, which is useful in modeling a large electrical system, is to divide the system into a finite number of topological volumes and then compute the electromagnetic field penetration into and propagation within the volumes. In many cases, the penetration and propagation of electromagnetic energy within a large system occurs on single or multiconductor transmission lines. Such lines may be either deliberate (signal cables, etc.) or unintentional (water pipes, hydraulic lines, etc.). In either case, however, energy can be transported from one part of the system to another, usually with small attenuation. For general applicability to many different systems, a transmission line analysis must be able to handle branching and/or looping of transmission lines, frequency dependent loads and lumped or field-induced sources.
This paper describes a number of recent developments in the analysis of multiconductor transmission line networks. The derivation of the BLT equation for the network will be discussed in detail, as well as the determination of the field-induced source terms. Sample calculations will be presented and a comparison of experimental data and theoretical results will be presented for both laboratory and actual aircraft test data. Finally, a discussion of planned future work in this area will be presented.

B3-4
0940

BOUNDARY CONNECTION SUPERMATRICES:

K. F. Casey, Dikewood Corporation
Westwood Research Branch
1100 Glendon Ave, Los Angeles, CA 90024

A boundary connection supermatrix (BCS) expresses a linear relation among the tangential components of the electric and magnetic fields on either side of a boundary layer between two regions. Since six such relations can be constructed, there exist six distinct forms of the BSC, each of which is analogous to a set of two-port network parameters of circuit theory. The elements of the various forms of the BCS are, in general, dyadic operators and each BCS is a 2×2 matrix of such operators.

The BCS is a practically useful tool when its elements can be calculated from a simple planar model of the boundary layer of interest, which may be inhomogeneous (in the direction normal to its boundaries) and/or anisotropic. The resulting BCS can then be applied to the analysis of problems involving curved boundary layers, provided that the principal radii of curvature are large in comparison to the thickness of the layer.

In this paper we define the six forms of the BCS and discuss certain of their properties, particularly those which follow as a consequence of reciprocity. We also present specific examples of the BCS for some commonly encountered types of boundary layers and discuss the construction of integral equations appropriate to the analysis of electromagnetic scattering and penetration problems involving hollow bodies.

Topic B: DIFFERENTIAL GEOMETRY

B3-5
1030

USE OF DIFFERENTIAL GEOMETRY FOR THE SCALING OF ELECTROMAGNETIC PROBLEMS IN INHOMOGENEOUS AND ANISOTROPIC MEDIA:

Charles T.C. Mo, R & D Associates,
Marina del Rey, California 90291

Scaling is one of the most useful methods among the various transforms that relate, seek, create, and identify problems and their solutions in one nature from those in another. Such transforms not only can make a problem easier to solve using one of its particular formulations, they often bring about deeper insight and open new areas of technology as a consequence of focusing upon the properties common to all these apparently unrelated but actually "equivalent" problems. Just as in the similarity solutions in mechanics and in fluid dynamics, the essence of the scaling of electromagnetic (EM) problems is to look for and study the appropriate dimensionless parameters and their combinations common to vastly different physical problems. Such a scaling encompasses controlled changes in the geometry and time, the distribution of the source charges-current, the properties of the media, and the EM fields. Starting with the simplest scaling produced by one single scalar that down-scales distance and time but up-scales sources and leaves the field unchanged, we show that a general scaling is obtained straightforwardly with a formalism using differential geometry. The general scaling creates a class of equivalent EM problems p each described by a complicated goemetry and in a complicated medium, which may be anisotropic, inhomogeneous, and time varying, from an EM problem p' described by a simple Cartesian geometry and in a simple medium. After high-lighting the details, the meaning, and the applicational restrictions of the general scaling, we exhibit its use by two examples. In one, an inhomogeneous bispherical lens that distortionlessly converts the spherical TEM wave of a conical transmission line to a plane one of a cylindrical transmission line is given. In the other, an anisotropic $\underset{\sim}{g}$ and inhomogeneous ε loaded matching section between two cylindrical coaxial waveguides is presented, with all EM quantities of the underlying simple problem and its three differently scaled versions in the three regions explicitly given.

B3-6 SCATTERING BY ROTATING BODIES: C. H. Papas, Department
1100 of Electrical Engineering, California Institute of Technology, Pasadena, CA 91125

One of the key problems of modern electromagnetic theory is the interaction of electromagnetic waves and fields with moving media. When the velocity of the medium is uniform, the system is inertial and can be handled with the aid of the Lorentz transformations. However, when the medium undergoes acceleration, the system is non-inertial, the interaction is more complicated, and there appear novel phenomena which deserve detailed study. In this paper we examine the theory of non-inertial systems and apply it to the problem of scattering of electromagnetic waves by rotating bodies. Moreover, we construct a simplified version of the theory and make plausible its adequacy for dealing with almost all practical situations involving the electrodynamics of accelerated media. Finally, we discuss the need for experimental verification of the theory which, for the sake of tractability, neglects the internal dynamics of the accelerated medium.

Topic C: FORMULATION OF MAXWELLS EQUATIONS

B3-7
1130

THE COMBINED FIELD: THEORY AND APPLICATIONS

B. K. Singaraju and C. E. Baum, Air Force Weapons Laboratory, Kirtland AFB, NM 87117

This paper is a review of some new concepts derived from the combined field. The combined field is defined as a special linear combination of the electric and magnetic quantities as $\vec{E}_q = \vec{E} + qjZ_o\vec{H}$ where $\vec{E}_q$ is the combined field, $\vec{E}$ the electric field vector, $\vec{H}$ the magnetic vector, Z_o the free space impedance, and q the separation index $= \pm 1$. Similar consistent set of definitions can be defined for currents, charges and potentials. Using this set of definitions, Maxwell's four equations can be reduced to two equations.

The combined field equation, continuity equation, and the Gauss's law for the combined field are derived in macroscopic and microscopic formulations. Boundary conditions between two different media for the combined field are derived. Integral equations in the scalar and dyadic formulations are derived for the combined field. Poynting's theorem and the reciprocity theorem for the combined field are derived along with the matrix representation of the combined field. Using the combined field, Babinet's principle was simplified and generalized to include impedance loadings.

Using the integral equations developed, various representations for electric and magnetic impedance loading on scatterers have been derived. Properties of these operators will also be discussed. Numerical results for the combined field integral equation for a perfectly conducting body are also obtained. Radar crossections and natural frequencies are found using this combined field integral equation. Advantages of this technique versus the "simple" electric or magnetic field integral equation will also be discussed.

COMPUTER NETWORKS
Tuesday Morning, 7 Nov., UMC 156
Chairman: P. E. Green, IBM Research, Yorktown Heights, New York 10598

C2-1
0830

APPLICATIONS OF QUEUEING THEORY TO COMPUTER NETWORKS:

Izhak Rubin, Department of System Science, School of Engineering and Applied Science, University of California, Los Angeles, CA 90024

Queueing models used to investigate the performance characteristics of computer communication networks are surveyed. The following topics are discussed: queueing network models; regenerative stochastic process methods; optimal control techniques; simulations, approximation and numerical procedures; channel sharing, multiplexing and multiple-access queueing models; network synthesis approaches; combined information/queueing theoretical models. For certain queueing network models, local balance techniques have been developed to yield analytical product form solutions for the distribution of the joint queue-size network state, when messages belong to a number of different classes. These models are limited in that they do not provide for the actual statistical dependences arising from network message transmission processes. Nor do they allow the computation of the message response-time distribution. Queueing network models allowing such dependences are described. Also discussed are queueing modeling and computational techniques that involve guided searching algorithms, hybrid numerical/simulation methods and approximation techniques. Such models incorporate blocking effects, flow control strategies, acknowledgment procedures, buffer conservation methods, various routing disciplines and channel-sharing schemes. Techniques for network synthesis, which involve the combined selection of the topological structure, flow routing and control strategy and link capacities under proper message queueing delay, complexity and cost measures, are reviewed. Using discrete-time bulk queueing process models, analytical results are obtained for various channel multiplexing strategies such as FDM, TDM, DA/FDM/TDM, or schemes where the user is assigned a channel (on a circuit-switching or message-switching basis) in a time-interrupted fashion. Combined information/queueing theoretical techniques are developed to study and evaluate joint performance measures describing the reliable and timely transmission of information through a computer communication network. The problem is noted to involve the allocation of the limited network resources, prescribing network bandwidth, power and structural constraints, to yield acceptable performance characteristics governed by the underlying noise-interference, message-flow and congestion situation.

C2-2 0900 SURVEY OF ROUTING TECHNIQUES IN COMPUTER COMMUNICATION NETWORKS: Mischa Schwartz, Dept. of Electrical Engineering and Computer Science, Columbia University, New York, N.Y. 10027

In this tutorial paper we focus on various packet routing procedures that have been either implemented or proposed for a variety of packet-switched networks. These include fixed path algorithms (e.g., shortest path and least time delay), adaptive algorithms, and combinations of the two.

A great deal of work has gone into simulating these algorithms in an attempt to develop quantiative measures of their performance. Performance measures studied include time delay, throughput, and cost of implementation of the algorithm. A combination of adaptive and fixed path routing has been found, through simulation, to provide impressive improvements in throughput with relatively little added cost in implementation.

Very little work has been done on analysis of the various algorithms, however, because of the inherent complexity of modeling the interactive queues used to represent the store-and-forward delays at the various nodes in the network. We present the results of some analyses carried out on small network configurations that attempt to remedy the dearth of work in this area. The analyses are carried out for simple routing rules incorporating both adaptive and fixed components. Improvement in performance obtained by adding simple adaptation to a fixed routing rule agrees with the results of simulation.

C2-3 0930 SURVEY OF FLOW CONTROL TECHNIQUES: Leonard Kleinrock, Computer Science Department, University of California, Los Angeles, CA 90024

Flow control is perhaps one of the most difficult problems yet remaining in the design of computer networks. In this survey, we present some of the well-known flow control phenomena and give examples of some of the more common techniques for controlling traffic flow upon entry to a network. Moreover, we give some general definitions and provide a global view of flow control for a whole class of control schemes.

C2-4
1030

FUNDAMENTAL ISSUES IN DATA LINK CONTROL

E. F. Wunderlich, Bell Telephone Laboratories, Holmdel, NJ 07733

Data link controls are the protocol rules by which senders and receivers transfer information over a data link. The minimum functional requirements for a data link control are usually considered to be (1) a method of identifying the beginning and end of a data transmission, (2) a method of specifying address information for the senders and receivers that share a communication facility, (3) a set of specific commands and responses to support such operations as polling on a multipoint facility and (4) a method of detecting errors and taking corrective action. These four functions are usually accomplished by separate mechanisms. A good example of this is the American National Standards Institute Advanced Data Communication Control Procedure (ADCCP) which is reviewed in this tutorial. Using a separate explicit mechanism for each function results in a significant amount of protocol information overhead. Reducing this overhead has become a fundamental research question. By reviewing the work in this area by Gallager (R. G. Gallager, IEEE Trans. Inform. Theory, 385-398, 1976), by Humblet, and by Hayes (J. F. Hayes, IEEE Trans. Communications, August 1978) the insight is developed that protocol information overhead can be reduced. This is done by recognizing how start/stop information, address information and polling strategies are all fundamentally related and that there exists implicit protocol knowledge that can be used. This relationship and the concept of implicit protocol knowledge are illustrated by an example of a concentrator on a multipoint facility.

C2-5 SECURITY ASPECTS OF DATA NETWORKS: Dennis K. Branstad, Institute for Computer Sciences and Technology, National Bureau of Standards, Washington, D. C. 20234
1100

Connecting various types of terminals and various computer systems together in distributed networks creates many technical problems. The requirement that data in the network must be protected against certain accidental and intentional threats adds additional technical problems. Cryptography is emerging as a practical means for providing the needed security in computer networks. The National Bureau of Standards has issued a Federal Information Processing Standard for providing the needed cryptographic protection in Federal computer networks.

The specific potential threats to computer data in a network will be discussed in this presentation. The Federal Data Encryption Standard (DES) and its commercial implementations will outlined. The major part of the presentation will center around the security equipment and procedures planned for the National Bureau of Standards internal computer network. Data communications and security are provided for each user of the network through special devices called Terminal Interface Equipments (TIEs). Each TIE will contain an optional security circuit board which encrypts (cryptographically scrambles) data before it is transmitted and decrypts (unscrambles) ciphertext (scrambled data) when it is received. A Network Security Center (microcomputer system) is used to provide the cryptographic keys required in each TIE participating in a secure connection. The NBS plans for developing the NSC will be described.

C2-6
1130 VARIABLE RATE PACKET SPEECH MULTIPLEXING OVER WIDEBAND CHANNELS:

Robert E. Kahn, Defense Advanced Research Project Agency, Arlington, VA, 22209.

Recent studies have shown that packet networks may be appropriate for handling voice traffic as well as data. In a packet network, only the "talk spurts" require transmission, while the remaining 60 to 70% of silence is simply not sent. This allows savings in network communications equivalent to that produced by a Time Assignment Speech Interpolation (TASI) system. Wideband packet networks may provide an effective vehicle for a network wide TASI capability. The application of variable rate speech communication to wideband packet networks is discussed.

RADIOOCEANOGRAPHY - SEASAT 1
Tuesday Morning, 7 Nov., UMC East Ballroom
Chairman: J. Dunne, Jet Propulsion Lab, Pasadena, CA
Organizer: C. T. Swift, NASA, Langley, VA

F2-1
0830

AN ASSESSMENT OF THE PERFORMANCE ACHIEVED BY THE SEASAT-1 RADAR ALTIMETER:

W.F. Townsend, Directorate of Applied Science, NASA Wallops Flight Center, Wallops Island, VA 23337

The SEASAT-1 spacecraft was placed into earth orbit on June 27, 1978. A radar altimeter, part of this ocean dedicated satellite instrumentation system, represents the first attempt to achieve 10 cm altitude resolution from orbit. The altimeter measures the spacecraft height above mean sea level, the significant waveheight, and the backscatter coefficient (σ_o) of the ocean surface beneath the spacecraft. It contributes to the overall SEASAT objectives of demonstrating global monitoring of waveheight; detecting currents, tides, storm surges, and tsunamis; and mapping the global ocean geoid. The instrument consists of a 13.5 GHz monostatic radar system that tracks in range only and has a 1 meter antenna pointed at the satellite nadir. Some of its unique features include a linear FM transmitter with 320 MHz bandwidth which can yield a 3 nanosecond pulse resolution. The high resolution permits a 10 cm altitude precision and a 10% or 0.5 m (whichever is greater) real-time waveheight accuracy for waveheights between 1 and 20 meters. The high pulse rate (1 KHz) reduces the sampling variability of the altitude and waveheight measurements. The altimeter was turned on for the first time on July 3, 1978, and subsequently declared operational on July 6, 1978. During the next 30 days of operations, a detailed assessment/analysis of performance was conducted. The altimeter was operated in various modes to acquire a set of data to determine the optimum configuration for future operations. Coupled with this activity, various surface truth data collecting activities were conducted in an attempt to evaluate/calibrate the real-time waveheight measurement. The total data set was analyzed in detail and results obtained from the evaluation process will be presented. In particular, altitude resolution, waveheight accuracy, and return pulse shape as a function of waveheight will be shown.

F2-2
0900 SEASAT-I SCATTEROMETER MEASUREMENTS-A PRELIMINARY REPORT: E. M. Bracalente, J. W. Johnson, L. C. Schroeder, W. L. Jones, Jr., and W. L. Grantham, NASA Langley Research Center, Hampton, VA 23665

A brief description of the SeaSat I scatterometer is presented with main emphasis of the paper on oceanographic measurements taken since launch (June 26, 1978). The scatterometer (SASS) which measures ocean surface wind is one of five remote sensors on the satellite. The active radars are a synthetic aperature radar, altimeter and scatterometer. The passive sensors are a multifrequency scanning microwave radiometer and a visible/infrared radiometer. Together these sensors are providing the oceanographic community with scientific and operational data to improve knowledge of the oceans and their ability to forecast ocean phenomenon.

An evaluation of the scatterometer performance in orbit is presented to show its ability to measure radar cross section of the ocean over its full dynamic range (low to high surface winds). In orbit the scatterometer overflies about 20 surface truth sites per day and a wide range of surface conditions have already been experienced. First comparisons of scatterometer derived winds with in situ data are good and includes some wind data from recent hurricanes.

Underflight NRCS values from a precision aircraft scatterometer are compared with SASS values to identify fixed biases that SASS has. The aircraft instrument was previously calibrated using precision radar spheres to an accuracy of ± 0.5 dB.

F2-3 0930 PRELIMINARY DATA AND PERFORMANCE OF THE SEASAT-A SCANNING MULTICHANNEL MICROWAVE RADIOMETER:

E. G. Njoku, J. M. Stacey, Jet Propulsion Laborarory, Pasadena, CA; D. B. Ross, NOAA/AOML, Miami, FL

The Scanning Multichannel Microwave Radiometer (SMMR) is a five-frequency dual-polarized radiometric system designed primarily to measure sea surface temperatures and wind speeds from space, on a global, nearly all-weather basis. Accuracy goals are 1.5 K and 2 m/s for ocean temperatures and wind speeds respectively. Three stages of instrument-related performance need to be assessed before the accuracy of the geophysical parameter derivations can be established. The engineering performance of the radiometer and antenna systems is periodically assessed during the mission by monitoring component temperatures and voltages, rms variations in the outputs, and switching and scanning modes. The radiometer calibration algorithm compensates for offsets and variations caused by the radiometer characteristics, and provides output data in units of antenna temperature. The antenna pattern correction algorithm corrects for effects caused by the antenna such as polarization mixing and sidelobe contributions, and outputs true brightness temperatures for the appropriate footprints on regularly-spaced subsatellite grids. A performance summary of these instrument-related algorithms will be made in terms of the brightness temperature output data quality. Preliminary comparisons of SMMR - derived quantities with surface truth measurements of winds and ocean temperatures from selected locations will be presented. This stage of data comparison while predominantely qualitative in nature will lead to more quantitative analyses when outputs from the full set of geophysical processing algorithms have been studied in more detail.

F2-4
1000 STATUS OF THE VISIBLE AND INFRARED RADIOMETER ON SEASAT-A: E. Paul McClain, National Environmental Satellite Service, NOAA, Washington, D.C. 20233

The Visible and Infrared Radiometer (VIRR) on Seatsat-A is a two-channel, visible (0.5-0.9 m) and thermal-infrared (10.5-12.5 m) scanner with a data swath width on Earth of 1500 km and a nominal spatial resolution at nadir of 9 km. The VIRR is not a primary sensor, but rather is considered a supporting instrument whose principal function is to provide images of visual reflection and thermal infrared emission from ocean, coastal, and atmospheric features that can aid in interpreting the data from the microwave sensors on Seasat-A. The VIRR is also expected to provide some derived quantitative measurements of sea surface temperature and cloud top height; and it is planned to use it, on that side of the track where SMMR (Scanning Multifrequency Microwave Radiometer) data are not available, for flagging SASS (Seatsat-A Scatterometer System) measurements that likely are contaminated by backscatter from precipitation.

Examples of VIRR image and digital data are presented and the results of geophysical evaluation of early measurements from Seasat-A are given.

F2-5 1030 PRELIMINARY RESULTS OF THE SEASAT-A SAR EXPERIMENT:

P.G. Teleki, Office of Marine Geology, U.S. Dept. of the Interior, Reston, VA

By virtue of the many uses of an imaging radar, the SAR Experiment encompasses a wide range of topical investigations in open oceans, coastal areas, regions covered by ice, and on terrestrial surfaces. The SAR Experiment has been primarily designed for the validation of the sensor's performance at pre-selected sites that are instrumented on the ground, as well as overflown with airborne sensors to allow correlation of radar backscatter measured by the satellite to geophysical processes on the earth's surface.

Since the June 26, launch of SEASAT-A, SAR data collection has been routinely carried out with the modified orbit. First priority was given to engineering assessment of the SAR and on checking out and improving the performance of the SAR Data Processor System (SDPS). SAR data acquisition began at the Goldstone and Merritt Island stations. Among the passes collected at these stations and processed (although without sensor data records) were Rev. No. 150, extending from the Baja California to the British Columbia coast, and Rev. No. 163, from Colombia, South America, to Lake Superior. Subsequent adjustments at the Fairbanks station allowed acquisition of sea ice data (Rev. No. 205). Upon activation of the Oakhanger (England) and Shoe Cove (Newfoundland) stations, on August 4 and August 22, respectively, SAR coverage became complete over North America and Europe. Examination of the SAR imagery shows that the anticipated saturation near coastal areas, resulting from the step function in dynamic range from the sea surface onto terrestrial surfaces due to increased scattering cross-section has not been realized. From the oceanographic viewpoint, the correlated SAR images contain a wider range of information than expected. While the extent of regions in which surface gravity waves were present have been limited (in part possibly caused by overall calm sea conditions), other features observed have been interpreted to be internal waves, surface roughness variations induced by wind as well as rainfall on sea and lake surfaces, and patterns resembling surface shear in currents. In ice covered areas, the SAR has performed well, clearly imaging various ice types, such as pack ice and shore-fast ice, as well as variations in the reflectivity that is thought to be related to both the age of ice and the extent of meltwater covering it.

It was anticipated that the foreshortening or fold-over problem would perilously reduce the geological interest in the imagery. However, the Seasat SAR has provided exceptional images of geologic and topographic features, primarily because the illumination is more uniform than that obtained by low depression airborne SLAR's. Since validation experiments have only recently begun, confirmation of the reality of observed features is yet incomplete.

Present speculations, therefore, will give way gradually to authenticated results, as the validation experiments, scheduled to last through September 1979, prove and disprove various hypotheses. It is important to remember that the Seasat radar has not been fully tested in airborne experiments preceeding launch; necessitating careful evaluation of the information contained in the images through comparison to ground truth and additional airborne data.

F2-6 PANEL DISCUSSION. Moderator: J. Dunne, Jet Propulsion
1130 Lab, Pasadena, CA

Members: P.G. Teleki, Office of Marine Geology, U.S. Dept. of the Interior, Reston, VA; J.R. Appel, Pacific Marine Environmental Lab, Environmental Research Labs, NOAA, Seattle, WA; W.F. Townsend, NASA Wallops Flight Center, Wallops Island, VA; E.P. McClain, National Environmental Satellite Service, NOAA, Washington, DC, and speakers from papers 2 and 3

IONOSPHERIC HEATING EXPERIMENTAL RESULTS
Tuesday Morning, 7 Nov., UMC Forum Room
Chairman: H. Carlson, NSF, Washington, DC

G1-1
0830

MODULATION OF IONOSPHERIC CURRENTS BELOW 90 KM BY MEANS OF A HIGH POWER R.F. HEATER:

A.J. Ferraro, H. S. Lee, and A. A. Tomko
The Ionosphere Research Laboratory, The Pennsylvania State University, University Park, PA 16802

Recent rocket measurements have established the presence of strong vertical electric fields in the D-region. Obviously such data imply the need to examine the role of electron transport in the formation of this region in addition to the ion-chemistry. A unique technique for monitoring the presence of these fields using ground-based measurements is described. Basically the technique relies upon modulating the ionospheric currents which result from these fields with a high power R.F. transmitter (or 'heater') and detecting the electromagnetic field radiated from the so-called 'ionospheric antenna'. This paper discusses the relevant theory, presents some calculations of the radiated power for different 'heater' modulating frequencies, and describes various models of the 'ionospheric antenna'. The calculated results are for a mid-latitude daytime D-region and include both the vertical and horizontal ionospheric electric fields which create vertically and horizontally polarized electromagnetic waves in the frequency range from 10 Hz to 10 KHz. In view of the construction of new high power heating facilities at Arecibo and EISCAT, future experiments to test the feasibility of this technique will be possible.

G1-2
0855

ION LINE ENHANCEMENT IN IONOSPHERIC MODIFICATION EXPERIMENTS

M.C. Lee
MEGATEK Corp., San Diego, CA. 92106

Ion line enhancement at 45° detected at Arecibo Ionospheric Observatory by 430 Mhz radar (T. Hagfors and C.J. Zamlutti, AGARD, No. 138, 5-1, 1973) is interpreted to result from the nonlinear coupling of weak plasma waves via ponderomotive force. Those weak plasma waves originate in the scattering of the O-mode heater wave and of the unstable plasma waves from the thermal ion acoustic waves. Weak plasma lines observed at Arecibo have been quite successfully reproduced in calculation by means of those weak plasma waves (J.A. Fejer and Y.Y. Kuo, Phys. Fluids, 16, 1490, 1973; F.W. Perkins et al., J. Geophys. Res., 79, 1478, 1974). Theoretical analyses show that those enhanced density irregularities associated with ion lines are forced ion acoustic modes whose frequencies, determined by the beat frequencies of plasma waves, are not necessarily their characteristic frequencies. It is expected that much stronger ion lines can be detected if the backscatter radar of lower frequencies (in the range of HF or VHF frequencies) is employed.

G1-3 PARAMETRIC EXCITATION IN SPORADIC E:
0920 F.T. Djuth, Dept. of Space Physics and Astronomy, Rice University, Houston, TX 77001

The diagnostic incoherent scatter radar at Arecibo, Puerto Rico has been used to study the interaction of a powerful HF radio wave in sporadic E. An extended series of observations indicate that the oscillating two-stream instability is the dominant instability mechanism responsible for observed enhancements in the ion and electron components of the incoherent scatter spectrum. Enhancements were detected only when the sporadic E blanketing frequency exceeded the HF pump frequency. In general, the results are consistent with existing parametric instability theory for excitation in a collisionally dominated plasma containing steep electron density gradients in the vertical direction. However, the development of the oscillating two-stream instability is readily understandable only if the sporadic E plasma exhibits large horizontal gradients. It is likely that the parametric interactions occur in a patchy plasma containing irregularities with scale sizes considerably less than 300 m.

G1-4 RADAR OBSERVATIONS OF THE HEATED IONOSPHERE
0945 OVER ARECIBO, PUERTO RICO: W.L. Ecklund, D.A. Carter, and B.B. Balsley, Aeronomy Laboratory, National Oceanic and Atmospheric Administration, Boulder, CO 80303

A portable 50 MHz radar was installed on the island of Guadeloupe in June 1977 to observe effects in the ionosphere generated by radio frequency heating at the Arecibo Observatory. Some of the Arecibo heating experiments were designed to simulate the intense radio beams that would be transmitted to earth from the proposed solar power satellites. Although no effects were observed at Guadeloupe when Arecibo transmitted on frequencies well above the critical frequency of the ionosphere, dramatic effects were observed when the transmitted frequency was below or near the critical frequency. These effects and some of the experimental details will be discussed in this talk.

G1-5
1040 CORRELATION BETWEEN LARGE-SCALE (km) AND SHORT-SCALE (3m) IRREGULARITIES GENERATED DURING AN HF IONOSPHERIC MODIFICATION EXPERIMENT: F. Frey, Dept. of Space Physics and Astronomy, Rice University, Houston, TX 77001; L. M. Duncan, University of California, Los Alamos Scientific Laboratory, Los Alamos, NM 87545

Intense HF radio waves incident on an overdense ionosphere can excite parametric instabilities near the altitude of reflection. In addition, self-focusing of the incident radiation can produce large-scale (~ kilometer) striations of enhanced electric field strength. Parametrically enhanced plasma waves and large-scale striations were observed during a recent HF ionospheric modification experiment at Arecibo using the 430-MHz incoherent backscatter radar. Simultaneous observations were made of short-scale (3 meter) field-aligned plasma irregularities within the heated volume using a 50 MHz radar located on Guadeloupe, looking perpendicular to the magnetic field over Arecibo at an altitude of about 250 km. These short-scale irregularities are thought to be generated as the result of thermal coupling associated with the parametric interactions. A comparison of the observations from Arecibo and Guadeloupe will be presented. The significance of detected correlations also will be discussed.

G1-6 1105 WAVE INTERACTION EFFECTS DURING HIGH POWER HEATING:

A. A. Tomko, A. J. Ferraro and H. S. Lee
The Ionosphere Research Laboratory, The Pennsylvania State University, University Park, PA 16802

Experimental techniques for monitoring D-region modifications during high power continuous wave heating of the ionosphere at radio frequencies and during the subsequent return of the plasma to ambient conditions following turn off of the heating transmitter are outlined. A four part experiment employing the wave interaction (or cross modulation) effect is proposed to study the four distinct states of the lower ionosphere during high power heating. These states result from the different time scales required for electron temperature and electron density modifications, and include: an ambient state prior to turn on of the heating transmitter, a state characterized by greatly enhanced electron temperature due to the thermal run away effect, a modified steady state in which the electron density distribution has changed in response to the enhanced electron temperature, and a final state following turn off of the heating transmitter in which the electron temperature has decayed to its ambient level but the electron density remains at some modified level. The first and last state can be monitored using conventional wave interaction techniques (Lee and Ferraro, J. Geophys. Res., 74, 1184-1194, 1969) while the other two states can be studied using the complimentary interaction technique (Sulzer, et. al., J. Geophys. Res., 81, 4754-4756, 1976). Calculations of the magnitude of the interaction effect for heating powers up to 100 MW ERP are presented and the relationship between the interaction effect, electron temperature, electron density and various ion chemistry parameters is discussed.

G1-7
1130 CONTROL OF PARAMETRIC INSTABILITIES IN THE IONOSPHERE THROUGH PUMP MODULATION

L. M. Duncan, University of California, Los Alamos Scientific Laboratory, MS664, Los Alamos, New Mexico 87545

Intense high-frequency electromagnetic waves incident on an overdense ionosphere are known to excite parametric instabilities, generating enhanced electron plasma waves observable by incoherent scatter radar. In a series of experiments at the Arecibo Observatory, control of the parametric interactions has been demonstrated through modulation of the pump radiation. In particular, sinusoidal modulation of the pump wave center frequency has been shown to suppress the parametric interaction by redistributing the pump energy over the sideband frequencies. This has been studied quantitatively by narrowband observations of plasma wave enhancements at the pump center frequency, and qualitatively by wideband measurements of the total signal backscattered from the enhanced oscillations. In addition, multi-pump parametric excitation, mathematically equivalent to amplitude modulation of a single pump wave, has been shown to increase the intensity of the parametric wave-plasma interaction by lowering the instability threshold when the frequency separation of the discrete pump waves is a multiple of the local ion-acoustic frequency. The motivation for control of parametric instabilities will be discussed in its application to underdense ionospheric heating experiments, solar-power-satellite ionosphere/microwave interaction studies, and laser fusion research.

Commission J Session 1

RADAR ASTRONOMY
Tuesday Morning, 7 Nov., UMC 157
Chairman: T. W. Thompson, Planetary Science Institute, Pasadena, CA 91101

J1-1
0830 POLARIZATION PROPERTIES OF RADAR-ASTRONOMICAL TARGETS IN THE OUTER SOLAR SYSTEM:

S. Ostro, G.H. Pettengill
Massachusetts Institute of Technology, Cambridge, MA 02139

Polarization properties of radar targets in the outer solar system differ considerably from those of the inner planets and the moon. Radar observations undertaken from 1976-1978, have been used to place constraints on the structure of Saturn's rings and the outer three Gallilean satellites. Measurements of the ratio μ of the echo power received in the same circular sense as transmitted to that received in the orthogonal sense, yield values averaging 1.4 for Europa, Ganymede and Callisto. (All astronomical targets previously studied by radar have $\mu \ll 1$.) Ostro and Pettengill (Icarus 34, 1978) have proposed a model which can explain this unusual polarization behavior in terms of double-reflection backscatter from nearly hemispherical icy craters. Observations (Ostro and Pettengill, in preparation, 1979) of Saturn's rings made in 1977-78 have yielded $\mu \tilde{\approx} 0.4$. A multiply-scattered component of the echo should have $\mu \approx 1$. Although the single-particle scattering properties of irregular particles are poorly known, available data indicates that $\mu \sim 0.4$ is a reasonable value for large particles. The backscattered echo from perfectly smooth spheres or very small particles would have $\mu \approx 0$. The results for Saturn's rings certainly suggest the importance of single scattering in the 12.6 cm echo, and can be interpreted in terms of either a monolayer of large, irregular particles or a many-particle-thick layer of particles with extremely low single-scattering polarization ratios.

J1-2
0900

3-STATION RADAR IMAGES OF VENUS:

R.F. Jurgens, R.M. Goldstein, R.R. Green,
H.C. Rumsey, Jet Propulsion Laboratory,
Pasadena, CA 91103

The radar images of the surface of Venus acquired during the 1977 inferior conjunction will be shown. These high resolution images extend the coverage south of the equatorial region. The maps shown have been made from a new procedure employing three simultaneous receiving stations. The solution of the north-south ambiguity has been accomplished by a new algorithm based on an n-station maximum-likelihood estimator. Using this procedure, both reflectivities and surface altitudes can be measured.

J1-3
0930

A NEW DETERMINATION OF THE AXIAL ROTATION OF VENUS.

S. Zohar, R. M. Goldstein, H. C. Rumsey
Jet Propulsion Laboratory
4800 Oak Grove Drive, Pasadena, CA. 91103

In the study of the surface of Venus by the methods of radar astronomy, several prominent surface features have been discovered. Some of these have been observed by now for over a decade and consistently show up as predicted. When one examines the positions of these features more closely, one observes that they seem to be moving slightly from one inferior conjunction to the next. Analysis shows that any error in the value of the Venus angular velocity vector ($\bar{\omega}$) used in the data processing, will yield an apparent motion of surface features. Obviously, one could exploit this fact to get a more precise $\bar{\omega}$ by perturbing its initial value so as to minimize this apparent motion. The precision attainable with this method will increase with the time interval separating observations of the same feature. It will also improve with a decrease in the size of the features.
An improved $\bar{\omega}$ was obtained by applying these techniques to 3 relatively small features, each of which was observed twice with a 19-month interval between observations. An interesting by-product of this effort is the conclusion that synchronous rotation seems to be ruled out.

J1-4
1030 RADAR STUDIES OF THE NON-SPHERICALLY SYMMETRIC CORONA: S. P. Owocki and G. Newkirk, Jr., High Altitude Observatory, National Center for Atmospheric Research, Boulder, CO 80307, and A. C. Riddle, Department of Astro-Geophysics, University of Colorado, Boulder, CO 80309

The results of radar studies of the sun made at El Campo, Texas from 1964-66 (James 1968, in J. V. Evans and T. Hagfors (eds.), Radar Astronomy, McGraw Hill Book Company, New York) are reviewed in light of recent evidence concerning the geometry of coronal structures. The characteristics of these radar observations are compared with those obtained from ray tracing studies which include the effects of refraction, scattering, and absorption in non-spherically symmetric models of the corona. Particular attention is given to the effect of geometrical focusing by coronal structures on the observed radar cross-section. Finally, the prospects of obtaining radar images of the sun with angular resolution are reviewed and some of the potential benefits of such a study are discussed.

J1-5
1100 MARE CRISIUM: TOPOGRAPHY MEASUREMENTS BY EARTH-BASED RADAR

S.H. Zisk, Haystack Observatory, Westford, Massachusetts 01886

Topographic maps can now be produced for a large fraction of the lunar Earthside hemisphere, using Earth-based radar measurements made several years ago. Small-scale maps of Earth-based Radar Topography (ERT) have been furnished for several geophysical analyses of the lunar surface and of lunar crustal history, although the accuracy of the elevation data has not been determined until now. It is known that the maps have an arbitrary zero-datum level, because of limitations in the lunar ephemeris used to obtain and process the radar data. An accurate datum level can now be added to some of the maps, however, and also an independent test made of their accuracy, by referring to the series of Lunar Topo-Orthophoto maps now being generated from the lunar-orbiting Mapping Camera data of the Apollo program.

An ERT map has been prepared of the Mare Crisium area near the eastern limb of the moon. Several interesting features of the Mare floor are shown as well as other patches of quasi-mare surface in the neighborhood of Crisium. These suggest a sequence of tectonic and lava-flooding events that contributed to the appearance and physical conditions of the present surface.

Finally, a detailed comparison between the ERT and Apollo topography maps is presented. This shows a deviation of less than 100 m rms between the two independently-derived maps, including one area of monotonic difference near the edge of the Apollo map which is probably a result of Apollo data limitations.

J1-6
1130

MODULATION OF LUNAR RADAR ECHOES BY SURFACE CHEMICAL COMPOSITION: T. W. Thompson, Planetary Science Institute, Pasadena, CA 91101

During the last few years, several multi-wavelength studies have indicated that radar backscatter is modulated by lunar surface chemical composition. Measurement of the electrical and optical properties of Apollo samples by Gold et al. (1976) showed that higher iron and titanium contents produce higher losses which absorb echoes from near surface rocks. A study of Mare Serenitatis by Thompson et al. (1973) identified five surface types where radar echo strength was correlated with surface composition. Schaber et al. (1975) showed that the earth-based 3.8cm and 70cm radar echoes from Mare Imbrium decrease in relationship to the color and age of mare units. Furthermore, Schaber et al. (1973) suggest that the reduction of radar backscatter from red to blue mare surfaces can be attributed to increased tiatnium and iron contents from ilmenite (FeT_iO_3). Pieters et al. (1973) showed that low 3.8cm radar echo strength associated with low optical albedos and distinct optical spectral types form a distinct lunar surface type, a mantle of ash or cinder with high iron and titanium contents. This distinct surface type is found at the Sulpicius Gallus formation and at the Apollo 17 Landing site. A study of the Aristarchus Plateau by Zisk et al. (1977) indicated that the Aristarchus Plateau is probably mantled up to depths of 50 to 300 meters by a pyro-clastic material, which resembles the orange glass beads found at Shorty crater during the Apollo 17 mission. All of these studies indicate that differing iron and/or titanium contents are reasonable causes for differences in radar backscatter from different lunar surface units.

References

T. Gold, et al, Proc 7th Lunar Sci Conf, 2593-2603, 1976.

C. Pieters, et al, Jour. Geophys. Res., 78, 5867-5875, 1973.

G. G. Shaber, et al, The Moon, 13, 395-423, 1975.

T. W. Thompson, et al, Apollo 17 Prel. Sci. Report Chap 33, 3-10, 1973.

S. H. Zisk, et al, The Moon, 17, 59-99, 1977.

TUESDAY AFTERNOON, 7 NOV., 1330-1700

NONDESTRUCTIVE ELECTROMAGNETIC PROBING AND TESTING
Commission A, Session 2, UMC 158
Chairman: H. E. Bussey, Electromagnetic Fields Division, National Bureau of Standards, Boulder, CO 80303

A2-1 1330 REVIEW OF ELECTROMAGNETIC METHODS IN NON-DESTRUCTIVE TESTING OF WIRE ROPES: J.R. Wait, Cooperative Institute for Research in Environmental Sciences, University of Colorado/NOAA, Boulder, CO 80309

Wire ropes are used extensively in many life sustaining situations. Elevator and mine hoist cables are two notable examples but we might also mention the support cable for aerial tramways, ski chairlifts and gondolas, helicopter and suspension cables. In this review, we will deal mainly with wire ropes used in mine hoists but the results are also relevant to testing support cables for ski lifts. There is an obvious need to perform tests of the integrity of such ropes without in any way impairing their function. Apart from careful visual examination and measurements of the external diameter, the non-destructive test methods available utilize electromagnetic fields, x-rays or mechanical waves. Here we will review progress in the electromagnetic methods.
The early history of the subject will be described briefly since this provides a remarkably good introduction to the working principles. We will then progress quickly in time up to the currently used techniques and operating procedures. Next we drop back in time to summarize some of the basic papers that deal with the basic concepts and the techniques for dealing with the testing of cylindrical conductors by both electric and magnetic methods. At this juncture, we call attention to the extensive related work on electromagnetic probing of geophysical targets such as ore bodies and other sub-surface conductors. Finally, we turn to the various investigations, primarily of a theoretical nature, that have been carried out; we include here the most recent work.

A2-2 1355 A NOVEL TIME-DOMAIN INVERSION TECHNIQUE FOR DIELECTRIC PROFILING: Wolfgang A. Bereuter, Kaman Sciences Corp., Colorado Springs, and David C. Chang, Electromagnetics Laboratory, University of Colorado, Boulder, CO 80309

Within the framework of easily implementable inversion methods the possibilities of pulse techniques were investigated. Recognizing that the first Piccard approximation for the reflection coefficient of an inhomogeneous profile possesses the form of a Fourier Transform, it is natural to develop the inversion in the time domain. One then discovers that the inversion equation for the profile can be expressed in closed form for many sensing pulse shapes of practical interest. For instance, for double exponential sensing pulses, $\exp(-\tau t) - \exp(-\tau_o t)$, the profile is given in terms of the measured response $\Gamma_p(t)$ as follows:

$$-\frac{1}{2}\ell n\frac{n(\alpha)}{n(o)} = \frac{1}{\tau_o-\tau}\left[\frac{d}{dt}\Gamma_p(t) + (\tau+\tau_o)\Gamma_p(t) + \tau\tau_o\int_o^t \Gamma_p(t')dt\right]_{t=2\alpha/c}$$

and where α is the optical length.
The limitation of the method is determined by the only approximation employed in its derivation, namely that $|\Gamma^2(\omega)| \ll 1$ inside the medium. In general, this implies that the profile must be slowly varying; however, by tailoring the spectral content of the sensing pulse shape, this can be relaxed, so that the method is quite versatile. The feasibility of extending this technique to dispersive media is also discussed.

A2-3 1445 MICROWAVE MEASUREMENTS OF SNOW STRATIGRAPHY AND WATER EQUIVALENCE, H.S. Boyne and D.A. Ellerbruch, Electromagnetic Fields Division, National Bureau of Standards, Boulder, CO 80303

This paper reports on a study of electromagnetic surface and subsurface scattering properties of snow using an FM-CW radar system operating in the frequency range 8 - 12 GHz. The scattering properties are interpreted and compared with the measured physical properties of snow such as density, stratigraphy, hardness and equivalent moisture content.
The electromagnetic scattering properties are measured in situ under natural environmental conditions and the physical analysis is done at each test site to correlate the physical properties of the sample with its electromagnetic signature. Application of this technique to the determination of water equivalence and avalanche hazard warning are discussed.

A2-4
1510

ELECTRICAL CHARACTERISTICS OF CORN, WHEAT AND SOYA IN THE 1-200 MHz RANGE:

R.N Jones, H.E. Bussey, W.E. Little, R.F. Metzker, Electromagnetic Fields Division, National Bureau of Standards, Boulder, CO 80303

In marketing, handling and processing grain, various measurements are made to determine grain quality. One important characteristic is moisture content and it is frequently determined by electrical capacitance-type moisture meters. To improve the accuracy of such measurements, additional information is needed about the dielectric properties.
A set of coaxial sample holders together with a measurement and data reduction technique has been developed and applied to the study of the dielectric properties ($\varepsilon^*=\varepsilon'-j\varepsilon''$) of wheat, corn, and soya over the 1 to 200 MHz range. Particular attention was given to the behavior of the dielectric properties as a function of percent moisture content, frequency, and packing density. Data was also taken to evaluate the dependence of dielectric properties on temperature and sample holder configuration. Some study was also devoted to the correlation between dielectric constant (ε'), loss factor ($\frac{\varepsilon}{\varepsilon'}$), and percent moisture content. Particular emphasis eas devoted to a study of high moisture corn (up to 40%).

A2-5
1535 DETERMINATION OF ELECTROMAGNETIC PROPERTIES OF MATERIALS BY HIGH RESOLUTION SENSING TECHNIQUES:

R. L. Jesch, Electromagnetic Fields Division,
National Bureau of Standards, Boulder, CO 80303

The National Bureau of Standards (NBS) is heavily involved in a number of projects in electromagnetic probing and nondestructive evaluation techniques that are pertinent in determining the electromagnetic scattering properties of soil, coal, snow, and slope-stability studies. NBS has been quite successful in using a remote sensing microwave measurement system to take measurements, as a function of frequency, in-situ under natural environmental conditions and obtain results that have a direct correlation to such physical measures as; density, moisture level content and subsurface physical strata.

Experimental results will be given for selected samples of data for soil which were obtained from measurements taken at several field sites under natural conditions. After taking the electromagnetic measurements, each test site was carefully characterized by digging a pit to visually inspect the subsurface and collect soil samples for measures of density and moisture content. Selected soil samples were also gathered from the test sites and measured in the laboratory to substantiate field results. Each sample was initially oven dried to remove all moisture. Then moisture was added to the dry weight sample to achieve a prescribed moisture content for measurement pruposes. The samples were then placed in special coaxial sample holders for the electromagnetic measurement.

EARTH EFFECTS AND SOMMERFELD INTEGRAL
Tuesday Afternoon, 7 Nov., UMC West Ballroom
Chairman: J. R. Wait, CIRES/University of Colorado, Boulder, CO 80309

B4-1
1330 QUASI-STATIC IMAGE THEORY FOR TRANSIENT FIELDS OF SOURCES OVER THE EARTH'S SURFACE: K. Tsubota, Geophysics Dept., Colorado School of Mines, Golden, CO 80401

Since the image representation of the quasi-static fields of a line current source and a vertical magnetic source was developed analytically by Wait (Elec. Lett., 5, 281-282, 1969) and Wait and Spies (Can. J. Phys., 47, 2731-2733, 1969), it has been applied to many geophysical problems involving the induced currents in the earth. The image theory, in which the presence of a conducting medium is replaced by the image of the external source located at some complex depth beneath the earth's surface, is valid when the distance between the source and the observer is *greater* than the "skin depth", δ. It is shown, in this presentation, that the image technique is also applicable to transient fields in early time regions.
The analytical expressions of the transient fields were derived for pulse type excitation for the configurations such that both the source and the observer are located on the uniform earth and they are compared with the exact forms of previous authors (e.g. J.R. Wait and D.A. Hill, IEEE Trans., AP-22, 145-146, 1974). For those configurations, where the analytical forms in the time domain are not possible, two different methods were used to evaluate the inverse Laplace transform. One is an expansion method into both integer s^{-n} and fractional $s^{-(n+\frac{1}{2})}$ power series and each term is then transformed by a known pair. The coefficients of each term were found in the least square sense by the digital computer. The other method uses the numerical inverse Fourier transform by means of digital convolution filter which was also used to evaluate the exact transient fields to be compared. The validity check was also extended to two and three layer earth models.
The results show that the image theory is useful also in the time domain especially when the source is raised above the earth's surface.

B4-2
1345 TRANSIENT FIELDS OF A VERTICAL MAGNETIC DIPOLE ON A TWO-LAYERED EARTH: S. F. Mahmoud and A. Z. Botros, Electrical Engineering Department, Cairo University, Giza, Egypt

A time domain solution for the fields of a small vertical magnetic dipole on a two-layered earth is obtained in closed form expressions. The displacement currents in the earth are neglected, but those in the air region are accounted for, hence the solution is valid at later times than the relaxation time in the ground. Two different approaches have been used to solve the problem. In the first, the fields in the frequency domain are obtained as a sum of contributions from waveguide modes and appropriate branch cuts in the complex plane of the longitudinal spatial wavenumber. The inverse Laplace transform is then applied to convert the solution to the time domain. In the second approach the natural frequency concept is used, hence, natural guided modes in the earth are identified by a set of complex frequencies which are characteristics of the earth's model alone.
In an earlier work (Botros and Mahmoud, Radio Science, March, 1978) an approximate solution to the same problem based on a quasistatic approach (Wait, Can. J. Phys., 50, 1055 - 1061, 1972) has been derived. It is demonstrated here that this solution is the late time part of the present more rigorous one. Numerical examples show that the waveguide mode contribution is significant at relatively early times and intermediate values of the separation between the source and receiver loops. Remote sensing considerations are discussed.

B4-3
1400

CURRENT INDUCED ON AN INFINITE HORIZONTAL WIRE NEAR THE EARTH BY A DISTANT VED LOCATED ON THE EARTH'S SURFACE:

R. G. Olsen, A. M. Aburwein
Department of Electrical Engineering
Washington State University
Pullman, WA 99164

Recently the formal solution to the problem of exciting a thin infinite horizontal wire by a vertical electric dipole (VED) has been reported (J.R. Wait, AEU, 31, 121-127, 1977). In addition to the exact solution an expression for the wire current which is valid when the VED is electrically close to the wire is given. An extensive numerical study of that case has recently been completed (A. Hoorfar, E.F. Keuster, D.C. Chang, Univ. Colo. Electromagnetics Report No. 31). A simple expression for the wire current in the case for which the VED is electrically far from the wire and the earth has recently been presented (R.G. Olsen, M.A. Usta, IEEE Trans., AP-25, 560-565, 1977). In that work the wave incident on the wire from the VED is assumed to be a plane wave and its reflection.

In this work the VED is assumed to be on the earths' surface and electrically far from the wire. The wave incident on the wire from the VED is assumed to be a ground wave. This case has important application for calculating distortions in VLF navigation signals caused by transmission lines and in computing induced currents on transmission lines due to cloud to ground lightning discharges. A simple closed form expression for the current has been found and will be presented along with a discussion of the approximations leading to it. Results based on this expression will be discussed.

B4-4
1415

TRANSMISSION LINE PARAMETERS FOR A THIN, INFINITELY-LONG WIRE EMBEDDED IN AN INTERFACE:*

James N. Brittingham, Lawrence Livermore Laboratory, University of California, Livermore, California 94550

In the past J. Wait ("Theory of Wave Propagation Along a Thin Wire Parallel to an Interface," Radio Science, Volume 7, Number 6, pp. 675-679, June 1972) developed a procedure to find the transmission line parameters for a thin, infinitely-long wire over a lossy half-space. He presented integral equations for the propagation constant down the thin wire along with integral representations for the series impedance and parallel admittance. Wait did not present any numerical results. In the present paper Wait's procedure will be applied to a wire embedded in the interface. The difficulty with using this procedure to obtain numerical results is that there are two Sommerfeld's integrals which must be evaluated numerically.

To prevent the necessity of numerically integrating these Sommerfeld's integrals a procedure, developed previously (J. N. Brittingham, "A New Series Solution for the Electric Fields from a Long, Thin Wire on an Interface," A.P.S. International Symposium, Stanford, California, June 20-22, 1977, pp. 162-165), will be used to evaluate the integrals. It consists of finding a series representation for the integrals. These series are developed by expanding the integrand in a Taylor's series and then interchanging the integration and summation. The new series is expressible in Hankel functions and is absolutely convergent. Because of the special nature of the series only the first two terms of the series are needed to accurately represent the integrals for thin wires. The new series representation is then substituted into the equation for the propagation constant.

A parameter study of the propagation constant for a thin wire on the interface was performed by using the new series approximation. These numerical results appear to have the correct physical behavior, which further demonstrate the accuracy of using the new series approximation for the Sommerfeld's integrals.

*Work performed under the auspices of the U.S. Department of Energy by the Lawrence Livermore Laboratory under contract number W-7405-ENG-48.

B4-5
1430 ON VERTICAL LOOP ANTENNAS ABOVE A FINITELY CONDUCTING GROUND: Ahmed S. Abulkassem and David C. Chang, Electromagnetics Laboratory, University of Colorado, Boulder, CO 80309

Performance of a loop antenna above a finitely conducting fround is of importance in geophysical probing, communication in mine tunnels and direction finding. Characteristics of a horizontal antenna were reported earlier by us (IEEE Trans. Ant. Prop., APS-21, 1973). In this work, the case of a vertical loop antenna is considered. An integral equation for current on the loop was derived taking the effect of the finite conductivity of the ground into account and Fourier series expansion was used, The moment functions are in terms of various Sommerfeld integrals integrating over the source and the observation angles θ' and θ. These triple integrals can be reduced to double integrals via the integral representation of the Bessel function, and were computed numerically using a double Gaussian Legendre scheme. It can be shown that numerical results obtained from this scheme agree with the special case of an isolated antenna as well as when the antenna is located above a perfectly conducting ground. For a loop of fixed height about a finite conducting ground, our result shows that as the frequency decreases, the input conductance decreases as expected like $(kb)^4$ where b is the radius of the loop. The input susceptance on the other hand is capacitive initially, but becomes increasingly inductive as the frequency goes down. In addition, proximity effect of the ground is pronounced only in the case when loop is near resonance, much like the case of two coplanar loop antennas.

B4-6
1505

AN EFFICIENT PROCEDURE FOR MODELING ANTENNAS OVER LOSSY HALF-SPACES:*

J. N. Brittingham, E. K. Miller,
J. T. Okada and G. J. Burke,
Lawrence Livermore Laboratory,
University of California, Livermore,
California 94550

In the study of practical antennas over lossy air-earth interfaces one needs to evaluate the Sommerfeld's integrals numerous times. In the past the time required to evaluate the Sommerfeld's integrals has been the limiting factor in the study of large antennas. This paper presents a numerical moment-method code that models thin wire antennas over lossy half-spaces which contains an improved method for evaluating the Sommerfeld's integrals. The key to this improved method is the realization that all the interaction between all points on any antenna over an interface can be modeled as a two-dimensional space. These two-dimensional representations are called the solution spaces.

When the separation between the field-point-source-point in the solution space is greater than 1.0 λ we use asymptotic series to evaluate the Sommerfeld's integrals. When the field-source-point distances are less than 1.0 λ and greater than .01 λ we use a previously presented bivariate interpolation procedure (J. N. Brittingham, E. K. Miller, and J. T. Okada, "Bivariate Interpolation Approach For Efficiently and Accuratley Modeling Antenna Near a Half-Space," Electronics Letters, Volume 13, pp. 690-691, 1977). This procedure uses a linear bivariate interpolation to find values of the Sommerfeld's integrals on a sparsely-spaced, prestored two-dimensional grid. The bivariate interpolation procedure is 1000 times faster than the numerical integration of the integrals. For field-source-point distances less than .01 we use a new series solution for the Sommerfeld's integrals (J. N. Brittingham and J. T. Okada, "A New Series Solution For Sommerfeld Integrals in a Two Media Problem," USNC/URSI Meeting 9-13 January 1978, p. 151). This new series solution is 10 times faster than numerically integrating the integrals.

*This work was funded by the U.S. Army Communication Electronic Installation Agency, Fort Huachuca, Arizona and performed under the auspices of the U.S. Department of Energy by the Lawrence Livermore Laboratory under contract number W-7405-ENG-48.

B4-7
1525

ANALYSIS OF ARBITRARILY ORIENTED THIN-WIRE ANTENNA STRUCTURES OVER A PLANE IMPERFECT GROUND

Tapan Kumar Sarkar, Department of Electrical Engineering, Rochester Institute of Technology, Rochester, New York 14623

Existing user-oriented computer programs (AP-23, p. 749, 1975; AP-24, pp. 907-908, 1976; AP-24, p. 546, 1976)* utilize reflection coefficient method to analyze thin-wire structures over a plane imperfect ground. When certain conditions are met by the antenna geometry excellent results may be obtained by the reflection coefficient method (SR-9, Dec. 1975)*. So to treat antennas near imperfect ground plane an exact formulation is made use of involving the well-known Sommerfeld integrals. User-oriented computer programs exist to treat vertical wire antennas touching the ground plane (AP-24, pp. 544-545, 1976)* and horizontal wire structures above a height of 0.03λ from the ground plane (AP-24, pp. 545-546, 1976)*. Under these restricted conditions arbitrary wire-configurations may also be analyzed using the Sommerfeld formulation (Electron. Lett., p. 462, 1976)*.

Presently efforts are being made for efficient calculation of Sommerfeld integrals for $z \leq 0.03\lambda$ and for different values of ρ. A bivariate interpolation scheme along with a series solution is being used at LLL. We are in the process of development of a scheme which would use the Gaussian and the Gaussian Laguerre quadrature formulas for evaluating the Sommerfeld integrals for $z \leq 0.03\lambda$ and for any values of ρ. It is too early to present data about the rate of convergence of this new approach, even though the initial results look too good to be true.

(* The user-oriented computer programs are available from the author).

B4-8
1545

SOLVING THE CURRENT ELEMENT PROBLEM OVER LOSSY HALF-SPACE WITHOUT SOMMERFELD INTEGRATIONS:

P. Parhami and R. Mittra, University of Illinois, Urbana, Illinois 61801; and Y. Rahmat-Samii, NASA/JPL, Cal. Inst. of Technology, Pasadena, California 91101

Repeated evaluation of the Sommerfeld integrals is required in the analysis and systematic design of antennas radiating over lossy half-space. Since the conventional evaluation of these integrals is an extremely time-consuming process, much attention has been devoted in recent years to developing techniques that can evaluate these integrals efficiently without unduly sacrificing the accuracy. The well-known reflection coefficient method (RCM) provides an extremely rapid means of computing the Sommerfeld integrals and yields the results in a simple, closed form. However, its application is limited to the asymptotic region of large kr, where k is the free-space wave number and r is the distance between the image and the observation points.

In this paper, we begin with the two-dimensional Fourier transform representation of the vector potentials instead of the conventional one-dimensional Sommerfeld integrals involving Bessel functions. These expressions are modified such that their inverse transforms can be obtained using a set of well-known identities. The approximation used in modifying the expressions for the vector potentials is valid for a wide range of kr and ground parameters of practical interest, as has been verified by Kuo and Mei (Radio Science, vol. 13, pp. 407-415, May-June, 1978). The above authors have presented a technique for numerically integrating the approximated forms of the vector potential integrals in an efficient manner. We show that under the same approximation, the vector potentials can be expressed in closed-forms, enabling one to evaluate the fields radiated by current elements over a half-space at speeds comparable to the RCM method.

B4-9
1610 PANEL DISCUSSION. Moderator: J.R. Wait, CIRES/University of Colorado, Boulder, CO 80309

Members: Y. Rahmat-Samii, Jet Propulsion Lab, Pasadena, CA 91103; E.F. Kuester, Electromagnetics Lab, Dept. of Electrical Engineering, University of Colorado, Boulder, CO 80309; James N. Brittingham, Lawrence Livermore Labs, Livermore, CA; Tappan Sarkar, Rochester Institute of Technology, Rochester, NY; and R.G. Olsen, Washington State University, Pullman, WA

Commission C Session 3

SATELLITE COMMUNICATIONS
Tuesday Afternoon, 7 Nov., UMC 156
Chairman: H. Kobayashi, IBM Research, P.O. Box 218, Yorktown Heights, NY 10598

C3-1
1330 SATELLITE CONNECTIVITY--DOWN TO EARTH LIMITS ON SPACE COMMUNICATIONS FOR THE 1980s:

Norman Abramson, The ALOHA System, University of Hawaii, Honolulu, HI 96822

Technological progress during the first decade of communications satellites has been centered primarily on the development of high capacity, high reliability point-to-point satellite channels. Thus most satellite communication systems in operation today require large multiplexing systems, microwave land links and costly switching systems to distribute data out of the earth station to the end user. The use of the small, customer-located earth station can eliminate the need for such equipment. But the network composed of large numbers of small stations requires a cost effective solution to the problem of earth station connectivity--how to distribute satellite capacity dynamically among large numbers of earth stations with rapidly varying traffic demands to and from varying destinations.

For networks composed of up to about thirty earth stations, a fixed allocation technique such as conventional frequency or time division multiple access (FDMA or TDMA) can provide adequate connectivity. But beyond that number of stations a fixed allocation communications architecture based on point-to-point channels begins to break down. The connectivity problem can be handled for networks of up to around 100 earth stations by allocation of point-to-point channels using a demand assignment multiple access (DAMA) technique such as SPADE in the INTELSAT system, the time division DAMA scheme planned for the SBS network, or the DAMA technique used in PALAPA, the Indonesian satellite network. However, the complexity of any DAMA scheme which operates by assigning point-to-point channels must still grow as the square of the number of stations in the network, and at about 100 earth stations the DAMA complexity and the DAMA cost become incompatible with the economics of the small earth station.

In this talk we provide some initial data on the connectivity limit for the INTELSAT, PALAPA and SBS systems. We then discuss the use of broadcast communication architecture in a satellite data network.

C3-2
1400

ACCESS PROTOCOLS FOR MULTIPLE BEAM COMMUNICATIONS SATELLITES

T.E. Stern
Dept. of Electrical Enginering and Computer Science, Columbia University, New York, New York 10027

New technological developments which are expected to be incorporated into the next generations of communications satellites will change dramatically the structure of future communication systems. Very high capacity systems with satellite-switched spot beams and with some degree of onboard processing capability will be feasible in the near future. The advent of small, inexpensive earth stations, which may be placed directly on the user's premises, and the expected increase in computer traffic will produce a new environment in which these satellites will operate. This paper discusses some new multiple access protocols adapted to satellite systems operating in a packet-switched mode using satellite-switched multiple beams.

We deal with a single satellite having multiple spot beams, each of which comprises a full duplex data link serving a narrow geographical zone, where up-link-to-down-link connections can be made rapidly, on demand. Each zone may contain many small "bursty" data sources each of which is transmitting to a destination in any zone (including its own). The objective of the access protocol is to provide for efficient sharing of the satellite channel; i.e., to reduce packet delays through the system while maintaining high throughput.

Fixed assignment access schemes (e.g. TDMA) are generally inefficient for the type of user population postulated here. Furthermore, random access and reservation schemes such as the ALOHA technique and its variants cannot be directly applied to the multiple beam configuration. The new access methods presented here are designed to operate in the multiple spot beam environment either with or without "intelligence" onboard the satellite. We show that the problem of optimal switching of the spot beams is equivalent to the problem of maximum matchings in bipartite graphs, a fairly complex combinatorial problem when many spot beams are involved. In view of this, some efficient sub-optimal techniques are proposed and their performance characteristics are presented and compared.

C3-3 1430 A PROCESSING SATELLITE TRANSPONDER FOR MULTIPLE ACCESS BY LOW-RATE MOBILE USERS:

Andrew J. Viterbi
Linkabit Corporation, San Diego, California 92121

A digital processing transponder is considered which performs a discrete 2^K -point spectral analysis over a bandwidth W for the received uplink signals and retransmits decisions on which of the 2^K frequencies contain significant energy. The processing transponder is intended for use with low datarate mobile users employing MFSK modulation with cide division multiple access (CDMA) by frequency hopping over the 2^K frequencies in the common bandwidth W. Error control coding minimizes the effect of mutual interference among the intended users. It is shown that the number of users, M, which may simultaneously transmit at data rate R, is as high as (3/8) W/R when the maximum doppler uncertainty-to-bandwidth ratio, D/W, is small and the bit energy-to-noise density, E_b/N_o, is very large. Bit error rate performance is determined for various values of M and K as a function of E_b/N_o and D/W, with results which compare favorably with FDMA and coherent PN/CDMA techniques. The technique described additionally has the major advantage of being far more robust than coherent PN techniques for mobile users, and much easier to acquire and track through large doppler rate motion.

C3-4 1530 PERFORMANCE EVALUATION OF SATELLITE COMMUNICATION SYSTEMS

W. C. Lindsey, University of Southern California, Los Angeles, California
J. K. Omura, University of California, Los Angeles, California

We present new computational techniques for evaluating bit error probabilities and computational cutoff rates for general satellite communication systems with noise and man-made interference signals. These techniques are based on the classical "moment problem" and are generalizations of the Gauss-Quadrature rules for integration. Conventional nonlinear satellite repeaters are compared with demod/remod processing satellites for both coherent MPSK modulation and noncoherent MFSK modulation. Interference on the uplink include intersymbol, co-channel, and CW tones.

C3-5 BANDWIDTH-EFFICIENT MODULATION AND DEMODULATION
1600 FOR SATELLITE COMMUNICATIONS*:

C. W. Niessen, M.I.T. Lincoln Laboratory,
Communications Division, Lexington, MA 02173

ABSTRACT

In digital modulation systems the traditional remedy for dealing with spectral crowding and the resultant adjacent-channel crosstalk has usually been severely filtered forms of standard modulations such as QPSK. The design of such filters is always a tradeoff between the crosstalk and filter-induced intersymbol interference and reduced detectability against Gaussian noise. Under some system constraints (such as linear channels and freedom from power constraints) this approach can yield impressive preformance in terms of bits/sec/Hz. However, new system constraints for satellite communications requiring small, low-powered, single-channel terminals and the use of satellite on-board signal processing place additional requirements on the modulation method. New modulation designs are now available which achieve rapid spectral roll-off by means of transmitter waveform shaping in the time domain, result in constant envelope signals (essential for use with hard-limiting power amplifiers), and have signal-to-noise (SNR) requirements similar to standard modulations. These new formats, their crosstalk and SNR performance, and digitally-implemented structures suitable for satellite on-board demodulation of multiple (FDM) uplinks will be the subject of this presentation.

*This work was sponsored by the Department of the Air Force.

C3-6
1630

PERFORMANCE ANALYSIS OF SINGLE CHANNEL AUTOTRACK SYSTEMS FOR COMMUNICATION SATELLITES: Daniel D. Carpenter, TRW DSSG, Redondo Beach, CA; William C. Lindsey, University of Southern California, Los Angeles, CA

Increasing performance demands and mission complexity for present day communication satellite systems place stringent pointing requirements on the antenna systems. The feed systems are often optimized for communication channel performance. In order to provide an automatic tracking capability error signals can often be provided by a five-horn or a multimode feed system. For satellite applications the use of a single channel autotrack system provides a means of saving space and weight and requires only a single receiver. The autotrack signal can be constructed from a beacon signal, a telemetry and command signal or a data signal.

The optimization of a communication channel produces a low cross-over level which reduces the antenna boresight sensitivity, or a scale factor, below that of a four-horn radar feed. Due to the inherently lower available antenna scale factor the determination of the additional complex gain-phase type scale factors is important to determine overall performance and tradeoffs. These include the receiver and its AGC which processes the autotrack signal and the demodulation process.

The performance analysis is given in terms of additive thermal noise, polarization mismatches, boresight-shifts and trajectory-spiral for several configurations and feed systems. For the noise process the time-dependent Fokker-Planck equation is derived from the dynamical equations which model the autotrack systems. From this equation the moments of the time to the first-passage of the antenna's ℓ dB loss contour are established. In addition, the joint probability density function of the azimuth and elevation tracking errors is established. From this distribution the variance of the pointing error is established as a function of the scale factors for the different configurations.

RADIOOCEANOGRAPHY - RADAR OBSERVATIONS
Tuesday Afternoon, 7 Nov., UMC East Ballroom
Chairman: D. Barrick, NOAA/ERL/WPL, Boulder, CO

F3-1
1330 THE EFFECTS OF SPACE AND TIME RESOLUTION ON THE QUALITY OF SEA-ECHO DOPPLER SPECTRA MEASURED WITH HF SKYWAVE RADAR

T. M. Georges, NOAA, Wave Propagation Laboratory
Boulder, Colorado 80302 and J. W. Maresca, Jr.,
SRI International, Menlo Park, California 94025

Measurements using the SRI Wide-Aperture Research Facility (WARF) HF skywave radar show that the radar's azimuthal beamwidth and integration time determine the quality of skywave (ionospherically propagated) sea-echo Doppler spectra. Using as a quality index the equivalent width of a portion of the Doppler spectrum in the vicinity of the stronger Bragg line, we find a reduction of ionospheric-multipath spectral contamination as beamwidth and integration time decrease. For nominal (3 dB) beamwidths of 1/2, 2 and 4 degrees and 256-sec averaging, the mean equivalent widths of 104 spectra were 0.090, 0.099 and 0.105 Hz, respectively. Experiments using 51-sec integration time gave average widths of 0.061, 0.075 and 0.079 Hz for the same three beamwidths. The additional contamination observed with the larger beamwidths and the longer averaging time is often sufficient to preclude the extraction of ocean wave height from the second-order spectral structure.

A geometrical-optics, rough-surface model of the ionospheric-reflection process explains this beamwidth dependence by relating the number and width of multipath spectral lines to the size, shape and number of "reflective glints" in the ionospheric area illuminated by the radar. The model also predicts a greater dependence of contamination on beamwidth as the integration time is reduced. We use ionospheric measurements made with CW Doppler sounders to estimate the statistical parameters of the rough-surface model and the amount of contamination the model predicts for finite beamwidth and integration time.

Our main conclusion is that the best way to avoid spectral contamination caused by short-term ionospheric motions is to involve the smallest possible spatial and temporal samples of the ionosphere in the radar measurement. Specifically, a successful sea-state radar should have a 3-dB beamwidth of less than 2 degrees and preferably as small as 1/2 degree, and should use coherent integration times shorter than about 100 s.

F3-2
1350

MEASUREMENT OF OCEAN SURFACE CURRENT AND CURRENT SHEAR BY HF BACKSCATTER RADAR: E.C.Ha,G.L.Tyler, and C.C.Teague, Center For Radar Astronomy, Department Of Electrical Engineering, Stanford University,Stanford,CA 94305

First order HF Bragg scatter from ocean waves exhibits peaks near the positive and negative Doppler frequencies $\pm f_B = \pm 0.102 \times \sqrt{f_c}$,as predicted by theory for deep water gravity waves in absence of currents, where f_c is the radar carrier frequency (MHz). The deviation of the peaks from $\pm f_B$ can be interpreted as a Doppler shift which is proportional to the Laplace Transform of the actual current profile with argument equal to four times the radio wavenumber (C.C. Teague, G.L. Tyler, and R.H. Stewart, IEEE Trans. Ant. & Prop., AP-25, No. 1, Jan. 1977).

During the months of August and September of 1977 and January of 1978, a series of HF backscatter experiments was performed at Pescadero on the California coast using the Stanford Four Frequency Radar. Concurrent in-situ measurements of ocean surface drifts were obtained by tracking motions of spar buoys. The radar inferred drifts were in good agreement with the component of the drifts of the buoys along the radar beam. We also found a steady temporal trend in the radar inferred drifts for all the days of the experiments. The variation of the Doppler shift of the Bragg lines as a function of radar carrier frequency is interpreted as indication of a horizontally stratified current field. Our data indicates that vertical gradient of the current field is no more than a few cm/s per meter, supporting the weak current shear assumption required by the perturbation approach used in obtaining the integral relation. Further work to invert the Laplace transform relation is in progress.

F3-3
1410 HF SKYWAVE RADAR MEASUREMENTS OF THE OCEAN WAVE FREQUENCY SPECTRUM: Joseph W. Maresca, Jr., SRI International, Menlo Park, CA, and Thomas M. Georges, NOAA Wave Propagation Laboratory, Boulder, CO

A method is described for computing ocean wave-frequency spectra and significant wave height from sea echo Doppler spectra measured by HF skywave radar. Surface-wave HF radars make such measurements out to about 100 km from shore; coverage out to 3000 km can be obtained with skywave radars by means of ionospheric reflection. To demonstrate this capability, skywave radar measurements of the sea backscatter were made near the National Data Buoy Office (NDBO) data buoy EB20 (41°N, 138°W) during the passage of a cold weather front on June 2, 1977, using the Wide Aperture Research Facility (WARF) skywave radar. The buoy-measured wave height doubled within a six-hour period and remained approximately constant for the next nine hours. The radar estimates of significant wave height and the ocean wave frequency spectrum were compared to those made at EB20. The relative agreement between the radar and buoy estimates of the significant wave height and the wave spectrum are within the reported accuracy of the buoy measurements. The radar estimates of significant wave height were within 0.1 m (4%) of those measured at the buoy.

F3-4
1430 HF SKYWAVE RADAR MEASURED TRACK OF HURRICANE ANITA: Christopher T. Carlson and Joseph W. Maresca, Jr., SRI International, Menlo Park, CA

Hurricane Anita was tracked across the Gulf of Mexico to land from 29 August 1977 to 2 September 1977 by using an HF skywave radar. The radar position estimates were made from California, 3 to 5 times per day, at the SRI-operated Wide Aperture Research Facility (WARF). The storm center was located from the WARF-derived surface wind direction maps. Seventeen independent wind maps were used to develop the WARF-derived track. The track was compared to the official track produced by the National Hurricane Center (NHC), and the relative agreement between the two tracks was 19 km.

F3-5
1510

RELATIONSHIP BETWEEN HURRICANE SURFACE WINDS AND L-BAND RADAR BACKSCATTER FROM THE SEA SURFACE

D.E. Weissman, Dept. of Engineering and Computer Sciences, Hofstra University, Hempstead, New York 11550
D.B. King, Jet Propulsion Laboratory, Pasadena, Calif. 91103
T.W. Thompson, Planetary Science Inst., Science Applications, Inc., Pasadena, Calif. 91101

Observations of the low altitude winds and microwave radar backscatter from a high altitude airborne L-band synthetic aperture radar were conducted (usually under near simultaneous conditions) in Hurricane Gloria on 28 and 30 Sept. 1976. The average radar cross section per unit area (over a few square kilometers on the surface) depends upon both the wind speed and the relative look angle between the radar and the wind direction. Flight paths through the eye and eye wall regions of Hurricane Gloria show that backscattered power from the surface varies with the surface wind speed.

The L-band instrumentation was an adaption of a synthetic aperture imaging radar (SAR) whose primary function was to obtain high resolution images of the large gravity waves generated in the hurricane. The data for this study were obtained by processing imaging radar signals so that the SAR was equivalent to a scatterometer radar. This scatterometer mode continuously monitored the average backscattered power from an area whose dimensions were much larger than the gravity waves, and viewed the surface at an incidence angle of 20^{o}, where the Bragg scattering mechanism controls the amplitude of the return signal.

The radar data to be discussed comes from several straight passes across the eye of the storm. The data were collected as part of a hurricane research program conducted jointly by NOAA and NASA.

F3-6
1530 DETERMINATION OF ELECTROMAGNETIC BIAS AT NADIR FOR 36 GHZ USING THE SURFACE CONTOUR RADAR: Edward J. Walsh, NASA Wallops Flight Center, Wallops Island, VA 23337 and James E. Kenney, Naval Research Laboratory, Washington, DC 20375

The Naval Research Laboratory and the NASA Wallops Flight Center have developed the Surface Contour Radar (SCR), an airborne 8.6 mm bistatic radar designed to measure the directional wave spectra of the ocean. The system produces a real-time false-color coded display of the surface elevations within a swath beneath the aircraft whose width is equal to half the aircraft altitude. The radar is computer controlled and uses an oscillating mirror to sinusoidally scan a pencil beam (0.85° x 1.2°) to interrogate the surface below the aircraft at a rate as high as 10 Hertz within a ± 15° sector perpendicular to the aircraft flight direction. Because the SCR simultaneously measures both surface elevation and relative backscattered power it can establish the magnitude of the electromagnetic bias that exists in the altimeter data. One of the greatest unknowns in terms of altimeter error is that difference between true mean sea level (MSL) and the electromagnetically measured MSL. Yaplee et al. (IEEE Trans. on Geosci. Elec., GE-9, 170-174, 1971) made some observations using an X-band radar mounted on a tower 20 m above the sea surface. They indicated a significant dependence of the relative radar backscatter on the height of the sea surface relative to MSL. It indicated that the electromagnetic centroid would be shifted away from MSL and towards the troughs of the waves. Yaplee et al.'s data was for SWH values of less than two meters. The SCR can generate the same information as Yaplee et al. did but for much larger wave heights. Data recorded by the SCR for SWH values up to seven meters will be shown to indicate the variation of the electromagnetic bias with sea state.

F3-7
1550 INTERPRETATION OF GEOS-3 SEA ICE REFLECTIVITY MEASUREMENTS: G. S. Brown, Applied Science Associates, Apex, NC 27502

An attempt is made to interpret sea ice reflectivity data acquired with the GEOS-3 radar altimeter in terms of effective surface characteristics. The pulse-to-pulse correlation data and the average return waveforms acquired over extended ice fields are shown to imply a highly anisotropic effective joint slope density function for the surface roughness. For such data, one component of the slope variance is shown to be extremely small, i.e. $\lesssim 10^{-7}$, and, consequently, the surface appears to be corrugated or very gently undulating in one direction. The Fresnel reflection coefficient computed from the altimeter data is shown to be significantly less than the nominal value for ice. This anomaly is attributed to surface inhomogeneity and it is shown how these results can be used to estimate the percentage smooth area of the ice. An optical technique is suggested whereby these results can be checked and verified. The application of these results awaits comparisons with appropriate ground truth data on ice surface characteristics.

F3-8
1610 SURFACE ROUGHNESS SLOPE DENSITY ESTIMATES FOR LOW SEA STATE CONDITIONS: G. S. Brown, Applied Science Associates, Apex, NC 27502

In addition to the sixteen waveform samplers in the GEOS-3 radar altimeter, there exist integrating samplers located at approximately 0.3° and 1° angles of incidence, i.e. the Plateau and Attitude/Specular gates, respectively. For very low surface wind speed conditions where the joint probability density function for the slopes of the surface roughness is very peaked, these two gates can be used to infer the form of the density. For two instances where this condition was observed, it was found that the GEOS-3 altimeter data implied that the joint slope density was closer to a Laplacian form than a Gaussian. A third case, in Lake Superior, did not agree with either of these forms; however, surface homogeneity was suspected to be a major source of error in the data analysis. These results indicate that under conditions of very low surface wind speed, the slopes of the surface roughness may depart rather markedly from the universally assumed Gaussian form. Such departures may be related to the trochoidal nature of small amplitude swell.

F3-9
1630

RECOVERING OCEAN WAVE HEIGHT FROM IONOSPHERICALLY CONTAMINATED SEA-ECHO DOPPLER SPECTRA

Jack Riley and T. M. Georges, NOAA, Wave Propagation Laboratory, Boulder, CO 80302 and
J. W. Maresca, Jr., SRI International, Menlo Park, CA 94025

Ionospheric motions broaden, shift and distort the spectra of sea echoes obtained with HF skywave radars. We have developed a signal-processing strategy for avoiding and minimizing such contamination, so that the weak second-order part of the spectrum can be more frequently recognized and processed for ocean waveheight.
Time series representing sea echoes are first screened to eliminate data that would yield excessively broad spectra. This is accomplished without using a Fourier transform by a simple method that estimates the variance of instantaneous frequency from the time series. This permits rapid scanning of large data quantities and focusing on the highest quality data subsets. We next compute 100-sec FFT's using overlapping time windows and sort further using equivalent spectral width as a quality index. After estimating and removing any ionospheric Doppler shift, we combine 40 or more spectral estimates, normalizing so that the overall spectral variance is minimized within the spectral interval of interest. Our model of multipath contamination predicts that contaminated spectral estimates have a positive bias, which distorts the chi-square distribution predicted for no contamination. We have devised a method of identifying and excluding the biased points from the averaging process. Wave height is computed from the ratio of second-order power to first-order power in the dominant half of the spectrum, using a power law derived empirically from computations with theoretical spectra. Wave heights measured near NOAA buoy EB-20 with the WARF skywave radar fall within 10 percent of buoy-derived values.

IONOSPHERIC BEHAVIOR AND PROPAGATION
Tuesday Afternoon, 7 Nov., UMC Forum Room
Chairman: K. Davies, NOAA/SEL, Boulder, CO

G2-1
1330 ARECIBO IONOSPHERIC MODIFICATION EXPERIMENTS: EFFECTS OF OHMIC HEATING AND PLASMA-INSTABILITY ACCELERATION OF F-REGION ELECTRONS ON THE 630.0 NM and 557.7 NM NIGHTGLOW INTENSITIES

Dwight P. Sipler and Manfred A. Biondi, Department of Physics and Astronomy, University of Pittsburgh, Pittsburgh, PA 15260

A dual-channel, sky-mapping filter photometer has been used to determine changes in the twilight and nightglow OI emission intensities at 630.0 nm and 557.7 nm produced by the heating wave during ionospheric modification experiments (I.M.E.) at Arecibo, Puerto Rico from 1972 to the present. In some cases these observations have been correlated with simultaneous radar backscatter and ionosonde observations of other ionospheric parameters such as electron density n_e and temperature T_e profiles and plasma line altitude. Two distinct effects are observed: (a) a suppression of the $(^1D \rightarrow {}^3P)$ 630.0 nm intensity resulting from reduced production of $O(^1D)$ by dissociative recombination between O_2^+ and e^- when the electron temperature is raised by ohmic heating and (b) an enhancement of the 630.0 nm and very occasionally the $(^1S \rightarrow {}^1D)$ 557.7 nm intensities resulting from impact excitation of O atoms to the ^1D and ^1S states by a small group of electrons accelerated by strong plasma waves generated by the absorption of the rf heating wave. Information derived from these studies includes electron energy gain/loss times, fraction of energetic (> 2 eV) electrons produced by the plasma instability, and quenching rates for the $O(^1D)$ excited state. The large variation in effects produced under similar ionospheric and heating conditions suggests that both the ohmic heating and the plasma instability generation depend critically on the electromagnetic wave-plasma coupling.

G2-2
1350 INCOHERENT SCATTER OBSERVATIONS OF AURORAL ELECTRIC FIELDS OVER $60^{\circ} \leq \Lambda \leq 75^{\circ}$ FROM MILLSTONE HILL:

J. V. Evans, J. M. Holt, R. H. Wand, Lincoln Laboratory, M.I.T., Lexington, Massachusetts 02173

As part of the U.S. plan for ground-based observations during the International Magnetosphere Study (1976-1979), the Millstone Hill radar, Westford, Massachusetts ($\Lambda = 57^{\circ}$) was upgraded by adding a 150' diameter fully steerable antenna. The antenna was moved 50 miles from Hamilton, Massachusetts, where it previously had been used for propagation studies by the Air Force Geophysics Laboratory. The steerable antenna has been connected to the existing UHF radar at Millstone and permits incoherent scatter ionospheric measurements over a wide range of latitudes. Initial use has been to explore the variation with latitude of the auroral and subauroral electric field. It appears that the gross features of the field can be measured over the range $60^{\circ} \leq \Lambda \leq 75^{\circ}$ with a time resolution of about 30 minutes. Results gathered to date clearly indicate the extent of the convection pattern and the changes in the pattern that accompany changes in the properties of the solar wind. It is found that the nighttime electric fields over Millstone are caused by magnetospheric convection rather than neutral air winds (dynamo effects).

G2-3 1410 THE USE OF THREE-DIMENSIONAL RAYTRACING IN ANALYSIS OF PLANETARY RADIO OCCULTATIONS:

Thomas A. Croft, SRI International,
Menlo Park, CA 94025

In December 1978, Pioneer Venus will commence daily radio occultations as it orbits the planet. For each of the first 80 days, an entry and an exit will be observed, although the final days are marked by shallow oblique occultations which will be treated as single events. The overall result will be a close-spaced set of observations spanning a wide range of latitude. To take advantage of this opportunity, a new approach to analysis is being attempted, one which for the first time makes use of the three-dimensional raytracing methods that have been developed for earth ionosphere work in the past decade. Other previous and current occultation analyses make the Bouguer-rule assumption that the refractive index exhibits perfect spherical symmetry. This yields a great increase in computation speed, but limits the applicability of the results. When applied to an oblate planet the old approach required the use of an offset center of symmetry in order to maintain the perfect spherical model that must be assumed in such calculations. The methods being developed for application of the more realistic raytracing will be described. The approach is comparatively difficult and time-consuming, but it is of general applicability regardless of the lateral gradients that may be present in the atmosphere or ionosphere of the planet. The method promises to be of most use when applied in conjunction with the conventional mathematics. Some aspects of the occultation analysis can be adequately treated with spherical symmetry as a basis, yielding the desired results with minimum effort. Other results cannot be derived without the three-dimensional mathematics. Between these extremes, there are several areas where the main applicability of the new computer programs will be to establish the limits of validity of the older methods, limits which are not presently well defined.

G2-4
1430

IONOSPHERIC BACKSCATTER REFLECTIVITIES

W. F. Ring and E. Richards,* Rome Air Development Center, Deputy for Electronic Technology Electromagnetic Sciences Division Hanscom AFB, MA 01731

Reflectivities have been determined using data recorded over a one-month period from a High Frequency radar operated in northern Maine to provide illumination of the auroral zone over a ninety degree sector. Volume backscatter reflectivities have been computed for the frequency range 8-20 MHz, using short range returns (less than 1500 km) to limit the uncertainty of propagation modes. The dependence of the ionospheric clutter reflectivities on height occurrence, observing frequency, geographic location and time of day are described. Both E and F layer reflectivities show a decreasing trend with frequency of the order of 5 dB/MHz in the 8-16 MHz range. In addition, F layer reflectivities consistently exceed E layer values in the 8-20 MHz range by 5 to 15 dB.

*Boston College

G2-5
1530

PROPAGATION OF VLF RADIO WAVES ACROSS THE NORTHERN PART OF THE CONTINENTAL UNITED STATES DURING DISTURBED IONOSPHERIC CONDITIONS

J. A. Ferguson, Naval Ocean Systems Center, EM Propagation Division, San Diego, CA 92152

VLF communications station signal strength measurements made aboard an aircraft flying towards and away from the station at Jim Creek, Washington are shown. These signal strength measurements are modeled using a full wave solution to the earth-ionosphere waveguide. An arbitrarily adjustable ionospheric profile in the full wave calculations allows us to determine the effective D region electron density distribution which applies to the aircraft measurements. Using an exponential electrons only profile our modeling shows that under distrubed conditions, the ionosphere over the northern continental US at night gives a reference height of 76 km which is very little different from that expected during the daytime. Additional measurements are for propagation along a magnetic meridian flying from the NOSC ten frequency sounder in Sentinel, AZ towards Thule, Greenland. Modeling of thes data suggest a latitudinal variation of the ionospheric reference height with the transition from middle to high latitudes beginning at about 55° magnetic latitude. The resulting reference height variation is from 87 km to 76 km over a magnetic latitude range of 4°.

G2-6
1550

EFFECTS OF SPORADIC E ON NIGHTTIME ELF PROPAGATION

R. A. Pappert, Naval Ocean Systems Center, EM Propagation Division, San Diego, CA 92152

Two features of attenuation enhancement at lower ELF ($\lesssim$100 Hz) associated with sporadic E layering will be addressed. First, the influential role played by ions in determining the peak and half width of the attenuation resonance will be stressed. Second, on and off path effects associated with a large patch of sporadic E have been estimated using a simple Kirchhoff-Huygens diffraction model. The patch is approximated by a lumped parameter phase amplitude screen allowed to move along a great circle path normal to the transmitter-receiver great circle path. The results indicate that sporadic E patches with areas on the order of 10^6 km^2, causing phase rate shifts and attenuation rate enhancements consistent with full wave modal evaluations, can account for the 6-8 dB fades observed in connection with 1600 km Wisconsin Test Facility (WTF) transmissions. The results also suggest that such disturbances can be expected to produce 2 to 4 dB fades over paths as long as 10,000 km.

G2-7
1610

VLF BEACON TRANSMISSION FROM THE SPACE SHUTTLE

P. A. Bernhardt, V. S. Sonwalkar, D. L. Carpenter, C. G. Park and R. A. Helliwell
Radioscience Laboratory, Stanford University, Stanford, Ca. 94305

The wave injection facility on board the Space Shuttle may be used to study the effects of the F-region and E-region ionosphere on VLF propagation. The wave injection facility should be designed to produce detectable signals at receiver sites on the ground. Factors affecting this design include (1) transmitter power, (2) transmitter antenna pattern, (3) transmission cone in the ionosphere, (4) attenuation of signals passing through the lower ionosphere, and (5) divergence of VLF rays as they enter the free space below the ionosphere. The received signals should provide information about the propagation characteristics of the ionosphere. Amplitude fluctuations in these signals may be produced by fading caused by multipath and by ground reflections. Changes in signal strength may also be produced by focusing (or defocusing) due to ionospheric irregularities. Doppler frequency shifts can indicate regions of the ionosphere that are not horizontally stratified. In a horizontally stratified medium, only waves with nearly vertical wave normals reach the ground. Since these waves are injected nearly perpendicular to the Shuttle velocity vector, they will have little Doppler shifts. The wave injection experiments may be used to diagnose chemical release experiments flown on the same Shuttle mission.

G2-8
1630 ENERGETIC PARTICLE PRECIPITATION INDUCED BY WAVES INJECTED FROM A VLF TRANSMITTER ON THE SPACE SHUTTLE:

U. S. Inan, T. F. Bell, and R. A. Helliwell,
Radioscience Laboratories, Stanford University, Stanford, Ca., 94305.

The energetic electron flux that is expected to be precipitated by coherent waves injected from a shuttle-borne VLF transmitter is calculated by using a recently developed computer code. The required radiated power levels that are necessary for producing measurable precipitated fluxes as well as stimulated emissions are estimated for various frequencies of operation. The effects of the diurnal variation of the ionosphere and a variable antenna orientation are also considered. Ray-tracing analysis is carried out to determine the range of latitudes from which injected waves will be focused by the plasmapause or by other large scale density structures. It is shown that these regions are very likely places for strong wave-particle interaction to take place.
The ionospheric perturbations produced by the precipitated flux are estimated and threshold values of radiated power for which the resultant perturbations can likely be detected by ground-based instruments are determined.

Commission J Session 2

PANEL DISCUSSION ON TECHNIQUES OF VERY LONG BASE-LINE INTERFEROMETERS

Tuesday Afternoon, 7 Nov., UMC 157

Chairman: A. T. Moffet, Owens Valley Radio Observatory, Caltech, Pasadena, CA 91125

J2-1 1330 ANALOG RECORDING: J.L. Yen, University of Toronto, Toronto, Canada

J2-2 1400 ANALOG SYSTEM CALIBRATIONS: D. Fort, National Research Council, Ottawa, Canada

J2-3 1430 MARK II DIGITAL SYSTEM: M. Ewing, Caltech, Pasadena, CA

J2-4 1530 MARK III DIGITAL SYSTEM: A. Whitney, M.I.T., Cambridge, MA

J2-5 1600 OPTIMAL ARRAY CONFIGURATIONS, T. Legg, National Research Council, Ottawa, Canada

J2-6 1620 OPTIMAL ARRAY CONFIGURATIONS: G. Swenson, University of Illinois, Urbana IL

J2-7 1640 AUTOMATIC OPERATION OF A RADIO TELESCOPE.

G.W. Swenson, Jr., J.C. Webber
Vermilion River Observatory
University of Illinois
Urbana, Illinois 61801

The 37.5-meter telescope of the Vermilion River Observatory operates completely unattended for most of its time in both continuum and spectroscopy modes. Features of the system are described. An appraisal of this experience is made in the context of single-observer VLBI Network operation. (If quality of telephone connections permits, a live demonstration will be conducted.)

GUIDED WAVES
Commission B, Session 5, UMC 158
Chairman: A. Q. Howard, Jr., University of Arizona, Tucson, AZ 85721

B5-1
0830 A GAUGE TEST TO REJECT ANOMOLOUS MODE SOLUTIONS WHEN USING THE SPECTRAL DOMAIN GALERKIN METHOD IN MICROSTRIP PROBLEMS, Chen Chang, L. Wilson Pearson, Department of Electrical Engineering, University of Kentucky, Lexington, KY 40506

The spectral domain application of Galerkin's method, pioneered by Itoh and Mittra, has proven useful in solving for the dispersion relations for the quasi-TEM and higher order modes in microstrip structures.

In this presentation we demonstrate the occurence of anomolous mode solutions using this technique with piecewise constant basis functions in a shielded microstrip structure. These solutions appear feasible physically if one simply observes the (apparent) dispersion curve obtained. They do not satisfy the boundary conditions on the strip, however. Consequentially, their presence in computed data can be highly misleading. An integrated electric field gauge of the degree to which boundary conditions are satisfied by the numerical solutions is found to be useful in rejecting these erroneous data. The results of a study of this gauge are presented. The gauge is useful, too, in judging the relative quality of a given basis set in representing the current distribution for a given higher order mode. Some comparisons of the full-domain basis set used by Itoh and Mittra with a piecewise-constant basis set are presented.

B5-2
0900

INTEGRAL OPERATOR ANALYSIS OF DIELECTRIC OPTICAL WAVEGUIDES--THEORY AND APPLICATION:

D.R. Johnson and D.P. Nyquist, Department of Electrical Engineering and Systems Science, Michigan State University, East Lansing, MI 48824

An integral-operator technique is described as an alternative to the conventional boundary eigenvalue analysis for wave propagation along cladded optical waveguides. The heterogeneous region, i.e., the core, of an optical waveguide is replaced by an equivalent current distribution which maintains a scattered electric field in the otherwise uniform, infinite cladding. Total electric field in the dielectric waveguide consists of this scattered wave superposed upon an impressed excitatory field. A volume electric-field integral equation (EFIE) for the unknown equivalent current (electric field) in the core is formulated. For guided-wave fields having exp $(-j\beta z)$ propagation dependence, this equation is converted to a 2-d EFIE for the $\underline{E}$ field over the guide cross section of arbitrary shape and index profile. When applied to slab waveguides, a 1-d EFIE is obtained, leading to the same characteristic equation for β obtained by conventional methods. Several advantages of the integral-operator analysis for dielectric waveguides are: 1) it is adaptable to core cross sections of arbitrary shape, 2) general core index profiles can be accomodated, and 3) the method leads directly to a theory for waveguide excitation by incident illumination.

B5-3
0930

ON THE AXIS OF PROPAGATION FOR NONUNIFORM TRANSMISSION LINES:

P.A. McGovern, Visiting Scientist, Dept. of Electrical Engineering, University of Colorado, Boulder, CO 80309. Permanent address, Physics Dept., University of Newcastle, NSW 2308, Australia

The choice of centerline for a nonuniform line with an axis of symmetry is clear, but identification of propagation distance along this line in terms of wall currents and fields elsewhere in the line is not so immediately clear. If the transmission line does not have this symmetry, curved two-dimensional tapered plate line being the prototype example, then both the axis and propagation behavior need to be identified. Direct definition on the normals of a previously specified centerline here appears the immediate choice, but this does not necessarily lead to the most economical field solutions nor is it the easiest to determine when only the line conductor profiles are given.

For nonuniform tapered plate and coaxial lines operated in dominant baseband mode, a systematic perturbation analysis (McGovern, MTT-S Symposium Digest, Ottawa 1978, pp. 189-191), separating transverse quasistatic and longitudinal wave behavior allows approximations to be ordered by powers of the taper scale parameter, η. Use of coordinate geometry based on radial arcs yields approximations with the first deviation from constancy on radial sections appearing in $O(\eta 4)$, and exact with a single term for the uniform wedge.

This paper extends the method to treat curved wedges yielding a similar but more complex structure of results, with the first deviation from constancy on arc sections being in $O(\eta 3)$, but directly obtainable from the basic solution at the level of distributed circuit theory. The arc centerline may be obtained from given conductor profiles without solution of a differential equation being necessary, unlike for the normal centerline from which it differs in second order. Rotation about an axis generates a coordinate description well adapted to treating nonuniform coaxial line, with primary emphasis on the propagation region between the conductors.

B5-4
1030

NONUNIFORM LINE TRANSITIONS WITH NONUNIFORM MEDIA: P.A. McGovern, Visiting Scientist, Dept. of Electrical Engineering, University of Colorado, Boulder, CO 80309. Permanent address, Physics Dept., University of Newcastle, NSW 2308, AUSTRALIA

Transitions using nonuniform transmission lines with nonuniform media have been synthesized using field transformation methods by Mo, Papas, and Baum (J. Math. Phys., 14. 479-483, 1973). This paper gives an analysis of some gradual but arbitrary baseband transmission line transitions involving both nonuniform boundaries and a restricted class of nonuniform media, constrained to be constant on transverse coordinate surfaces and varying along the general direction of propagation.

A perturbation expansion technique (McGovern MTT-S Symposium Digest, Ottawa 1978, 189-191) in the length scale parameter of the nonuniformity is extended to the nonuniform medium case. For a nominally transparent situation in lowest order (equivalent to distributed circuit theory) explicit solutions are obtained for the first correction term for both plane and radial transverse geometries in tapered plate and coaxial lines.

The laboratory problem inspiring this analysis is that of making a gradual transition between coaxial lines of the same characteristic impedance but different dielectrics.

B5-5
1100

A NOTE ON THE TRANSVERSE DISTRIBUTIONS OF SURFACE CHARGE DENSITIES ON MULTICONDUCTOR TRANSMISSION LINES

D.V. Giri, F.M. Tesche and S.K. Chang
Science Applications, Inc., P.O. Box 277,
Berkeley, CA 94701

Over the last few years, there has been a revival of interest in the subject of multiconductor transmission lines, partially because of a direct application in the area of nuclear electromagnetic pulse (NEMP). Since NEMP frequency spectrum extends over a wide range (dc to, say, 500 MHz), various procedures that are applicable in certain frequency ranges are required. At high frequencies, a method is available (G.S. Smith, J. Applied Physics, 43, 2196-2203, 1972) for determining the transverse high frequency current distributors for systems of parallel and coplanar conductors. On the other hand, electrostatic systems made of bare, as well as dielectric coated wires immersed in free space have received considerably more attention (e.g., W.T. Weeks, IEEE Trans., MTT-18, No. 1, 35-43, January 1970, and J.C. Clements, et al., IEEE Trans., EMC-17, No. 4, 238-248, November 1975). Typically, the method of moments has been efficiently applied to compute the transverse charge distributions and the capacitive coefficients matrix of multiconductor transmission lines with prescribed *voltages* on each conductor (potential problem).

This paper, however, is concerned with the related problem of finding the transverse charge distributions given the *net charge* on each conductor (charge problem). Similar to the case of the voltage problem, a system of Fredholm integral equations is formulated for the angular distributions of charge. Some fairly standard methods of investigating the kernel singularities, often used at high frequencies, were found useful in this electrostatic problem. By way of an interesting example, we consider a balanced two-wire transmission line for which charge distributions are known in closed form from other methods. For this simple case, very good agreement is seen between the numerical solution of the integral equation and available analytical solutions. The potential problem is more often used since it can also yield the capacitive coefficients matrix as a by-product. It is observed, however, that in a realistic situation, where the potentials are prescribed and the elements of capacitive coefficients matrix have been experimentally measured, the present formulation provides an alternate way of evaluating the charge densities accounting for the proximity effects.

SCATTERING-II
Wednesday Morning, 8 Nov., UMC West Ballroom
Chairman: R.M. Bevensee, Lawrence Livermore Lab, Livermore, CA 94550

B6-1
0830 Scattering By Inhomogeneous Dielectric Bodies of Revolution-A First Order Solution: T. K. Wu and D. R. Wilton, Electrical Engineering Department University, Mississippi 38677

The scattering by inhomogeneous lossy dielectric body is an area of current concern. The exact analysis of this scattering problem usually requires tedious analytic formulation and awesome computer programming work. Practically, however, a simple approximation can adequately provide a solution to that problem. In this paper, an Approximate Integral Equation (A.I.E.) method is employed to obtain the first order solution to the scattering problem of a missile with an inhomogeneous plume.
The model consists of a conducting cylinder modeling the missile, with an inhomegeneous lossy dielectric body of revolution trailing behind. The approach here is to derive an approximate integral equation relating the tangential fields at the outer surface of the missile/plume and to model the effect of the plume by an impedance type boundary condition on the fields at the plume surface. The approximate integral equation is then solved by the method of moments. Extensive results are given for the missile skin currents as functions of the frequency and incident angle of the plane wave excitation, in order to determine the effects of the presence of the inhomogeneous plume.

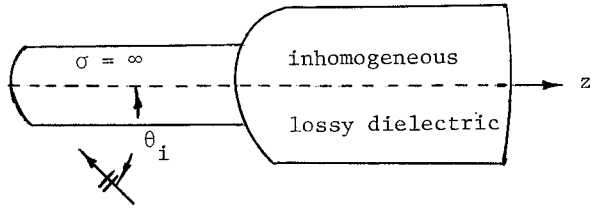

Scattering configuration of a missile/plume.

B6-2
0850

SCATTERING FROM INHOMOGENEOUS DIELECTRIC BODIES OF REVOLUTION

S. Govind and D. R. Wilton, Department of Electrical Engineering, University of Mississippi, University, MS 38677

Recent studies on scattering from inhomogeneous dielectric bodies have adopted the extended boundary condition approach of Waterman. However, this technique, which uses entire domain expansion functions, is not well suited for thin scatterers. Other approaches have made use of the volume equivalence principle, which requires the computation of the three vector components of the polarization current at every point interior to the volume of the scatterer and is therefore often wasteful of computer storage. The use of surface equivalence principle and subdomain type basis functions, on the other hand, generally requires less computer storage than the volume equivalence principle and, at the same time, provides a highly stable numerical algorithm regardless of the scatterer shape. The matix equation obtained by approximating the inhomogeneous body by layers of homogeneous media, would ordinarily tax the memory of even the largest computer. However, it has been noted (R. J. Pogorzelski, IEEE Trans. AP-26, 616-618, 1978) that the matrix is block tridiagonal and hence one can iteratively solve for the equivalent surface currents on successive surface layers, thus reducing the requirement for computer storage. For a scattering problem, the surface currents on the outermost layer are sufficient. If one, however, desires the fields on the inside, a back substitution process can be utilized to obtain the fields on any of the interior surfaces.

Numerical solutions obtained by this procedure have been successfully compared with the Mie series solution for a three-layered dielectric sphere with complex permittivities. The propagation of numerical errors can be estimated by treating a homogeneous body as being modeled by a series of ficticious layers all with the same physical parameters, as the homogeneous body. The results thus obtained show very good agreement with conventional calculations of scattering by homogeneous bodies. Numerical experiments on a three-layered dielectric sphere treated as a five-layered sphere, i.e. with two ficticious layers, have demonstrated the versatality of the computer code. Work is now in progress on an iterative solution for a composite missile/plume configuration, for which the overall impedance matrix is not strictly block tridiagonal. However, through a judicious partitioning of the sub-matrices the overall matrix can again be reduced to a block tridiagonal form, thus permitting the use of the iterative algorithm.

B6-3
0910

FINITE ELEMENT COMPUTATION OF MICROWAVE INDUCED CRANIAL HEATING: M.A. Morgan, Department of Electrical Engineering, University of Mississippi, University, MS 38677

Using an axisymmetric inhomogeneous lossy dielectric model of the human cranial structure, Figure 1, calculations yielding interior microwave fields and absorbed power density spatial distributions are presented. These computations are performed using a finite element computer program, which is based upon the coupled azimuthal potential formulation (M.A. Morgan, et al, *IEEE Trans. on Antennas Propagat.*, vol. AP-25, 413-417, May 1977).

Results are considered for various angles of plane wave incidence, with two orthogonal polarizations, at the frequencies of 1 GHz and 3 GHz. Comparisons are made with an early multilayered spherical model (A.R. Shapiro, et al, *IEEE Trans. Microwave Theory Tech.*, vol. MTT-19, 187-196, Feb. 1971). Attention is given to the sensitivity of spatial positions and intensities of "hot spots", as well as total absorbed power, as functions of incident field orientations and data uncertainties.

FIGURE 1 Axisymmetric Cranial Model

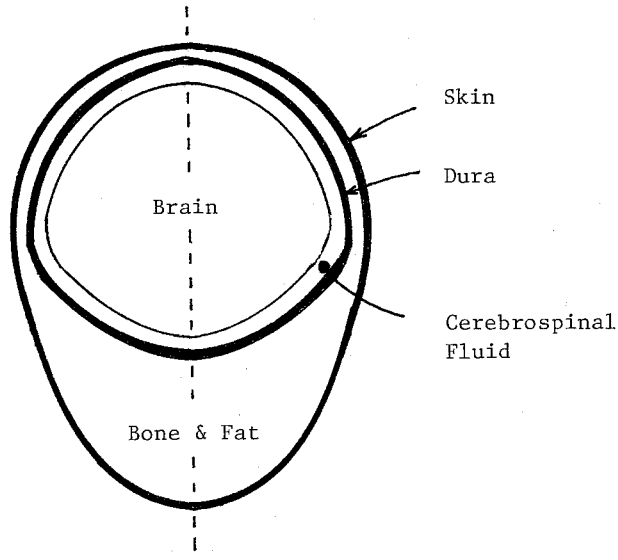

B6-4
0930 NUMERICAL COMPUTATION OF ELECTROMAGNETIC SCATTERING BY TWO BODIES OF REVOLUTION: J.F. Hunka and K.K. Mei, Department of Electrical Engineering and Computer Sciences and Electronics Research Laboratory, University of California, Berkeley, CA 94720

Numerical codes utilizing the unimoment technique (K.K. Mei, IEEE Trans. Ant. & Prop., AP-22, 760-766, Nov. 1974) have been developed which compute the scattering by metal and inhomogeneous dielectric bodies of revolution. The research described in this paper uses these codes to solve the two-body scattering problem. First, interior field solutions (i.e. interior to the unimoment surface) for each scatterer are solved with the unimoment routines and stored in the form of system solution matrices. These matrices contain the "individual isolated scatterer information" for each scatterer and this information need be obtained only once for each scatterer. Second, an iterative scheme is used to solve for the scattering coefficients for each sucessive scattering. Rotation and translation addition theorems are employed to rotate and translate incident and scattered fields between coordinate systems for each scatterer. The iterative scheme has been tested on the special case of two perfectly conducting spheres and has proven to be well behaved and accurate.

B6-5
0950 SURFACE CURRENT AT THE REAR OF A FINITE-LENGTH CYLINDER.

V. V. Liepa, Radiation Laboratory, Department of Electrical and Computer Engineering, The University of Michigan, Ann Arbor, MI 48109

To resolve a controversy about the behavior of the surface fields at the rear of a finite-length cylinder excited by a plane electromagnetic wave at broadside incidence, surface fields were measured as a function of frequency on a number of metallic cylinders with open and closed ends. The measurements cover the range of ka from 0.086 to 1.97 and ℓ/λ from 0.32 to 19.7 and thus span over the so called "thin wire" and "fat cylinder" regimes. The amplitude and phase data are examined in detail at the rear of the cylinder as a function of frequency and for a majority of the cases considered, it is shown that the primary excitation of the currents at the rear of the cylinder is not over the curved surface but rather via the ends. This shows that the current behavior on the infinite cylinder has little bearing on interpretation and understanding of the surface fields at the rear of a finite cylinder. Finally, the experimental data are compared to the results computed using thin wire and patch model computer codes.

B6-6
1030

ANALOGIES OF MULTIPLE SCATTERING PROBLEMS IN ACOUSTIC, ELECTROMAGNETIC AND ELASTIC WAVE FIELDS

V.K.Varadan, V.V.Varadan, V.N.Bringi and
T.A.Seliga, Wave Propagation Group,
The Ohio State University, Columbus,OH 43210

The study of wave propagation and scattering is a classical subject dating back to Rayleigh. The electromagnetic field is generally a transverse field while the acoustic field is a longitudinal one, and both wave fields are characterized by a single wave velocity. In contrast the elastic field admits both longitudinal and transverse waves propagating at two distinct speeds leading to a more complex mathematical problem as well as different physical phenomena like mode conversion. Due to this difference, often well tried methods for electromagnetic and acoustic fields apparently failed for the elastic field. The extended integral equation method or the T - matrix method introduced by Waterman for single scatterers has now been extended by the authors to multiple scattering and works very efficiently for all three wave fields. The paper will focus on the inherent unity in the structure of the three fields. The T - matrix formulation for multiple scattering of waves by a random distribution of arbitrary shaped scatterers will be presented and analogies will be discussed. Numerical results will be presented for the frequency dependent phase velocity and attenuation of electromagnetic and elastic waves in such media will be presented. The results have important applications in many fields like satellite microwave communication links, in studies of the properties of inhomogeneous media, fiber reinforced composite materials, porous media, under water signal transmission etc..

B6-7
1050

BACKSCATTERING FROM RESISTIVE STRIPS

Thomas B. A. Senior, Radiation Laboratory,
The University of Michigan, Ann Arbor,
Michigan 48109

Strips made of a resistive sheet material have lower backscattering cross sections than the corresponding perfectly conducting strips, and this is true in particular when the illumination is edge-on with the electric vector parallel to the edge. Attention is focused on this case. Using the moment method applied to an appropriate integral equation, data are obtained for the surface and backscattered far fields of resistive strips for a variety of strip widths w and uniform resistances R. The front and rear edge contributions to the far field are then extracted. It is shown that for strips whose width is greater than about a half wavelength the former is the same as for a half plane having the same resistance, whereas the latter is proportional to the square of the current at that point on the half plane corresponding to the rear edge of the strip. The implications of these results on the selection of a strip resistance for low backscattering are discussed.

B6-8
1110

THE REFLECTION OF ELECTROMAGNETIC WAVES FROM ALMOST PERIODIC STRUCTURES

D. L. Jaggard, Department of Electrical Engineering, University of Utah, Salt Lake City, Utah 84112.
A. R. Mickelson, Department of Electrical Engineering, California Institute of Technology, Pasadena, California 91125.

Almost periodic structures occur both in nature and in manufactured devices. Structures with almost periodic properties include crystals and fabricated optical devices. In this paper, the problem of electromagnetic reflection from a finite almost periodic slab is treated. The slab is characterized by a spatially varying almost periodic permittivity. Here the reflection characteristics of the almost periodic slab are compared to those of a periodic slab.

Under certain approximations, the two-point boundary-value problem of the figure below can be cast into the form of vector coupled mode equations. These equations are generalizations of the scalar coupled mode equations introduced by J. R. Pierce [*J. Appl. Phys.* 25, 179 (1954)]. The vector technique of invariant imbedding so aptly treated by Bellman and Wing [*An Introduction to Invariant Imbedding*, John Wiley and Sons, New York (1975)] is employed here to convert the boundary-value problem into an initial-value problem. This transformation results in the matrix Riccati equation for the reflection coefficient matrix

$$\underline{\underline{R}}'(z) = i\underline{\underline{\chi}} + i\left[\underline{\underline{\delta}}_F \underline{\underline{R}}(z) + \underline{\underline{R}}(z)\,\underline{\underline{\delta}}_B\right] + i\,\underline{\underline{R}}(z)\,\underline{\underline{\chi}}^{\dagger}\,\underline{\underline{R}}(z)$$

Here the prime signifies differentiation with respect to the coordinate z, the dagger denotes the matrix hermitean transpose. The coupling matrix $\underline{\underline{\chi}}$, and the phase-mismatch matrices $\underline{\underline{\delta}}_F$ and $\underline{\underline{\delta}}_B$ are composed of constants characterizing the medium and are taken from the vector coupled mode equations. The distinction between the periodic and the almost periodic cases is placed in evidence by the possible inequality of the dimensions of the matrix $\underline{\underline{R}}(z)$.

The above equation is amenable to numerical integration. The reflection coefficient R of the slab (see figure) is simply related to the matrix $\underline{\underline{R}}(z)$. Graphical results of R display the similarities and differences between reflection from periodic and almost periodic slabs. The reflection characteristics in some sense mimic the differences found previously in the Brillouin diagrams. Paradoxically, the most periodic slab possesses preferable filter characteristics.

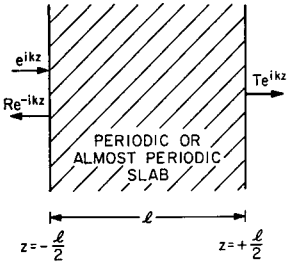

B6-9
1130

ELECTROMAGNETIC WAVE PROPAGATION IN ALMOST PERIODIC MEDIA

A. R. Mickelson, Department of Electrical Engineering, California Institute of Technology, Pasadena, California 91125.
D. L. Jaggard, Department of Electrical Engineering, University of Utah, Salt Lake City, Utah 84112.

In 1923 Harold Bohr found the almost periodic generalization of Fourier series [see e.g., C. R. 177, 737 (1932) or *Almost Periodic Functions*, Chelsea Publishing Company, New York (1962)]. According to Bohr, an almost periodic function is one which can be resolved into "pure vibrations" or tones. Therefore, an almost periodic function f(z) exhibits a spectrum of discrete lines. That is,

$$f(z) = \sum_{M} a_M \exp\left(i \kappa_M z\right)$$

where z is a coordinate, the tones or wave numbers κ_M are real, and the harmonic strengths a_M are complex. For the case when all κ_M's are commensurable, f(z) becomes a periodic function. The term "almost periodic" is often applied in a restricted sense, that is, only when at least two of the κ_M's are incommensurable. This latter definition will be used here. An example of a periodic and an almost periodic function is shown in the figure below.

In this paper we consider electromagnetic wave propagation in an infinite medium which is electrically characterized by a longitudinally varying almost periodic dielectric permittivity. A generalization of Floquet theory is presented which explicitly accounts for the difference between propagation in periodic and almost periodic media. Through the use of dispersion relations and Brillouin diagrams, this difference is clearly placed in evidence and becomes most apparent whenever the tones are closely spaced, i.e., whenever the bandgaps due to individual tones overlap.

We expect that physically measurable quantities will reflect the properties and differences noted in the Brillouin diagrams for periodic and almost periodic media.

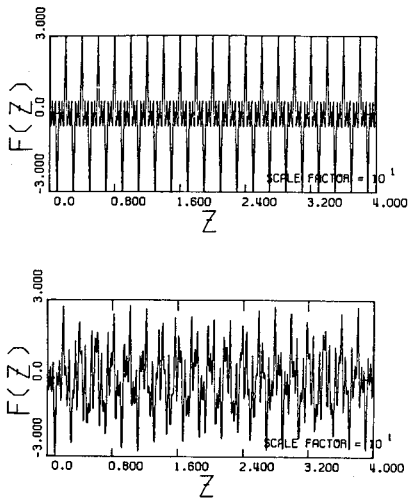

A comparison of a periodic function (a) $f(z) = f_p(z)$ with an almost periodic function (b) $f(z) = f_{Ap}(z)$ where $f_p(z) = \cos[\pi z] + \cos[3\pi z] + \cos[5\pi z]$ and $f_{Ap}(z) = \cos[\pi z] + \cos[3(1.7)\pi z/3^{\frac{1}{2}}] + \cos[(5)3^{\frac{1}{2}}\pi z/1.7]$.

COMMUNICATION THEORY AND SYSTEMS
Wednesday, Nov., 8, UMC 156
Chairman: J. K. Wolf, University of Massachusetts, Amherst, MA

C4-1
0830

APPLICATION OF SPREAD SPECTRUM TO MOBILE COMMUNICATION

G. R. Cooper, School of Electrical Engineering
Purdue University, W. Lafayette, IN 47907

A spread-spectrum technique for cellular high-capacity mobile communications is described and some results from an analytic study are summarized. The technique uses a very large set ot frequency-hopped signals which are designed for minimal mutual interference. No synchronization of the mobile units is required, and each user is permanently assigned his own signal, which serves as an identifying signal and as a carrier for the biphase-modulated digital message.

The spectral efficiency of the spread-spectrum system is analyzed and compared with the efficiencies of developmental FM/channel re-use schemes. It is concluded that even with relatively simple speech digitization schemes, the efficiency of the spread-spectrum scheme may exceed those of the narrowband schemes by a factor of almost five. More ambitious bit-rate-reducing speech digitization methods could improve still further on these figures.

Additional benefits of the spread-spectrum scheme include privacy, immunity from fading and interference, more consistent speech quality, simpler system control algorithms, more flexible blocking properties under overload conditions, and no channel switching as the user moves from cell to cell.

C4-2
0900 SIGNAL FILTERING WITH GAUSSIAN QUANTUM STATISTICS: R. O. Harger, Department of Electrical Engineering, University of Maryland, College Park, Md. 20742

The classical theory of signal filtering requires fundamental extension to account for quantum mechanical restraints on measurement when applied to optical communications. The linear minimum variance estimate of a vector signal sequence, given present and past measurement outcomes, has been discussed (J.S. Baras and R.O. Harger, IEEE Trans. Inform. Theo., IT-23, 683-693, 1977): necessary and sufficient conditions satisfied by the optimal present quantum measurement and weighting of past measurements have been given.

The work discussed here concerns the more concrete case with Gaussian statistics. We account for the effect of measurement on the quantum state which depends on a vector random "signal" process and evolves according to the Shrödinger equation. The quantum measurements are restricted to be "canonical" and a system Hamiltonian that results in a Gauss-Markov measurement outcome sequence is assumed. The weighted mean-square error is minimized over choice of current quantum measurement and linear weightings of past measurements. It is shown that the optimal weight matrices satisfy certain normal equations and necessary and sufficient conditions for the optimal canonical measurement are given. Sufficient conditions for the "separation" into a canonical measurement independent of past measurements and classical "post" filtering are given. An optical communication application is given.

C4-3
0930

On the Independence Theory of Equalizer Convergence

J. E. Mazo, Bell Telephone Laboratories
Murray Hill, New Jersey 07974

We consider the convergence of a mean-squared adaptive equalizer using the popular stochastic gradient algorithm for tap adjustment. The average of the error vector, or of the mean-square error, can be written as the average of the product of dependent matrices. We make use of the Markov nature of the dependence between successive stochastic gradient directions to recast the problem in a higher dimensional space in which study of the average matrix product is replaced by investigation of the equation $V_{n+1} = A(\alpha)V_n$. Here V_n is a vector from which the error at the n-th stage may be determined. The quantity $A(\alpha)$ is a matrix depending explicitly on the step size α of the original tap adjustment algorithm, and in practice is usually chosen to be small to assure convergence. The principal result of our study is the demonstration that if our basic matrix equation is treated using perturbation theory for small α, then the leading term is identical to the answer which one would obtain if one had assumed that the successive stochastic gradient vectors were independent.

C4-4 1030 ERROR CONTROL FOR CHANNELS WITH CROSSTALK: J.K. Wolf, Department of Electrical and Computer Engineering, University of Massachusetts, Amherst, MA 01003

A signalling system is discussed where more than one user transmits digital information over a common channel using exactly the same set of frequencies. It is shown how codes can be used to combat the resulting crosstalk. Examples are given whereby the overall transmission rate exceeds the rate which would result from time division multiplexing the various users.

C4-5 1100 FM DISTORTION IN THE OUTPUT OF AN ADAPTIVE PROCESSOR RECEIVING FSK PLUS TONE JAMMERS: D. R. Anderson, Systems Engineering Laboratory, TRW Defense Systems Group, Redondo Beach, Ca. 90278

For the case of FSK with interference made up only of tones at the instantaneous FSK frequency, this paper provides an unaveraged transient analysis of the output of any adaptive processor of the bootstrap type, i.e., any adaptive processor in which the reference signal is either a bandpass-filtered version of the processor output (AGIPA processor) or else a bandpass-limited version of the processor output (conventional bootstrap processor). Such an analysis has been given by Di Carlo for the case of interference by noise alone to predict the cycling of array weights. The present analysis shows the dependency of the transient output on

1) adaptive processor gain,
2) phase and amplitude variations of the reference loop bandpass filter transfer function,
3) power in the sum of the signals from the antenna elements input to the processor.

In particular, significant phase-distortions dependent on the latter three parameters have been found. The resulting degradation in the output SNR of the FSK detector has also been determined.

INTERFERENCE AND ITS SUPPRESSION
Wednesday Morning, 8 Nov., UMC 159
Chairman: John W. Adams, National Bureau of Standards, Boulder, CO 80302

E1-1
0830 HIGHLIGHTS OF THE COMMISSION E SCIENTIFIC SESSIONS AT THE XIXTH URSI GENERAL ASSEMBLY, HELSINKI 31 JULY - 8 AUGUST 1978: G.H. Hagn, SRI International, 1611 North Kent Street, Arlington, VA 22209

The scientific program of Commission E consisted of eight different sessions:

E-1 Global Location of Atmospherics and Lighting Instrumentation, H. Ishikawa (Japan)
E-2 Man-made Noise and Interference (Sources), G.H. Hagn (USA)
E-3 Radio Noise and Interference (Environment), R. Lindquist (Sweden)
E-4 CCIR Topics, F. Horner (UK)
E-5 New Topics, G.H. Hagn (USA)
OS-5/1 Natural Noise in Space, Ja. I. Likhter (USSR)
AE-1 Signal and Noise Measurements, P.I. Somlo (Australia)
CE-1 Effects of Non-Gaussian Noise on System Performance, A.D. Spaulding (USA) and J.K. Skwirsynski (UK)

These sessions contain 47 papers excluding those papers contributed to session E-5. This paper will summarize the scientific and technical highlights of these sessions.

E1-2 0900 GEOMAGNETIC INDUCED CURRENTS IN POWER LINES:

W.-M. Boerner, Communications Laboratory, Info. Eng., UICC, P.O. Box 4348, Chicago, IL 60680; W.R. Goddard, AEM Spec. Studies, Elect. Eng., University of Manitoba, Winnipeg, Can. R3T 2N2

The increasing use of the immense hydro-electric generating capacity in Northern Manitoba requires long HV-DC/AC transmission lines to serve Southern Manitoba and Northern U.S. power utilities. The auroral zone covers three-quarters of the province and the power generating and transmission systems are strongly affected by auroral activity (L.J. Lanzerotti, SCOSTEP Survey, April 1977, Bell Labs.). The cause of these problems is transient geomagnetic field variations associated with the growth, the decay and the rapid movement of the auroral electrojet producing induced earth-surface-potentials which in turn causes currents in conducting cable (pipe) systems that are grounded to earth at two (several) separate points. The objective of our study is to determine the expected effects on a new 500KV-AC line from Winnipeg to the Twin Cities. We have used spectral analysis of induced current records from La Verendrye and magnetograms from the closest magnetometer (IMS) station to the line's route at Whiteshell. These analyses and results of studies by Albertson (IEEE Trans. PAS-89(4), 578, April 1970), and by Campbell (Pure & App. Geoph. 116, 31p., 1978) and Akasofu (Geophys. Inst., U. of Alaska, Fairbanks, Alas. 99701, 1978) on the Alaska pipeline and Golden Valley line induction problem (1978) were used for prediction of periodic and surge currents. We conclude that the surge currents will produce significant level of harmonics and corresponding operating problems for the electric utilities as will corresponding radio noise interfering with various communication systems (W.R. Goddard, W.M. Boerner, Tech. Rep. AEMSS 75.05.01, May 1978).

E1-3
0930

ON SHIELDING EFFECTIVENESS OF METALLIC ENCLOSURES IN A COHERENT AND AN INCOHERENT ELECTROMAGNETIC ENVIRONMENT:

David C. Chang, Electromagnetics Laboratory, University of Colorado, Boulder, CO 80309
Ronald Prehoda and Vincent Puglielli, Naval Surface Weapons Center, Dahlgren, Laboratory, Dahlgren, VA 22448

In assessing the electromagnetic compatibility of electronic circuits, it is often necessary to determine the shielding effectiveness of metallic enclosures at both system and subsystem levels. Various definitions of shielding effectiveness, as well as test procedures in measuring their values were used in the past. However it is often very difficult to interpret the precise meaning of a given shielding effectiveness measurement, let alone the intercomparison of measurements based upon different procedures. The non-uniqueness in defining a shielding effectiveness number for enclosures of size comparable to free space wavelength, is further complicated by the fact that penetration of electromagnetic energy in most cases is influenced by both the external and internal resonances that might occur at a test frequency. Based upon some well-known antenna theories, attempt is made in this work to present a unified viewpoint on shielding effectiveness of enclosures exposed in either a coherent or a completely incoherent electromagnetic environment. It is shown that, by associating the shielding of an enclosure with antenna mismatch, measurements in the two entirely different environments are directly related to each other. Advantages and disadvantages of measurement in an incoherent environment are then discussed.

E1-4 1030 THE PERFORMANCE OF ADAPTIVE WORLD-WIDE HF COMMUNICATIONS:
S. Lehto, J. Kekäläinen, J. Kajava, Laboratory of Telecommunications, Department of Electrical Engineering, University of Oulu, Linnanmaa, 90570 Oulu 57, Finland

This report describes the results of the experimental work done since 1976 at the University of Oulu using a controllable (azimuth and elevation) HF array antenna for 14.2 MHz. The array is equipped with a microprocessor-based data acquisition and main beam steering system for medium and long-term control and a 3-channel adaptive receiving system for short-term control. An extensive world-wide test program including a series of five 24-hour tests has been carried out since January 1977. The results indicate that a world-wide availability in excess of 90 % over the natural noise-level can be achieved on a single frequency in the 10-15 MHz range with high-gain (24-26 dBi) rotatable antenna arrays with transmitter power of 10-50 kW for low-capacity transmissions. The unavailability due to low MUF during night-time and high absorption during day-time can be combated by long-term frequency selection using antenna arrays for 2-3 discrete bands supported by a single rotating structure.

This leaves abnormal ionospheric conditions occuring a few percent of the time as the limiting factor for the availability. The tests have verified that off-great-circle reflection and scatter can be very effectively used during these periods. Also high-angle modes on selected frequencies often provide communications. The systematic use of these propagation methods has been made possible by the development of the controllable high-gain antennas.

Achieving the high availability in actual HF operation requires reduction of the man-made interference level. The systems engineering approach where world-wide HF communications is developed into the direction of a complex system of adaptive links able to adapt to the changes in their environment coordinated in real-time by regional and world-wide centers offers a modern solution. Presently, systematic effort is directed towards implementing the algorithms and methods on all levels of HF communications meeded for this approach. Results indicate that the required noise reduction of 20-30 dB can be achieved in practical HF operation.

E1-5
1100

HF INTERFERENCE SUPPRESSION

G. J. Brown
Naval Ocean Systems Center
San Diego, California 92152

Several methods were investigated for suppressing other user interferences that occur on the high frequency radio channel. The interferences were divided into two types: those that occupy a narrow bandwidth with respect to the communicator's signal, and those that occupy a bandwidth approximately equal to or greater than the communicator's bandwidth. The processing techniques were based on large time-bandwidth (TW) product signals, where TW is much larger than the symbol alphabet size, whereby significant portions of the symbol TW space could be altered while still maintaining quality communications.
The suppression problem was considered in two parts: identification of the interference, and elimination of it. A simple threshold algorithm was used for identification and several elimination techniques including excision, clipping, and non-linear weighting were evaluated using computer simulations. The suppression techniques were found to work well with simple interferences consisting of narrowband interference alone or broadband interference alone. However with both interference types present together, a more complicated technique was required. An approach that divided the TW space into a time-frequency grid showed good results in this case.

E1-6
1130 OPTIMUM THRESHOLD DETECTION IN BROADBAND IMPULSIVE NOISE EMPLOYING BOTH TIME AND SPATIAL SAMPLING

A.D. Spaulding, National Telecommunications and Information Administration, Institute for Telecommunication sciences, Boulder, Colorado 80303

Because communication systems are seldom significantly interfered with by classical white Gaussian noise, it is necessary to consider more appropriate interference models in order to obtain realistic estimates of system performance. In this paper, we employ Middleton's recently developed statistical-physical models for non-Gaussian noise to investigate the optimum detection of a weak signal, where this signal is dominated by impulsive noise. It has been suggested that using a form of space diversity reception, it would be possible to "look between the large noise pulses" and thereby detect a signal well buried in the noise. It is well known that "normal" detection techniques, i.e., those known to be optimum in white Gaussian noise, are very inefficient in impulsive noise and can be greatly improved upon. The threshold (or locally optimum Bayes) detector is derived for the case of "pure detection" (Neyman-Pearson) of a weak signal and its performance determined. In addition, a form of space diversity is considered where the noise value which has the minimum absolute value from among n samples (n receivers) is used with the optimum detection algorithm. Substantial improvement, or processing gain, can be obtained with one receiver, with substantial, but less, additional improvement obtainable by then going to many additional receivers (receiving sites). Illustrative examples for atmospheric noise are given.

PROPAGATION THROUGH RANDOM MEDIA WITH APPLICATIONS TO REMOTE SENSING
Wednesday Morning, 8 Nov., UMC East Ballroom
Chairman: Earl Gossard, NOAA/ERL/WPL, Boulder, CO

F4-1
0830 PULSED PROPAGATION THROUGH A RANDOM MEDIUM:

V. H. Rumsey, Department of Applied Physics and Information Science, University of California, San Diego, San Diego, CA 92093

The space-time (or space-frequency) statistics of signals transmitted through a medium with random variations of refractive index, such as the atmosphere at optical frequencies, may be expressed in terms of the four dimensional correlation functions for the signal fluctuations at n different places and times with n = 1, 2, 3, ---- ∞. Only two of these statistics can be expressed simply for any level of turbulence, the mean and complex covariance, and then only when the spatial statistics of the signal are homogeneous. Otherwise machine computation from the equations for propagation of the correlation function is necessary and the computations are extremely laborious. The statistics of the medium are usually represented in the propagation equation by the Kolmogoroff Two Thirds Law or some more general postulate. Empirically some modification of the Kolmogoroff law often gives a better fit to measurements so that one may choose a postulate for the statistics of the medium that is typical of actual conditions and at the same time simplifies the solution of the propagation equations. By using such a postulate it is possible to obtain fairly simple formulas for the statistics of laser beam propagation through a turbulent atmosphere.

F4-2 0850 MEASUREMENTS OF THE ANGULAR SPECTRUM AND INTENSITY FLUCTUATIONS DUE TO A POINT SOURCE IN A TURBULENT MEDIUM: W.A. Coles and R. Frelich, University of California, San Diego, La Jolla, CA 92093.

Measurements of a HeNe laser with a divergent beam have been made over a 2 km horizontal path. The experimental objective was to measure the spatial correlation of intensity in a simple geometry under well determined conditions. The results are used to test the various approximation calculations, particularly those for saturated scintillations. The simplest geometry we can approach experimentally is that of a point source in a uniform medium. Since we can also calculate the mutual coherence function (MCF) for a diverging beam we are able to choose a divergence which makes the MCF experimentally indistinguishable from that of a true point source. We avoid difficulties in measuring the structure constant, C_n, and assumptions about the spectral shape by measuring the angular spectrum and the intensity scintillations simultaneously. From the angular spectrum we determine the MCF by Fourier transformation, and the MCF is simply related to the two dimensional phase structure function, $D(\bar{s})$. Of course $D(\bar{s})$ is sufficient to completely characterize the second order statistics of intensity. A full range from weak to strong scintillation is obtained over a single path using the diurnal variation of turbulence over a superheated dry lake bed. The intensity scintillations are measured with an array of PIN diodes on a minimum redundancy spacing. This permits estimation of the spatial correlation instantaneously as the detectors need not be scanned. The temporal spectrum, pattern velocity, and point statistics of intensity are also determined from these detectors. The angular spectrum is measured using a long focal length telescope and photographic film. The film is calibrated as it is exposed. It is digitized with a densitometer at the Visibility Laboratory of UCSD and the MCF and structure function are then estimated numerically.

F4-3
0910 Nth-ORDER MULTIFREQUENCY COHERENCE FUNCTIONS: A FUNCTIONAL PATH INTEGRAL APPROACH:

C. M. Rose, Naval Surface Weapons Center, Dahlgren, VA 22448 and I. M. Besieris, Department of Electrical Engineering, Virginia Polytechnic Institute and State University, Blacksburg, VA 24061

A functional (or path) integral applicable to a broad class of randomly perturbed media is constructed for the n^{th}-order multifrequency coherence function, a quantity intimately linked to n^{th}-order pulse statistics. This path integral is subsequently carried out explicitly in the case of a non-dispersive, deterministically homogeneous medium with a simplified (quadratic) Kolmogorov spectrum, and a series of presently unavailable results are derived. Special cases dealing with the two-frequency mutual coherence function for plane and beam pulsed waves are considered, and comparisons are made with recently reported findings in this area [e.g., I. Sreenivasiah et al., Radio Sci. 11, 775 (1976); C. H. Liu and K. C. Yeh, J. Opt. Soc. Am. 67, 1261 (1977); R. L. Fante, IEEE Trans. Ant. Prop. AP-26, 621 (1978)].

F4-4
0930

A FUNCTIONAL PATH INTEGRAL APPROACH TO PULSED BEAM PROPAGATION IN FOCUSING MEDIA WITH RANDOM-AXIS MISALIGNMENTS:

I. M. Besieris, Department of Electrical Engineering, Virginia Polytechnic Institute and State University, Blacksburg, VA 24061 and C. M. Rose, Naval Surface Weapons Center, Dahlgren, VA 22448

Recently formulated asymptotic techniques based on functional (or path) integration are used to compute n^{th}-order pulse statistics in connection with beam propagation in focusing media (e.g., graded lightguides) characterized by random-axis misalignments. Particular emphasis is placed on second- and fourth-order pulse statistics. Analytical and numerical results concerning on- and off-axis average pulse intensities and variances of pulse intensity fluctuations are presented, and comparisons are made with previously reported results, which are based for the most part on ray and modal methods.

F4-5
1010 REMOTE SENSING AND SOLAR-TERRESTRIAL STUDIES OF TROPOPAUSE HEIGHT:

E. A. Hall, J. P. Basart, R. E. Post, W. P. Birkemeier, L. D. Bacon, G. E. Fanslow, and D. T. Stephenson,
Department of Electrical Engineering,
Iowa State University, Ames, Iowa 50011

A forward-scatter CW radar link operating at a frequency of 940 MHz has been established from Iowa State University to the University of Wisconsin at Madison. This system has been developed as a facility to routinely provide data for developing new equipment for tropospheric scatter systems, for studying tropospheric scatter propagation, and for meteorological studies. A RAKE receiver and spectrum analyzer produce information on signal intensity and Doppler velocity of particles as a function of height in the common volume. Intensities at zero Doppler frequency are converted to potential temperature gradient for heights above the majority of the water vapor. The high average CW power of 10 kW and the signal processing capability of the RAKE receiver provide the necessary sensitivity to detect scattered signals off the tropopause. Continuous monitoring of the tropopause height for time periods of several days will give data for solar-terrestrial studies. Solar data which is available on nearly a real time basis from the Solar Environment Laboratory Data Acquisition and Display System is then compared with the tropopause heights to search for height dependencies on solar phenomena. Customarily tropopause heights are measured twice a day by radiosonde which is useful for studies on a time scale of days. The continuous monitoring capability of the forward scatter system makes it possible to study tropopause height fluctuations on a shorter time scale of minutes to hours.

F4-6
1030

LONG TERM MEASUREMENTS OF C_n^2

R. B. Chadwick and K. P. Moran, Meteorological Radar Program Area, Wave Propagation Laboratory, Environmental Research Laboratories, Boulder, CO 80302

A major problem for aviation is low-level wind shear at airports. To determine the feasibility of using radar to detect hazardous wind-shear, a year long experimental program was carried out under Air Force sponsorship.

From March, 1977 to February, 1978, the 10-cm FM-CW Doppler radar used to make C_n^2 measurements in the Boulder, Colorado area. During this period, the radar was operated all or part of 161 days, and the total operating time was 2827 hours. Measurements were made at nine equally spaced heights up to 1610 m. Averaged measurements were made at one minute intervals and then arranged into hourly histograms of C_n^2. These histograms can then be analyzed for specific long term effects such as diurnal trends, yearly trends, and probability density functions on C_n^2. The diurnal trend is such the C_n^2 maxima occur at midnight and shortly after mid-day. Minima occur at sunrise and sunset. As might be expected, the yearly trend is such that C_n^2 is lowest in the winter months. The data shows that C_n^2 closely follows a single-parameter log normal probability distribution. The variance of the distribution seems to change very little with time of day or year.

The main conclusion of the experiment is that a modest radar offers an all-weather method of detecting hazardous wind shear at airports. The radar must be capable of operating at an elevation angle of 5°-10° and measuring winds from a few hundred meters range to 5 km range.

This work was fully supported by Air Force Project Order No. Y77-847 entitled "FM-CW Doppler Radar Wind Shear Detector."

F4-7
1050 FEASIBILITY OF GLOBAL WIND MEASUREMENTS USING SATELLITE-BORNE PULSED COHERENT LIDAR: P.A. Mandics, R.M. Huffaker, T.R. Lawrence, R.J. Keeler, and F.F. Hall, Jr., Wave Propagation Laboratory, Environmental Research Laboratories, National Oceanic and Atmospheric Administration, Boulder, CO 80303

Recent advances in laser technology and the recognized need to provide better wind input for numerical weather prediction have led NOAA to investigate the feasibility of measuring the global wind field using a satellite-based pulsed coherent CO_2 lidar. The feasibility study consisted of evaluating existing data on CO_2 laser attenuation in the atmosphere, aerosol backscatter, and refractive turbulence and the construction of appropriate models for various meteorological conditions. Computer simulations including all major lidar system parameters, space platform constraints, atmospheric propagation effects, and wind-field models have been performed to study system design alternatives and to evaluate expected performance. Using realistic lidar system parameters (10 J pulse energy, 7 μs pulse duration, 10 Hz pulse repetition frequency, and 1 m telescope diameter) we concluded that it should be possible to measure winds with a 300 km horizontal and 1 km vertical resolution from the surface up to 15 km height. Depending on backscatter intensity and measurement geometry the accuracy of the deduced horizontal wind components should be in the range of 1-2 m s^{-1}. Our current efforts are focussed on refining the wind field models used in the simulation, introducing and evaluating the effects of clouds, and performing critical ground-based experiments to verify various aspects of lidar system performance.

F4-8
1110

EXCITATION OF WAVES BY IRREGULAR TERRAIN IN A NEUTRAL ATMOSPHERIC BOUNDARY LAYER:

R. Michael Jones, Wave Propagation Lab.
U.S. Dept. of Commerce, Boulder CO 80302

To correctly interpret the measurements soon to be available from the meteorological tower of the Boulder Atmospheric Observatory, it is necessary to calculate the effect of the irregular terrain in the vicinity of the tower on the boundary layer at the tower.

The effect considered here is that of a series of three hills: that upon which the tower sits, Gun Barrel Hill, and the Haystack Mountain-Table Mountain Complex to the west and slightly north of the tower. To first order, the effect of these hills is that of a spatially harmonic surface with a wavelength of 13 km, the approximate spacing of the hills. We calculate the perturbation to a horizontally stratified boundary layer due to the presence of such a spatially harmonic surface when the wind blows normal to the terrain variation (that is, from the west, a typical wind direction). We calculate only the Fourier component of the perturbation that has the same horizontal wavelength as the terrain (i.e., 13 km). Nonlinearities also generate other Fourier components, as do the deviations of the actual terrain from the model spatially harmonic surface, and these would introduce corrections having a smaller scale height structure. Neglect of the effect of the earth's rotation is justified because that effect would introduce corrections having a much larger scale height structure. Although the effect of the Rocky Mountains (which start some 30 km west of the tower) on the boundary layer should be significant, the scale of the horizontal structure is probably large enough that we can consider its effect already taken into account in the background horizontally stratified boundary layer. We neglect compressibility and use a second order closure model for a neutral boundary layer (a simplified version of the model used by J. C. Wyngaard, Boundary Layer Meteorology, 9, 441-460, 1975).

The terrain excites two kinds of waves in the boundary layer: First, there are evanescent pressure waves, whose vertical decay length is about the same as the horizontal wavelength (about 13 km for our case). Second, there are viscous waves, whose vertical wavelength depends on the horizontal wavelength, the horizontal wind velocity of the background boundary layer, the background turbulence level, and the length scale of the turbulence. The vertical wavelength for the viscous waves (about 100 m for our case) is much smaller than that for the pressure waves. Calculations show that this particular second order closure model gives nearly the same results as an eddy viscosity model in which the eddy viscosity depends in a particular way on the turbulence level and the turbulence length scale. Results include height profiles of wind and Reynolds stress.

IONOSPHERIC EFFECTS OF SOLAR POWER SATELLITES
Wednesday Morning, 8 Nov., UMC Forum Room
Chairman: C. Rush, NTIA/ITS, Boulder, CO

G3-1
0830 SOLAR POWER SATELLITES: THE IONOSPHERE CONNECTION

L. M. Duncan, University of California, Los Alamos Scientific Laboratory, Los Alamos, NM 87545

A review will be presented of potential ionosphere/microwave interactions associated with the operation of a solar power satellite. Three major interactive mechanisms are identified. The first of these relates to electron heating and a thermal runaway instability in the lower ionosphere, resulting in substantial increases in the local electron temperature. A second potential phenomenon is associated with thermal self-focusing of the SPS microwave beam. This interaction leads to large-scale (kilometer) irregularities in the ionospheric F-region. A third effect which might accompany ionosphere/microwave interactions is the formation of short-scale (meter) plasma striations. These striations are known to produce serious communications interference. A preliminary assessment of the probability of occurrence and possible impacts of these interactions will be given. In addition, a summary of the current status of ongoing studies will be included.

G3-2 0850 POTENTIAL TELECOMMUNICATIONS EFFECTS OF SOLAR POWER SATELLITES: L. E. Sweeney, Jr., Remote Measurements Laboratory, SRI International, Menlo Park, CA 94025

The possible effects on the ionosphere by the Solar Power Satellites (SPS) S-band (2450 GHz) beam, which has power densities on the order of 20 mW/m^2, are presently unknown but potentially significant. Experiments with high-powered HF heating of the ionosphere indicate a variety of possible effects on the ionosphere by the SPS power beam, some having potentially significant impacts on commercial and military telecommunication and radar systems. This paper discusses these possible ionospheric effects and the potential telecommunications impacts, with special emphasis on artificially produced field-aligned ionospheric irregularities that may scatter RF energy from below 1 MHz to above 300 MHz. Such irregularities may adversely affect vertical ionosondes, OTH radars, VHF line-of-sight radars, and satellite downlinks. These irregularities might also affect communications systems (HF and VHF), navigation systems, and broadcast systems (shortwave, AM, FM and television).

G3-3 0910 THE MICROWAVE BEAM SUBSYSTEM OF THE SATELLITE POWER SYSTEM:
R. M. Dickinson, Transmitter Group Supervisor
Jet Propulsion Laboratory, Pasadena, CA 91103

The overall beamed RF power transmission efficiency design for currently proposed orbiting solar energy conversion spacecraft-to-earth power transmission links are reviewed in terms of the transmit and receive aperture sizes and the aperture power density distribution for the proposed S-band (2.45 GHz) operating frequency. A calculated beam transmission efficiency of greater than 95% is shown to be potentially achievable from the proposed 1 km diameter transmit array to the 10 km diameter receiving array under optimum conditions.
The pilot beam steered, retrodirective, power transmitting phased array resulting antenna pattern characteristics are presented for a particular point design. System and propagation factors that affect the performance of the beamed power link are presented and discussed. Design factor uncertainties, technology shortcomings in RF power conversion efficiency, harmonic and noise suppression, beam forming and beam pointing, propagation modeling and analysis and subsystem modeling are identified relative to the desired and currently achievable or demonstrated performance.
Multiple satellite beam effects, such as sidelobe addition are examined. Possible mitigation strategies for alleviating undesirable effects are discussed.

G3-4
0930

SPS PILOT BEAM PHASE CONTROL SYSTEM

A. H. Katz, Raytheon Company, Wayland, Massachusetts 01778

Accurate beam pointing of the SPS (Solar Power Satellite) downcoming microwave power beam toward the ground-based rectenna relies on the phase stability of a retrodirective beam control system. The retrodirective system consists of a microwave carrier (pilot beam) transmitted from the ground and beamed upward toward the SPS microwave antenna at GEO (Geosynchronous Earth Orbit). Phase measurements of the pilot beam across the GEO array are used to position the power beam onto the ground based rectenna. Ionospheric perturbations (both natural and induced by the downcoming power beam) will produce phase front distortions on the pilot beam itself, the extent of which must be considered in the pilot beam system design and performance evaluation. This paper reviews the pilot beam concept and describes the potential ionospheric interactions. Finally, a program designed to perform early measurements of the ionospheric affects (both natural and those induced by HF Heater experiments to simulate the microwave power beam) is described.

G3-5
1020

AN EXPERIMENTAL STUDY OF ELECTRON HEATING IN THE LOWER IONOSPHERE:

D.S. Coco, Dept. of Space Physics and Astronomy, Rice University, Houston, TX 77001; L.M. Duncan, University of California, Los Alamos Scientific Laboratory, Los Alamos, NM 87545; R.L. Showen, 1638 Edmonton Ave., Sunnyvale, CA 94087

An ionospheric heating experiment has been performed at the Arecibo Observatory (NAIC) using the 430 MHz incoherent backscatter radar both as a heater and as a diagnostic. Radar pulses up to 9 msec in length were transmitted with 2.5 MW peak pulse power, yielding an average power flux of approximately 20 W/m^2 at 100 km altitude. A 20 μsec diagnostic radar pulse offset in frequency from the heating pulse was used to measure the resultant ohmic heating of electrons in the lower ionosphere. The heating was calculated to be well above threshold for an electron thermal runaway below 100 km, with a predicted saturation electron temperature of approximately 2000°K. The experimental results show heating only of about 200°K, with no indication of a thermal runaway. Possible sources of the discrepancy between experiment and theory will be discussed.

G3-6
1040 A PRELIMINARY LOOK AT EMC FOR A SOLAR POWER SATELLITE SYSTEM: W.B. Grant & E.L. Morrison, Institute for Telecommunication Sciences, National Telecommunications Information and Administration, 325 Broadway, Boulder, CO 80303

The potential EMC problems generated by a Solar Power Satellite System (SPS) were investigated. Information was obtained from the National Aeronautics and Space Administration on SPS system definition including: single microwave power transmission system radiation characteristics; geostationary earth orbit locations for multi-satellite operation; emission power spectra; side lobe structure; and candidate receiving antenna (rectenna) sites. A representative rectenna site in the Mojave desert of Southern California was chosen for EMC analysis. Equipments and systems near the rectenna site that would be susceptible to SPS radiation were identified by selective retrieval from existing files, and categorized in relation to function, coupling modes, location, and interconnectivity. Various atmosphere parametric interactions were investigated which effect the power efficiency of the SPS system as well as contributing to the EMC problem. These are: gases and stratification, attenuation and scatter due to precipitation in rain, hail, etc; attenuation and scatter due to dust and other particulates; and wavefront distortions due to turbulence. There were more than 1500 operating EM systems within a boundry 145 Km by 145 Km with the proposed Mojave site at center. Based on the probable operational system degradations near the Mojave site and the mobility to establish mitigating strategies without unacceptable probability of operational compromise to some of the systems, a new site for Southern California was chosen.

G3-7
1100 IONOSPHERIC HEATING BY RADIO WAVES: R. Roble, NCAR, Boulder, CO; and F. Perkins, Princeton University, Princeton, NJ

LONG-LENGTH RADIO ASTRONOMY
Wednesday Morning, 8 Nov., UMC 157
Chairman and Organizer: W. C. Erickson, University of Maryland, College Park, MD 20742

J3-1
0830 EVIDENCE FOR VERY ENHANCED ANGULAR BROADENING AND SCINTARS: James J. Rickard and W.M. Cronyn, Department of Physics and Astronomy, University of Iowa and Clark Lake Radio Observatory, Borrego Springs, CA 92004

Estimates of angular broadening can be derived from measurements of pulsar pulse decay times and coherence bandwidths. If an extragalactic source is subjected to exactly the same scattering as a pulsar, i.e., if the scattering medium extends from earth to pulsar and then abruptly ends, the full-width half maximum scattering angle for the extragalactic source will be $\theta_e = (x + 1)\sqrt{8\tau c/xz}$, where τ = pulse decay time constant, z/c = pulsar-to-earth propagation time, and x = distance ratio of (earth-to-scattering screen)/(pulsar-to-scattering screen). Applying this relationship to measurements of τ, estimates of z/c based on measurements of dispersion measure and assuming an average density of .03 electronic cm^{-3}, and assuming x = 1 yields values of θ_e at 81 MHZ of $\gtrsim$1 arcsec for $|b| < 10^o$ and a scale height of 400 psc for the galactic electron layer or $\geq$5 arcsec for $|b| < 10^o$ and a scale height of 1000 psc. Thus the presence of $\sim$80 Cambridge IPS sources with sizes $\leq$ 1 arcsec at $|b| < 10^o$ presents a conflict with 3 possible resolutions: (1) pulsar pulse smearing is governed by turbulence in the immediate vicinity of the pulsar and is unrepresentative of the general interstellar medium through which extragalactic sources are observed, (2) the pulse smearing is caused by random variations in the real-time group delay propagation time introduced by large scale irregularity structure, not the simple geometric relationship discussed and (3) the deduced angular broadening scale is generally correct and the $\sim$80 small angular diameter sources are in large measure a group of nearby (in front of the scattering screen) galactic sources, not extragalactic. We favor a combination of (2) and (3) and propose to call such sources scintars, sources whose sole distinguishing characteristic at the present time is a display of scintillating activity implying a small angular diameter, in spite of the fact that they are observed in a region of the sky in which there is such large angular broadening that extragalactic sources would not display IPS. Scintars may, in fact, be nothing more than perhaps steep spectrum pulsars (similar to the Crab pulsar) for which the pulse decay time constant exeeds the pulse period, or perhaps spun down pulsars.

J3-2
0845

SPATIAL DISTRIBUTION OF INTERSTELLAR SCATTERING:

W.M. Cronyn and James J. Rickard, Department of Physics and Astronomy, University of Iowa and Clark Lake Radio Observatory, Borrego Springs, CA 92004

A critical reanalysis of source structure parameters in the Cambridge interplanetary scintillation catalog (A.C.S. Readhead and A. Hewish, Mem. R.A.S., 78, 1, 1974) reveals no statistically significant evidence for increased interstellar angular broadening in a galactic plane, in conflict both with previous studies (cf A.C.S. Readhead and A. Hewish Nature, 236, 440, 1972, and M.N. R.A.S., 176, 571, 1976) and with a recent study of indirect estimates of angular broadening based on measurements of pulsar pulse broadening as described in a companion paper. Implicit in the previous studies is the assumption that the population mix of sources is the same at low and high galactic latitudes, i.e., the sources are all extragalactic with a homogeneous distribution of intrinsic angular size. However, there is a significant contribution to the decrease in the ratios of scintillators/non-scintillators and strong/weak scintillators near the plane from known galactic SNR's which were included in the previous studies of source counts. Such SNR's introduce a large angular diameter bias in the distribution of source sizes in the plane. We do find a 500 square-degree scintillator-deficient region roughly centered on $\ell = 60^{o}$ extending from $b \sim 10^{o}$ to 65^{o} near the North Polar Spur (NPS) continuum radio feature, a suspected SNR; the deficit may be caused by enhanced scattering associated with the NPS.

J3-3 WHERE ARE THE INTERSTELLAR ELECTRONS LOCATED?

0900 Carl Heiles and Y.H. Chu
Astronomy Department
University of California, Berkeley

We suppose that van der Laan's theory applies, in which the radio continuum emission from old supernova remnants (SNR) arises from compression of interstellar relativistic electrons and magnetic field in the expanding shock front. Since the field is "frozen" into the matter, the interstellar gas density should also be higher in continuum-emitting regions. Contrary to this expectation, the 21-cm line intensity is not correlated with the radio continuum brightness temperature in the North Polar Spur (NPS). However, Faraday depolarization is strong in the NPS and the product $n_e B \cong 8$ cm^{-3} uG. From the absence of detectable Zeeman Splitting in nearby neutral gas, and the absence of detectable Hα optical emission, we estimate that the gas in typical filaments in the NPS region is nearly fully ionized with $n_e \cong 3$ cm^{-3}, B $\cong 2$ uG. A filament having diameter 5 pc contributes dispersion measure of about 15 cm^{-3} pc and a rotation measure of about 30 rad m^{-2}, which is comparable to typical values found in pulsars located at high galactic latitudes. In van der Laan's theory, the radio continuum emissivity is approximately proportional to the fourth power of the compression, so that regions somewhat less compressed than the NPS filaments will not stand out in the radio continuum; they may therefore be plentiful, and we suggest that the dispersions of pulsars, and interstellar scintillation, are caused by a superposition of these small, relatively dense regions instead of the canonical, smoothly distributed electron density of 0.03 cm^{-3}.

J3-4 0915 COMPACT SOURCE STRUCTURE AT METER WAVELENGTHS FROM INTERPLANETARY SCINTILLATIONS (IPS):

S. Ananthakrishnan*, W.A. Coles and J.J. Kaufman, University of California, San Diego, La Jolla, CA 92093

Three station IPS observations of radio sources at 74 MHz are used to estimate the angular structure of compact components (~ 0.5 arc sec) utilizing two different methods. First, the solar wind velocity and the temporal spectrum of the intensity fluctuations are measured and the velocity is used to convert the temporal spectrum to a spatial spectrum. This reflects the angular diameter of the source directly in strong scattering. Second, the anisotropy of the compact structure is inferred from the systematic variations of the apparent flow angle of the IPS pattern. The sources studied are 3C48, 3C144, 3C161, 3C237, 3C273, 3C298 and 3C459. A comparison of the results with those obtained from the temporal second moment and scintillation index shows fair agreement although there are large uncertainties and limitations in all the methods. Within these uncertainties the results also agree with the published VLBI measurements. We also present some recent results on the effect of interplanetary medium on VLBI observations.

*On leave from TIFR, Ooty, India

J3-5 NON-THERMAL GALACTIC CONTINUUM EMISSION:
0930 H.V. Cane, Dominion Radio Astrophysical Observatory*, Penticton, Canada

The spectra of continuum emission from the Southern and Northern Galactic Polar Regions have been observed and calibration differences between southern and northern galactic continuum surveys have been reconciled. Surveys of the Galaxy at five frequencies in the range 2 to 20 MHz have been obtained using the Llanherne low-frequency array and the data have been assembled into maps covering the area $320° \leq \ell \leq 30°$ and $-25° \leq b \leq 22°$. The data from these maps are combined with data from seven earlier continuum surveys to produce galactic radio spectra in various directions.
A summary is made of most of the measurements, at frequencies less than approximately 400 MHz, of the galactic background radiation and their interpretation. Two new composite maps, at 10 and 30 MHz, are presented. These, combined with the 85 MHz all-sky map, are used to illustrate the variation of the galactic non-thermal radiation across the sky and with frequency.
The galactic spectra are interpreted in terms of a model of the Galaxy in which synchrotron emission, and absorption in HII regions, predominate in spiral arms. It is found that the synchrotron emission arms and the arms defined by HII regions are not coincident. In addition to the HII absorbing gas the model incorporates a much broader uniform absorbing HI gas which is responsible for high latitude absorption, pulsar signal dispersion, and Faraday rotation.

J3-7 1020 METER-WAVELENGTH OBSERVATIONS OF FOUR GIANT RADIO GALAXIES: R.A. Perley and W.C. Erickson, Clark Lake Radio Observatory, University of Maryland, College Park, MD, 20742.

A method of aperture synthesis employing successive fan-beam scans taken with the E-W arm of the CLRO TPT antenna has been utilized to synthesize the brightness distribution of four large radio galaxies in the 26 to 110 MHz range.
The head-tail radio galaxy 3C129 was mapped at 43 and 73.8 MHz. These low frequency maps show that the tail is both longer and brighter relative to the head than seen on WSRT maps taken at 610 and 1415 MHz. These maps indicate the spectrum is straight at all points but steadily steepens with increasing distance from the head. The absence of curvature indicates that electron reacceleration mechanisms are required at all points in the tail.
The double radio sources DA240 and 3C236 were mapped at 43 MHz, and showed little change in structure from that observed by the WSRT at 610 MHz. This implies little change in spectral index in the outer lobes of these sources. The fractional flux of the central component of 3C236 is much lower at 43 MHz than at 610 MHz.
The Perseus cluster was mapped at 26, 38, 43, 73.8 and 109.2 MHz. From these observations we found the fluxes of 3C83.1B and 3C84. The source 3C83.1A was not detected at any frequency, implying a turnover in its spectrum near 100 MHz. Due to the synthesis technique employed, the extended cluster halo was not detected, but may have been detected in subsequent observations with different techniques.

J3-8 1035 THE SECULAR VARIATION OF CAS A BELOW 100 MHZ: C.L. Bennett, W.C. Erickson, M.J. Mahoney and S. McCorkle, Clark Lake Radio Observatory, University of Maryland, College Park, MD 20742

The flux of Cas A appears to be evolving in a complex fashion at frequencies below 100 MHz. Early Teepee Tee observations (W.C. Erickson and R.A. Perley, Ap.J. 200, L83, 1975) showed an anomally in the flux of Cas A at 38 MHz. Comparison with older observations showed no evidence of the secular decrease in flux observed at higher frequencies. These conclusions were independently confirmed by Read (Mon. Not. R. Ast. Soc., 178, 259, 1977). Our present observations indicate that a long wavelength flare occurred in this SNR and that an increase in its radio flux has spread to higher frequencies. In particular, the flux appears to have increased in the 80 MHz region, i.e. that frequency range in which the rate of secular decrease was originally determined.

J3-9 1050 CORONAL CHARACTERISTICS AT 2.0 $R_\odot$ DERIVED FROM OBSERVATIONS OF DECAMETER RADIO BURSTS:

T.E. Gergely, W.C. Erickson, M.R. Kundu and M.C. Reardon, Clark Lake Radio Observatory, University of Maryland, College Park, MD 20742

We discuss the evolution of two solar radio bursts, which occurred during the ATM/SKYLAB period. The radio observations were obtained with elements of the two-dimensional swept-frequency array, called the Teepee Tee of the Clark Lake Radio Observatory. Additional data from SKYLAB, as well as from other ground based experiments, allow us to derive some of the physical conditions present in the corona at the time of the bursts.

The first radio burst, associated with a white light coronal transient, occurred on August 21, 1973. White light observations of the disturbance are available in the form of a series of photographs taken by the High Altitude Observatory's coronagraph aboard SKYLAB. The radio emission was continuum in nature and lasted for almost five hours. The source of emission was observed to be co-spatial with the lower part of one of the secondary white light loops. This fact, along with considerations of radio wave propagation in the corona allowed us to estimate, for the first time, a lower limit for the depth (extension along the line of sight) of the loop. It turned out to be 0.6 $R_\odot$, comparable to the extension of the loop on the plane of the sky. The radio source showed no dispersion of height with frequency, and therefore we attribute the emission to gyrosynchrotron radiation. Based on this assumption we estimate the magnetic field strength in the lower part of the loop to be in the 2.0-4.5 gauss range at a height of 2.1 $R_\odot$ from sun center. Very few estimates of the magnetic field exist at comparable coronal heights. One recent observation implies a field strength of 3.3 gauss at 2.0 $R_\odot$ from sun center (G.A. Dulk et al., Solar Phys., 49, 369, 1976).

The second radio burst, which occurred on September 5, 1973, was associated with one of the best observed flares of the SKYLAB period. A series of type III/V groups of increasing intensity were observed, followed by a continuum burst, possibly a type II. The first type III group coincided in time with the filament activation observed in the H_α line (E.J. Schmahl et al., submitted to Solar Phys., 1978). A single type III burst coincided in time with the flash-phase of the flare; its direction followed closely that of a spray knot crossing the equator. Subsequent type III bursts occurred above different regions of the corona, which appeared to be linked by high magnetic arcades, indicating that these structures fill up with energetic electrons at the time of the flare. In contrast, although the size of the continuum source varied, its centroid was confined to a small area above the H_α flare.

J3-10
1105

A Compressive Receiver for Radio Astronomy

R. G. Peltzer and J. W. Warwick
University of Colorado, Boulder CO 80309

Compressive receivers offer unique advantages in radio astronomical spectroscopy. This type of receiver was originally developed for high sensitivity radars and has further applications for military spread spectrum receivers. In the spectroscopy of solar and planetary radio emissions, and the spectroscopy of pulsars, this technology will provide new standards for simultaneously high sweep rate (and range), spectral resolution, and sensitivity. The high stability required for molecular line studies probably rules out any application of this technology in this field.

A compressive receiver is in final construction phase at the University of Colorado Radio Astronomy Observatory. It features surface acoustic wave delay lines for local oscillator sweep and for compression of the swept signal band. Its output is one spectrum covering 1 to 80 MHz in each 100 microsecond interval. Spectral resolution is 50 kHz, and output is adapted for either analogue (e.g., CRT and film record display) or digital tape record. The receiver will operate at Nederland, Colorado, in conjunction with either of two antenna systems: a circularly polarized array of 14 dB gain (over an isotrope), or an interferometer with 10 dB gain. These combinations permit state of the art spectroscopy of high speed solar and planetary bursts. They may also provide spectra of the largest pulses from the strongest pulsars, but this type of study in general requires larger collectors than our Nederland arrays.

This work has been supported by the National Science Foundation.

J3-11 1120 A SEARCH FOR CORRELATION BETWEEN SOLAR ACTIVITY AND JUPITER'S DECAMETER-WAVE RADIO EMISSION:

C. H. Barrow,* Astronomy Program, University of Maryland, College Park, MD 20742

The possibility of a short-term correlation, between Jupiter's decameter-wave radiation and solar activity, has been investigated for the fourteen apparitions between 1960 and 1975, using the catalogs of Jupiter events published by the University of Colorado Radio Astronomy Observatory (UCRAO) and by Goddard Space Flight Center (GSFC). Artificial periodicities in the Jupiter data, due to beat periods and harmonics between Io revolution and Jovian and Earth rotation, have been considered and the most serious of these are found to be Io-dependent. Using the geomagnetic A_p index as the indicator of solar activity, the method of superposed epochs is applied to Non-Io events selected from the UCRAO catalog and separated into two-month periods before opposition and two month periods after opposition, as an additional test for correlation. While significant positive correlation appears from all of the Jupiter data the effect is enhanced by selection of Non-Io events and implies that much of the Non-Io emission is somehow activated by solar particles having velocities within the range 300-500 km/sec. Interestingly, the Io-dependent periodicities are also apparently removed by use of the GSFC catalog, without event selection, as this is based upon a round-the-world network of observing stations and is thus largely free of terrestrial rotation effects.

An alternative approach to the problem is to examine some limited period, during which a clear pattern of solar behaviour is known to be present, and to search for some effect of this pattern to appear in the Jupiter radiation. This method is discussed briefly and some problems arising are outlined.

---

* On leave from the Department of Physics, University of the West Indies, Kingston 7, Jamaica, W.I.

J3-12
1135 A THEORY OF JUPITER CONTROL OF IO-RELATED RADIO EMISSION:

A. J. Dessler and T. W. Hill, Dept. of Space Physics and Astronomy, Rice University, Houston, TX 77001

The decametric radio emissions from Jupiter are, to a large degree, controlled jointly by the rotational phase of Jupiter and the orbital phase of the inner Galilean satellite Io. We address the problem of why the Io-related emissions occur for only certain favorable orientations of Jupiter. (This is in addition to the requirement for a favorable viewing angle, which is provided by Io being in the proper phase relative to the Earth.) We have investigated a mechanism in which longitudinal asymmetries are created in both the conductivity and the electron content of the Jovian ionosphere because of the non-dipolar character of the Jovian internal magnetic field. These ionospheric inhomogenieties are created in regions where the Jovian magnetic field is anomalously weak and trapped energetic electrons preferentially precipitate. A low-pressure electric arc can be struck in Jupiter's ionosphere when the foot of Io's flux tube passes into such ionospheric "hot spots", thereby enhancing the Birkeland (magnetically field-aligned) current between Io and Jupiter, which then generates detectable levels of decametric radio emissions.

J3-13
1150 SEARCH FOR COHERENT RADIO PULSES FROM MXB1730-335

I.R. Linscott, J.W. Erkes, Dudley Observatory, Latham, NY 12110, and N.R. Powell, General Electric Co., Syracuse, NY 13221

A search for asynchronous radio pulses from the Rapid Burster MXB 1730-335, has been implemented on Dudley Observatory's 100-foot radio telescope at 327 MHz. Detection of highly dispersed radio pulses, asynchronous in time, is attempted using a combination of on-line hardware, and off-line software signal processing to deconvolve dispersion, and in some cases, multipath scintillation distortion. The deconvolution relies on transforming real-time signals into frequency spectra with a Fast Fourier Transform (FFT) 1024-point processor operating at 2 MHz. Dispersion spectra, representing the dispersion compensated pulse as a function of dispersion, are constructed from the frequency spectra. The construction involves a homomorphic mapping of the frequency spectra followed by an additional FFT, and has a signal to noise gain of 30 dB for coherent pulses. These dispersion spectra are searched for strong power fluctuations and pulses may be detected over a wide range of simultaneous dispersions. Results of the search, and the application of this technique to multipath deconvolution will be discussed.

J3-14 1205 DEKAMETRIC MEASUREMENTS OF JUPITER'S ROTATION PERIOD

T. D. Carr, Department of Physics and Astronomy, University of Florida, Gainesville, FL 32611
J. May, Observatorio Radioastronomico de Maipu, Universidad de Chile, Santiago, Chile
M. D. Desch, Goddard Space Flight Center, Code 695, Greenbelt, MA 20771

A total of 26 measurements of Jupiter's 12-year average rotation period were made at frequencies of 18, 20, and 22.2 MHz at observatories in Florida and Chile. An improved method was employed in which histograms of occurrence probability vs. central meridian longitude obtained at the same frequency and observatory during apparitions about 12 years (one Jovian year) apart were cross correlated. The longitude shift giving maximum cross correlation was used to correct the initially assumed rotation period. The mean value of all the measurements was found to be 9 hr 55 min 29.689 sec, with a standard deviation of the mean of 0.005 sec. This is about 0.02 sec, or 4 standard deviations, less than the System III (1965) value. Although the difference is small, it is probably significant. No evidence of a change in the rotation period was found.

WEDNESDAY AFTERNOON, 8 NOV., 1330-1700

RECENT ADVANCES IN MICROWAVE, MILLIMETERWAVE MEASUREMENTS
Commission A, Session 3, UMC 158
Chairman: Ramon C. Baird, National Bureau of Standards, Boulder, CO

A3-1 1330 A NEW MICROWAVE INTERFEROMETER: G. Tricoles and E. L. Rope, General Dynamics Electronics Division, P.O. Box 81127, San Diego, CA 92138

Microwave interferometers are used to measure the complex-valued transmittance and reflectance of flat dielectric panels as functions of incidence angle. Transmittance is determined by a receiver that measures phase and intensity while a panel is rotated in a free space path between a transmitting and a receiving antenna. Reflectance requires moving one antenna, as well as the panel, to receive the specular reflection. The measurements have several purposes. They test the panel design and the fabrication process. Dielectric constant can be determined by comparing measured data with calculations based on exact theory. Interferometers are especially useful for evaluating anisotropic panels that have corrugated surfaces because they are less restrictive than waveguide and cavity methods. However, interferometers have disadvantages at high incidence angles because direct radiation between antennas introduces errors into reflectance data. These errors reduce the accuracy of absorptance estimates.

This paper describes a new interferometer that is accurate for both high and low incidence angles. The main improvement the addition of a convenient method for eliminating direct radiation and multipath. The test panel is supported on a small turntable that is placed on a larger turntable. The transmitting antenna and the panel are rotated together by the larger turntable, and the received field is continuously recorded during the rotation. The incidence angle can be varied by the smaller turntable. Measurements are made with and without the panel, and the data are subtracted to eliminate direct and multipath fields. The complex-valued fields require a receiver that measures both phase and intensity. Measured data are given and compared with exact calculations for flat sheets with known properties. These data demonstrate that accuracy is increased by subtracting the field measured without the panel.

A3-2 1400 A HIGH RESOLUTION MILLIMETER WAVE PHASE METER FOR DISPERSION SPECTROSCOPY

H. Liebe and A. Diede, Institute for Telecommunication Sciences, National Telecom & Inf. Adm., DoC, Boulder, CO 80302

A sampling, digital millimeter wave phase meter was developed capable of resolving the phase of a 60 GHz resonance signal to better than 2×10^{-8} degrees (corresponding to a frequency resolution of $< 1 \times 10^{-9}$) without being affected by an equivalent 60 dB/km change in signal amplitude. The phase meter is the key to accurate absolute intensity measurements of gaseous millimeter wave spectra by means of detecting refractive dispersion (Liebe et. al., IEEE Trans. AP-25(3), 327-335, 1977). Care was exercised to isolate reference and measurement channel. Time period averaging is employed. A novel gating logic generates the time interval to be counted over one sampling (sweep) period. The phase result is displayed as the average of 10^3, 10^4 or 10^5 samples; the repetition rate is 1, 2.5, or 5 kHz hence a time resolution between 0.2 s (10^3, 5 kHz), and 100 s (10^5, 1 kHz) can be attained. Such flexibility permits to adapt to different measurement situations arising from the need to cope with the dynamic response of the high Q ($> 2 \times 10^5$) preselecting resonance filters while still obtaining an optimum S/N. The operating principle and various results in connection with 60 GHz oxygen line and band shape studies will be presented and discussed.

A3-3
1430

ON THE USE OF STATISTICAL DESIGN AND ANALYSIS IN ASSESSING THE PROPERTIES OF A RECEIVER IN A COMPLEX ENVIRONMENT:*

Richard Mensing and Justin Okada,
Lawrence Livermore Laboratory,
University of California, P.O.
Box 808, Livermore, California 94550

In recent years there has been an increasing recognition of random CW and systematic variation that exists in basic measurements (current, energy, etc.). Awareness of such variation is important, for example, in realistically assessing the survivability of a system due to various electromagnetic environments. Thus, many experiments are being planned for the purpose of evaluating the random distribution of measurements in many situations. This paper discusses the use of statistical design and analysis in such experiments.

The principles of statistical design (e.g., replication, randomization) as well as the important question of the number of replications necessary for a valid statistical analysis are discussed. Some statistical methods (e.g., tests of goodness of fit, distribution function estimation) are outlined and a method of describing the random variation is suggested.

An experiment planned to assess the effect of scatterers on properties of a receiver in a complex environment is critiqued. The use of statistical design and analysis is illustrated to the extent possible for this experiment.

*Work was performed under the auspices of the U.S. Department of Energy by the Lawrence Livermore Laboratory under contract number W-7405-ENG-48.

POSTER SESSION
Wednesday Afternoon, 8 Nov., UMC West Ballroom
Chairman: C. M. Butler, University of Mississippi, University, MS

Topic A: SEM

B7-1
1400

ANALYTIC DETERMINATION OF SEM POLES AND RELATED COEFFICIENTS FOR THIN-WIRE DIPOLE ANTENNAS

David C. Chang and Ahmad Hoorfar, Electromagnetics Laboratory, University of Colorado, Boulder, CO 80309
S.W. Lee, Electromagnetics Laboratory, University of Illinois, Urbana, IL 61801

Analytical expression for the frequency-domain current induced on a thin-wire antenna of radius a and half-length h has been previously obtained by Shen (IEEE-APS, 16, 5, 542-547, 1968) in terms of the current existing on an infinite antenna, plus the multiple reflections from the two ends. More recently, we have shown the formula can be modified to yield a satisfactory result for both a transmitting and a receiving antenna of all incidence angles, and to cover a very broad frequency range within the assumption of a thin-wire, i.e., $(\ell n\ 2h/a)^2 >> 1$ and $(ka)^2 << 1$. Equipped with these results, we investigate in this work how the formula of a transmitting antenna can be recast in a form thereby the positions of the SEM poles in the complex frequency plane can be determinied analytically. In addition, the explicit expression for the current distribution of each mode, as well as the admittance function in terms of the product of modal functions, can be uncovered. More specifically, we can show the SEM poles can be determined from the resonant condition of

$$F(\omega) = 1 - \Gamma^2(\omega) I_\infty^2(\omega; 2h) = 0 \qquad (1)$$

where Γ is the reflection coefficient of an incident current wave onto the end of a slim-infinite antenna; $I_\infty(\omega; z-z')$ is the current at z on an infinitely-long antenna eminating from a source at z'. At $\omega = \omega_s$ so that $F(\omega_s)=0$, the current on the finite antenna is then given as

$$i_s(z) = I_\infty(\omega_s; h-z) \pm I_\infty(\omega_s; h+z) \qquad (2)$$

where (±) sign is for the even and odd modes on the antenna. It is shown that results obtained from (1) and (2) compared well with the numerical work of Tesche [IEEE-APS, 21, 1, 53-63, 1973].

B7-2
1400

COMPARISON OF PRONY'S METHOD (COVARIANCE METHOD - CV) AND AUTOCORRELATION METHOD (AM)

Tapan K. Sarkar, Dept. of Electrical Engg., Rochester Institute of Technology, Rochester, N.Y. 14623

It happened that Gaspard Clair François Marie Riche (1755-1839) a Lyonnais mathematician, physicist and civil engineer in eighteenth-century, France, with particular aptitude and inclination toward numerical analysis and its applications to the interpretation of measurements, became interested in the behavior of aqueous gases. He tried to fit exponentials to some measured data in 1795 (J.Ecole Polytech., t.1. An.IV, Dec. 1795). The period in which Riche lived was one that made everyone's life rather exciting, and his was no exception. But we cannot stop to explain how he fared in the Revolution, under Napoleon, and in the Restoration. Suffice it to say that he went on through a very rich life to become Baron de Prony in 1828 and a peer of France in 1835. It is also interesting to note that the name Prony to a civil and mechanical engineer implies the work brake and not transient phenomenon.

It is well known that Prony's method (which might better be called Riche's method) yields excellent results of characterizing transient waveforms by poles and zeros, when the data is noise free. However when noise is present, Prony's method may fail. Hence a pseudo least squares extension of Prony's method is made which yields the popularly known CV and not AM. The basic difference between the two methods is that the coefficients f_i of the polynomial equations are obtained from different equations. In

$$\sum_{\tau=0}^{M-1} f_\tau \left[\sum_{t=k}^{K-1} x_{t-\tau}\, x_{t-j} \right] = 0 \; ; \text{ for } j=0,1,\cdots,M-1; \; f_0 = 1$$

where x_t is the sampled data of length K and M is the order of the filter, k = M yields CV and k = 0 is AM. The difference in the results due to change of the lower limit sometimes could be castastrophic. The basic differences are: 1) AM yields a biased estimate for the poles whereas CV yields an unbiased estimate. 2) AM windows the data by assuming it to be zero outside the K-samples and CV does not. 3) CV sometimes yield non-physical power-spectral density and AM always yields stable poles. The details of the 3 conclusions may be found in (T.K. Sarkar, AFWL,SR2). In spite of these basic fundamental differences, the Prony practitioners use AM and not CV.

As an example Dudley (AFWL,MN51) shows why his AM yields a biased estimate for the poles. Had he used CV, his poles would have been unbiased. Also Van Blaricum and Mittra (AFWL, IN301) uses AM instead of CV. It is not a big deal which method one uses, but one must be aware of the pitfalls of that method. Otherwise it may lead to erroneous conclusions.

B7-3
1400

ON THE PHYSICAL REALIZABILITY OF BROADBAND EQUIVALENT CIRCUITS FOR WIRE LOOP AND DIPOLE ANTENNAS:

L. Wilson Pearson and G. W. Streable, Department of Electrical Engineering, University of Kentucky, Lexington, KY. 40506

Baum (Interaction Note 295, March 1976) has introduced a formal equivalent circuit construction for antennas in a lossless medium based on the Singularity Expansion Method representation of the current on the structure. The bandwidth over which the equivalent circuit approximates the impedance of the antenna can be made arbitrarily large, in principle, by including a sufficient number of SEM poles. Singaraju and Baum (1978 Nuclear EMP Meeting, University of New Mexico, June, 1978) have investigated the physical realizability of resulting admittances for the thin dipole based on an approximate application of Hallen's solution for the current on the wire in order to test the positive real (p.r.) properties of the terminal admittance function. They concluded that the admittance components contributed by each conjugate pole-pair are individually p.r. when treated in Baum's modified pole admittance form.

This paper presents the results of a study of the p.r. properties of wires loops and dipoles based on the existing numerically-derived SEM represintation for these structures. The pole-pair admittance p.r. result for the dipole by Singaraju and Baum is not corroborated by the numerically-derived data. The departures from p.r. are quite small, however, and are potentially attributable to numerical errors. The individual pole-pair admittances for the loop are substantially in violation of p.r. conditions. The admittances formed by summing all of the pole-pair admittances associated with a single eigenmode (terminal eigenadmittances) exhibit p.r. behavior.

The terminal eigenadmittances are amenable to Bott-Duffin synthesis techniques. Results are presented comparing computed terminal currents at the driving point of the antenna with a circuit analysis program computation of the equivalent circuit currents.

B7-4
1400

NOISE PROCESSES RESULTING FROM USE OF SAMPLING OSCILLOSCOPES IN SEM MEASUREMENTS:

T. L. Henderson, Department of Electrical Engineering, University of Kentucky, Lexington, KY 40506.

One method for physically determining the SEM description of a metallic body is to record the resonance decay curve at one or more points on the body following experimental application of an impulsive electromagnetic excitation at another point, and determining the poles and residues of the resulting waveform $y(t)$. If the bandwidth requirements are severe, as is often the case when miniature scale models are being used, then it is practical to use a sampling oscilloscope with a digital output interface. However, only one ordinate of $y(t)$ is recorded during each "shot" (i.e., presentation of impulsive excitation), so repeated shots are necessary to record the complete waveform. At least two types of errors can result: (1) An inherent "time-jitter" within the triggering circuitry of the oscilloscope, and (2) the effects of slight shot-to-shot variations in the amplitude of the excitation. Under suitable assumptions the effect of both errors is that of an additive, non-stationary, zero-mean, white, discrete-time noise process. The type (1) errors produce a contribution whose time-dependent variance, $S(t)$, is proportional to the squared derivative, $(y'(t))^2$. Type (2) errors produce two correlated effects; one masquerades as a type (1), the other produces a variance proportional to $(y(t))^2$. The net effect is that $S(t)$ is proportional to

$$[a\ y(t) + b\ y'(t)]^2 + [c\ y'(t)]^2$$

where a, b, c are constants. Effects of non-unity loop gain ("dot response") in the sample/hold circuit are also discussed, as are signal averaging and processing of data from experiments with multiple points of excitation and measurement.

B7-5
1400

CONDITIONS OF VALIDITY FOR THE CLASS 1 AND CLASS 2 SEM COUPLING COEFFICIENTS

L. Wilson Pearson[1], Donald R. Wilton[2], Fwu-jih Hsu[1], and Raj Mittra[3]

In his initial exposition of SEM(Baum, Interaction Note 88, AFWL, 1971), Baum presented several alternative forms for the coupling coefficient in the SEM construction of transient skin currents. He also identified the potential existence of a contribution to the total transient current resulting from an entire function in the transformed domain representation of the current. Subsequent work has demonstrated that an interrelationship exists between these two issues.

The Class 1 coupling coefficient form appears to provide the correct solution for the transient currents induced on a conducting sphere, and no entire function contribution is required. On the other hand, the use of the Class 1 coupling coefficient with Tesche's thin-wire SEM results(Tesche, Interaction Note 102, AFWL, 1972) produces clearly anomolous current responses, while the Class 2 form provides favorable results.

In the present work we present evidence that the critical factor in the sucess of the Class 1 coupling coefficient is the ordering of the pole summation according to the eigenmodes with which the poles are associated. Because such ordering includes poles deep in the left half of the s-plane, this representation may depend critically on the numerical accuracy of the poles. The straight wire and the wire loop are used as test structures to demonstrate these issues.

The Class 2 coupling coefficient is justifiable based on a consideration of the asymptotic behavior of the current in the s-plane. A representation in terms of this coefficient is potentially useful when one does not posess complete eigenfunction pole set data. Such a situation might arise, for example, when a problem is treated numerically or when the SEM representation is derived from transient data by way of the Prony method.

1. Department of Electrical Engineering, University of Kentucky, Lexington, KY 40506
2. Department of Electrical Engineering, University of Mississippi, University, MS 38677
3. Electromagnetics Laboratory, Department of Electrical Engineering, University of Illinois, Urbana, IL 61801

Topic B: DETECTION AND SENSING

B7-6
1400 NON-DESTRUCTIVE TESTING OF A CYLINDRICAL CONDUCTOR WITH AN INTERNAL ANOMALY - A TWO DIMENSIONAL MODEL: J.R. Wait and R.L. Gardner, Cooperative Institute for Research in Environmental Sciences, University of Colorado/NOAA, Boulder, CO 80309

There is a need to evaluate the internal structure of wire ropes and similar cylindrical conductors. This has led to an extensive technology called non-destructive testing (NDT). A good survey of the electromagnetic methods are given by Libby ("Introduction to Electromagnetic Nondestructive Test Methods", New York, John Wiley & Sons, 1971). One of the basic configurations is a solenoidal coil that tightly encircles the wire rope specimen. As indicated in a two-dimensional analysis (J.R. Wait, "The electromagnetic basis for non-destructive testing of cylindrical conductors", (in press), IEEE Trans. I&M, Sept. 1978), the impedance of the solenoid can be related uniquely to the conductivity and permeability of the wire rope if it can be assumed homogeneous. It is the purpose of the present analysis to examine the effect of an internal flaw. While more complicated cases (D.A. Hill and J.R. Wait, "Scattering by a slender void in a homogeneous conducting wire rope", (in press), Applied Physics, 1978) can be treated, we consider here an idealized two-dimensional anomaly or cylindrical flaw of radius c that is contained within the otherwise homogeneous cylinder of radius a.
Even for the assumed two-dimensionality, a rigorous solution is complicated. However, since we are interested in the threshold of the detectability of an internal anomaly, a perturbation approach is quite permissible. Here the anomaly is assumed to be "excited" by the field that would exist if the anomaly or flaw were not present. This primary field actually induces a monopole, dipole, and higher order multipoles. In the case where the wire rope is encircled by an idealized uniform solenoid, the primary magnetic field has only an axial component and the primary electric field is entirely azimuthal. These excite, respectively, a line magnetic monopole and a line electric dipole within the anomaly. If the transverse dimensions of the cylindrical flaw are small (in terms of skin depth of the wire rope material), the higher order multipoles are negligible. The secondary fields of the induced monopole and the dipole are the external observables. In the simplest case, they manifest themselves as a modification of the impedance of the encircling solenoid.
A preliminary problem that we need to consider is the excitation of a cylindrical flaw by a known form of primary field. In this manner, the polarizabilities or strengths of the induced monopole and dipole can be ascertained. We then use these results in the composite problem where the exciting field is produced by the encircling solenoid.

B7-7 1400 PERTURBATION BY AN INTERNAL VOID IN A CONDUCTING CYLINDER EXCITED BY A WIRE LOOP:

D.A. Hill and J.R. Wait, ITS/NTIA and ERL/NOAA, U.S. Department of Commerce, Boulder, CO 80303

Electromagnetic NDT (Nondestructive Testing) is widely used for inspection and evaluation of metals (H.L. Libby, "Introduction to NDT Methods", McGraw-Hill, 1971), and electromagnetic methods in NDT of wire ropes have recently been reviewed (unpublished report for U.S. Bureau of Mines by J.R. Wait). Both DC and AC methods are currently in use. In both methods, the magnetic field is applied along the axis of the rope, and rope irregularities produce magnetic field changes which induce voltages in the sensing coils. A two-dimensional model of solenoidal excitation of a homogeneous wire rope has now been analyzed fully (J.R. Wait, IEEE Trans. I&M, Sept. 1978). The toroidal coil excitation was also treated by invoking the principle of duality. A further analysis deals with a two-dimensional model for a wire rope with an internal anomaly (J.R. Wait, R.L. Gardner, unpublished report, March 1978), and the resulting change in the input impedance of the surrounding solenoid.

Here we consider a three-dimensional model in which an electric current ring is used to model a thin solenoid or multi-turn wire loop. The analogous problem of a magnetic current ring has already been solved (D.A. Hill and J.R. Wait, Jour. Appl. Phys., 48, 4893-4897, 1977); thus the needed primary field expressions can be obtained from the magnetic ring current solution by duality. We allow for the presence of a small slender void within the otherwise homogeneous rope. Such a void can be considered a model for a broken wire within the rope or similar internal flaw. The void is allowed to be oriented at any arbitrary angle to the rope axis to account for the winding geometry. Following a previous analysis (D.A. Hill and J.R. Wait, Appl. Phys., in press, 1978), we compute the induced electric and magnetic dipole moments from the primary fields and the electric and magnetic polarizabilities of the void. The external fields of the induced dipole moments are then calculated using the previous formulation for dipoles of arbitrary orientation. These external fields are the observable quantities in any nondestructive testing method.

The most common methods of wire rope testing detect the average or integrated value of the circumferential electric field with a receiving solenoid which completely encircles the rope. Usually, this is done by making a measurement of the mutual impedance of two coaxial loops or similar arrangements. But, in addition, one should be able to probe the detailed structure of the external magnetic field components with small sensing coils.

B7-8 1400 COMPUTER AIDED DESIGN OF TEM HORN ANTENNAS FOR ELECTROMAGNETIC PROBING: Donald R. Belsher, Robert H. McLaughlin, Electromagnetic Fields Division, National Bureau of Standards, Boulder, CO 80303

Initial work with a short pulse system using a constant impedance TEM horn antenna showed it to be a broadband, high fidelity radiator. It was desired to lower the aperture reflections and improve the efficiency, especially at the lower frequencies, in order to achieve a flat very wide band response. For this work a simple and rapid approach to the design and construction of these antennas was needed. For evaluation a two-section antenna model was used. A feed section, containing a coaxial to strip line connector, having a length l_1 and constant impedance was followed by a transition section of length l_2 having a variable impedance. A short basic program was written for use on a minicomputer to evaluate Wheeler's conformal-mapping approximation for the impedance of wide parallel strips (H.A. Wheeler, IEEE Trans. MTT, 1964). The program was arranged to accept a selected impedance curve, a length and height at the aperture and then to print out a listing of the strip width, strip spacing, strip length and impedance at selected points along the antenna axis. Several of these antennas were fabricated and the on axis frequency response and ringing evaluated using a pulse system approach.

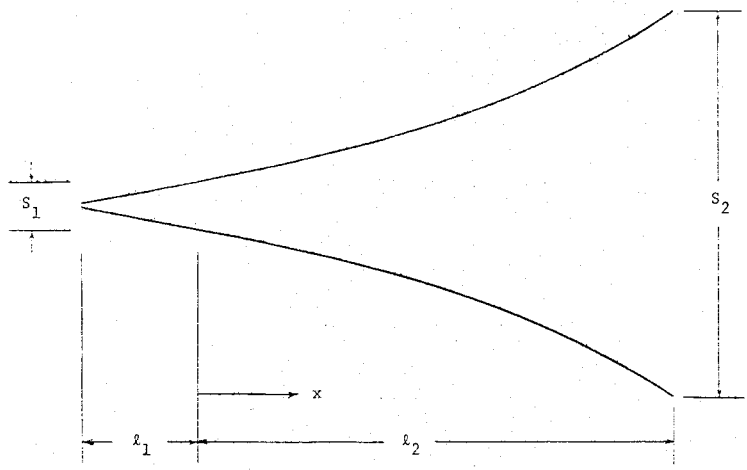

Separation Profile (Side View)

B7-9
1400

PLANE-POLAR TECHNIQUE FOR FAR-FIELD COMPUTATION FROM NEAR-FIELD MEASUREMENTS: V. Galindo-Israel, Y. Rahmat-Samii, and R. Mittra[+], Jet Propulsion Laboratory, California Institute of Technology, Pasadena, CA 91103

Recent advances in "near-field" techniques have demonstrated that the method of measuring the near-field and reproducing the far-field by computation can be used with a high degree of accuracy for microwave antennas (D. M. Kerns, NBS J. Res., Jan-Mar. 1976; D. Paris, W. M. Leach, Jr., and E. B. Joy, IEEE Trans. Ant. Prop., Vol. 26, May 1978, and G. V. Borgiotti, IEEE Trans. Ant. Prop., Vol. 26, July 1978). There are three basic geometrical configurations that have been used for measuring the near-field data. These configurations are: 1. planar, 2. cylindrical, and 3. spherical. In this paper we address ourselves to only the planar configuration. In this case, past attempts have concentrated on using a rectangular scan geometry together with an FFT algorithm to compute the far-field.

An alternative useful geometry is the plane-polar geometry. With this geometry it is still possible to correct for the probe pattern when this is desirable. Furthermore, this geometry permits application of a new series expansion for the radiation integral to evaluate the far-field (V. Galindo-Israel, and R. Mittra, IEEE Trans. Ant. Prop., Vol. 25, pp. 631-641, Sept. 1977; and R. Mittra, Y. Rahmat-Samii, V. Galindo-Israel, and R. Norman, IEEE Trans. Ant. Prop. - submitted). This expansion has several advantages over the FFT. First, the polar grid measurements require an interpolation to rectangular coordinates before an FFT can be used. If a large number of far-field data points are required, the series expansion has been shown to be at least comparable to the FFT in efficiency. The choice of far-field observation points is not limited with the series, thus permitting accurate and fast interpolation. Finally, there is no need for a 'zero fill in' when the series expansion is used, and thus, in general, fewer data measurement points are usually required. Other important advantages exist.

Mechanically, there are advantages in this measurements scheme since only a single scan (radial) is required for the probe. The antenna under measurement is then moved rotationally. This is similar to the cylindrical geometry (G. V. Borgiotti, IEEE Trans. Ant. Prop., Vol. 26, July 1978), but the plane-polar geometry permits the measured antenna to point upward towards a clear sky - thus providing both mechanical and electrical advantages. Details of the method including techniques for probe corrections as well as results (as available) will be presented.

[+]The order of the listing of the authors is arbitrary.

Topic C: CAVITY BACKED APERTURE

B7-10
1400

Measurement and Calculation of Interior Fields and Impedance of One-Port and Two-Port Coaxial Cavities

Michael G. Harrison and Chalmers M. Butler, Department of Electrical Engineering, University of Mississippi, University, MS 38677

Measurements have been accomplished on the relative magnitude and phase of the normal electric field and the tangential magnetic field on the inner surfaces of the forward and rear end plates of one- and two-port coaxial cavities. The range of measurement frequencies included both the first axial and transverse resonances of each cavity. The input impedance of the two-port cavity has been measured over the same frequency range.

The measured field and impedance values have been compared to results obtained from solutions to integral equations. The integral equations are similar to those presented by Schwinger and Saxon, Marcuvitz, and Collin. In the earlier treatments, variational solutions for the susceptance of the geometry of interest were obtained. The present formulation, which includes the dominant TEM terms and infinite series of higher order mode terms, has been solved by numerical techniques. The major difficulty overcome in this solution technique was the extreme slowness of convergence of the series of terms in the kernel involving Bessel functions.

The calulated and measured impedance of the two-port cavity showed very good agreement over the entire range of measurements (500-1700 MHz). The impedance values also agreed very well with those computed from a combination of data from Marzuvitz's Waveguide Handbook and transmission line theory. This transmission line approach began to fail as the first transverse resonance was approached. Very good agreement has also been obtained between measured and calculated values of interior fields for both cavities. It is important to note that this method of calculating cavity impedance and fields is not limited by cutoff frequencies of transverse modes as was earlier published work. This solution technique is, therefore, suitable for broadband or time-domain application.

B7-11
1400

A PARAMETRIC STUDY OF ELECTROMAGNETIC COUPLING INTO SHIELDED ELECTRONIC SYSTEMS:

R. J. Prehoda and R. M. Swink, Naval Surface Weapons Center, Dahlgren, VA 22448, and D. C. Chang, Electromagnetics Laboratory, University of Colorado, Boulder, CO 80309

The coupling of electromagnetic energy into electronic systems can cause severe degradation of system performance. In those cases where EM coupling enters the system through cables, seams, holes or other inadvertent coupling paths, the parameters which determine the degree of coupling such as angle of incidence, internal configuration, etc. cannot always be well defined. Any theoretical or experimental approach to examine the interaction of these parameters results in a mass of data which is often very difficult to interpret. In the approach to be presented, the canonical problem of penetration of electromagnetic energy into a cylindrical enclosure through a small aperture is solved in terms of an equivalent circuit. Through analysis of this equivalent circuit, a procedure is then derived for performing an efficient parametric analysis. The mass of data resulting from this parametric analysis is then condensed and interpreted by utilizing basic statistical methods. Data will be presented to illustrate the power distribution of antenna patterns associated with external configurations, the distribution of energy resulting from variations of internal configurations and probabilities associated with the interactions of load impedances with the equivalent circuit representing the structure.

B7-12
1400

EXTERIOR-INTERIOR COUPLING OF A CAVITY BACKED APERTURE IN AN INFINITE PERFECTLY CONDUCTING PLANE SCREEN: W. A. Johnson* and D. G. Dudley, Department of Electrical Engineering, University of Arizona, Tucson, AZ 85721

This paper is a continuation of previous work (W. A. Johnson and D. G. Dudley, "Complete Dyadic Formulation of Aperture Coupling into a Rectangular Cavity," URSI Meeting, Boulder, Jan. 1978). The exterior-interior coupling of a cavity backed aperture in a perfectly conducting plane screen is considered. The cavity is rectangular, has perfectly conducting walls, and contains a straight, thin wire perpendicular to one of the cavity walls. Integral equations for aperture fields and wire currents are reviewed. A summation method for potential dyads allows extraction of the singularity, Real $\frac{e^{-ikR}}{2\pi R}$, provided source and observation points are close together. This summation technique holds under the restriction that the smallest cavity dimension in the aperture is less than 1/2. Numerical results for the aperture fields are given along with some comments concerning their symmetries. The paper concludes with a discussion of the numerical difficulties involved in obtaining the transient fields.

* Currently at University of Mississippi, Dept. of Electrical Engineering, University, Mississippi 38677

Topic D: ANTENNA ARRAY

B7-13
1400

POWER-APERTURE PRODUCT CONSIDERATIONS IN THE DESIGN OF A DISTRIBUTED TRANSMITTING ARRAY

B.D. Steinberg, Valley Forge Research Center
University of Pennsylvania, Philadelphia

Sometimes it is desired to achieve a larger power density at the focal point of a transmitting array, or on the axis of the far field pattern, than the power-aperture product will permit. Splitting the aperture into several subaperatures may help, provided that the radiation launched from the several antennas arrive cophased at the focus.
Once the array is distributed, i.e. different portions are fed from different sources, conventional wisdom regarding power-aperature product may be inadequate for system design purposes. For example, in some systems the total available power is constrained while in others the limit is on the power per antenna. In some the maximum individual antenna size is limited while in others the total real estate covered by the antennas is constrained. Sometimes also the problem of electric field breakdown in the RF circuitry or in the immediate vicinity of the antenna limits local radiated power and thereby imposes a constraint which can only be overcome by using multiple antennas.
Tradeoffs are examined and rules for maximizing power density on axis, subject to these constraints, are discussed.

B7-14
1400

ACTIVE IMPEDANCE OF DIPOLE ELEMENTS IN A HARDENED PHASED-ARRAY ANTENNA:

J.A. Fuller and R.L. Moore, Engineering Experiment Station, Georgia Institute of of Technology, Atlanta, Georgia 30332

The performance of a planar phased-array antenna that incorporates dipole elements is discussed. The dipoles are embedded in a dielectric layer that protects the array face, and the dielectric is assumed to be imperfect (dissipative). The array performance is described in terms of beam-scan limitations that result from excessive variation of active element impedance. The results to be discussed are concerned with horizontal dipoles, and the effect of the layer is of primary interest. The results clearly indicate the sensitivity of the usable beam-scan range to the thickness and electrical properties of the dielectric layer and to the array and element dimensions.

The analysis is accomplished by a moment-method calculation for a periodic array of thin-wire elements. The elements are located in the central layer of a general three-layer space; but for most practical cases the lower layer is taken as a ground plane, and the upper layer is air. The array is assumed to be of infinite extent, and periodicity is utilized to develop a Green's function. The Green's function is just the solution for a periodic array of Hertzian dipoles located in the three-layer space, and a "grating lobe series" representation is derived directly from the well-known solution for a single dipole in a three-layer space (J.R. Wait, Electromagnetic Waves in Stratified Media, Pergamon Press: New York, 137-146, 1962). The array elements are modeled by piecewise-linear wire segments that may have arbitrary orientation. The element current distribution is expanded in piecewise-sinusoidal basis functions, and a solution is obtained by Galerkin's method. The convergence questions that arise concern, first, the grating lobe series for the Green's function and, second, the basis for the current distribution. Convergence is examined in terms of numerical behavior and by comparison with results of others (e.g., V.W.H. Chang, Proc. IRE, 56, 1892-1900, 1968). Experimental validation of the model by measurements in array simulators is currently in progress.

B7-15
1400

EFFICIENT COMPUTATION OF COUPLING BETWEEN CO-SITED ANTENNAS FROM THE FAR FIELD OF EACH ANTENNA:

Arthur D. Yaghjian and Carl F. Stubenrauch,
National Bureau of Standards, Boulder, CO 80303

The plane-wave scattering-matrix description of antennas, introduced by D. M. Kerns at the National Bureau of Standards (NBS) nearly twenty years ago, forms an ideal theoretical framework on which to base the determination of mutual coupling between two co-sited antennas. Three important tasks were accomplished in order to translate the existing formulas into a convenient program which computes coupling efficiently.

First, the Kerns coupling formula or transmission integral was expressed in terms of the far field of each antenna, assuming the receiving antenna was reciprocal, and neglecting evanescent modes and multiple reflections. The far field conveniently characterizes an antenna and is the most common output generated either from a PO-GTD (physical optics-geometrical theory of diffraction) program or determined from near-field scanning measurements. Secondly, the coupling formula was generalized to apply explicitly to arbitrary relative orientations of the antennas. Since the far field of each antenna is usually expressed in a coordinate system fixed in each antenna, and the original coupling formula involves an integration of the dot product of the two vector far fields in a mutually reoriented system, the proper Eulerian angle transformations between the fixed and mutual coordinate systems were required to accomplish this second task. Thirdly, an efficient scheme of computation was developed to numerically evaluate the resulting coupling integral (double Fourier transform), which now involves only the far field of each antenna (expressed in its coordinate system), and, of course, their mutual separation and orientation (three Eulerian angles of each antenna). Although the sampling theorem and FFT algorithm apply to the coupling integral, initially computer time became prohibitive for typical microwave antennas when separation exceeded more than a few antenna diameters. Fortunately, it was shown analytically that essentially only the far fields within the sheaf of angles mutually subtended by the antennas are needed to compute the coupling. Beyond this sheaf the far fields can be set equal to zero with little degradation in accuracy. This effective reduction in far-field spectrum in turn artificially band limits the coupling quotient, thus allowing (via the sampling theorem) larger integration increments with an accompanying reduction in computer time.

Mutual coupling curves have been computed from far fields generated by PO programs and from far fields determined from NBS near-field scanning. Comparisons have been made between the computed coupling curves and directly measured coupling between antennas co-sited on an outdoor range.

Commission C Session 5

CIRCUITS AND SYSTEMS
Wednesday Afternoon, 8 NOV., UMC 156
Chairman: L. Weinberg, CCNY, EE Dept., 140th and Convent, New York, NY 10031

C5-1
1330 STATISTICAL CIRCUIT DESIGN: R. K. Brayton, Thomas J. Watson Research Center, Yorktown Heights, NY 10598

This talk will provide a survey of some recent developments in statistical circuit design. An optimal statistical circuit design is one which is optimized in the presence of statistical uncertainties about the circuit parameters and components, or environmental factors. These statistical variations happen either through uncertainty at the time of manufacture or during the lifetime of the circuit. The objective of the design may be to maximize manufacturing yield, maximize circuit performance subject to yield being greater than a given value, or to minimize the manufacturing cost by assigning optional tolerances on the components. Although the particular application is electrical circuit design, the methods, which are extensions of optimization theory, can be used in a wide variety of applications.

C5-2
1400 NONLINEAR CIRCUITS: R.W. Newcomb, Electrical Engineering Department, University of Maryland, College Park, MD 20742

Progress in certain areas of nonlinear circuits most familiar to the author will be surveyed. The field is developing rapidly. Turning to our own work, which will be most fully discussed in the talk, an almost "all-encompassing" nonassociative algebra of nonlinear systems will be presented. It is most useful for polynomic driven systems.

C5-3 1430 MIXED LUMPED - DISTRIBUTED FILTER NETWORKS: Louis Weinberg, Department of Electrical Engineering, City College and The Graduate School, New York, NY 10031

An important problem in system theory is the synthesis of mixed lumped - distributed networks that realize a given transfer function. It is only in the past few years that this problem has been solved. Nearly all of the solutions make use of functions of two complex variables.
However, it is also possible - and, in fact, desirable - to solve this problem using a single complex variable. In the paper we present an efficient algorithm that is based on a set of necessary and sufficient conditions for realizability formulated by A. J. Riederer and L. Weinberg. The network that is realized is the filter configuration of a lossless two-port network terminated at both ends in resistances. In driving and using our algorithm we work with the associated driving-point function to realize a cascade connection of lumped two-port networks alternating with uniform commensurate transmission lines with the overall lossless network, terminated in a resistance. The driving-point function that is realized is a quotient of two functions, each of which is an exponential polynomial whose coefficients are polynomials.

C5-4 1545 CIRCUIT LAYOUT: E. S. Kuh, College of Engineering, University of California, Berkeley, CA 97420

With recent advances in microelectronics, the field of circuit layout has become more important than ever. Unfortunately, most layout designs for LSI chips are still being done manually. In this paper, we present a new approach to both the placement problem and the routing problem. The basic idea is to solve first the simple one-dimensional problems and then apply the one-dimensional results to the general problem of layout. In the one-dimensional placement problem, an efficient algorithm has been developed based on key properties of interval graph. In the one-dimensional routing problem, the necessary and sufficient condition for optimum single-row routing has been obtained.

C5-5 APPLICATIONS OF MATROIDS TO PROBLEMS IN NETWORK DESIGN:
1615 A. Kershenbaum, Polytechnic Institute of New York, Brooklyn, NY 11201

The theory of matroids provides a unifying framework for the solution of many of the most important problems in the area of network design. First, the basic theory is briefly introduced, including properties of matroids which give rise to effective algorithms for the solution of problems definable within the framework. Problems of network layout, terminal assignment, and network flows are then discussed along with their interrelationship within the theory. In particular, a common approach to their solution is presented. Finally, the solution of more complex problems which have recently been approached with the matroid theory will be discussed. Among these problems are the capacitated minimal spanning tree problem and the traveling salesman problem.

THE CHARACTERIZATION AND MODELING OF NOISE AND INTERFERENCE
Wednesday Afternoon, 8 Nov., UMC 159
Chairman: P. M. McManamon, NTIA/ITS, Boulder, CO 80302

E2-1
1330 VARIANT LINEAR PROCESSES : John B. Smyth and John A. Durment, Smyth Research Associates, San Diego, California 92123

Fourier and Laplace transforms have wide application in the solution of problems representing linear processes which are invariant. Neither is applicable when the linear process is variant. Indiscriminate use of these methods has created a great deal of science fiction. For example, the Fourier analysis of the radio emissions from the transient lightning discharge has led to many erroneous conceptions of the basic physical process, thwarting an adequate description of the observables of the phenomenon.

When the coefficients in the equations representing a linear process are not constant, "Laplace integrals" may not be used to rescue one from the horrendous task of evaluating the convolution integral.

E2-2
1405

NEW RESULTS FOR STATISTICAL-PHYSICAL MODELS OF ELECTROMAGNETIC NOISE

David Middleton, Contractor, National Telecommunications and Information Administration, Institute for Telecommunication Sciences, Boulder, Colorado 80303 and 127 East 91st, New York, New York 10028

Recent work of the author (D. Middleton, IEEE Trans. Electromagnetic Compatibility, Vol. EMC-19, No. 3, August 1977, pp. 106-127, and NTIA (U.S. Dept. of Commerce) Contractor Technical Reports NTIA-CR-78, June, September 1978) has demonstrated experimentally verified, tractable, analytic models of man-made and natural electromagnetic noise. These models provide the basic first-order statistics needed to describe both qualitatively and quantitatively the three basic classes (Class A, B, C) of such noise, and, to enable one to calculate probability measures of receivers performance in such EMI environments (A. D. Spaulding and D. Middleton, IEEE Trans. on. Comm., Vol. COM-25, No. 9, September, 1977, pp. 910-923). The key feature of these models is that they are canonical: they are independent in mathematical form of the particular physical noise source, and the model parameters are (i) physical and (ii) measurable. The canonical nature of these models permits one to describe all noise and interference mechanisms in practice, subject only to the two conditions that: (1) the noise sources emit independently, and (2) the receiver in question is narrow-band, conditions very rarely violated in applications.

Among the new results obtained are (i) the demonstration that Class C noise (≡ Class A + Class B) can be effectively regarded as a form of Class B noise ($\Delta f_{receiver} < \Delta f_{noise}$); (ii) pdf's and APD's for the Class B (and C) envelopes (E) and amplitudes (X); (iii) approximate and "exact" procedures for determining the $P_3 \equiv (A_A, \Gamma_A', \Omega_{2A})$ and the $P_6 \equiv (A_B, \Gamma_B', \Omega_{2B}, \alpha, b_{1Q}, N_I)$ model parameters of the (approximate, i.e., tractable) analytic models; and (iv) various important questions regarding the statistical estimation of model parameters, subject to finite data samples.

E2-3 1450 MARKED POINT PROCESS MODEL FOR VLF NOISE: Stanley R. Robinson and Joseph W. Carl, Air Force Institute of Technology, Department of Electrical Engineering, Wright-Patterson AFB, OH 45433

A new statistical model is presented for the combination of atmospheric/thermal noise encountered in very low frequency (VLF) systems. We represent the noise as a sum of two independent inhomogeneous point processes, each with arbitrary rate parameters. In addition, one of the processes is assumed to have random amplitude weights (marks) at each occurance time. The marked process is used to represent the impulsive atmospheric noise, while the (filtered) unmarked process is used to represent the thermal noise.

The advantage of such an approach in contrast to previous work is that the random process model is totally impulsive rather than a mixed sum of continuous and impulsive processes. Thus, this model has a statistical characterization that is more nearly complete compared to the usual first order densities commonly used. We physically justify such a model by assuming the events times are representing the electron flow induced in the antenna. Furthermore since any measurement can be thought of as the output of a filter, the measurements can be made continuous just as if a continuous, thermal-like noise were introduced at the input in addition to the impulsive component due to atmospheric noise. We are further encouraged in that the optimal detector for a point process model becomes a matched filter in the limit of a large rate parameter. The optimal detector for Gaussian noise measurement is therefore, a special case of the optimal detector for a point process model.

As an indication of the validity of the approach, we suppose the marks are statistically independent, identically distributed, Gaussian random variables. The new noise model is then passed through a suitably chosen bandpass filter and statistics of the output envelope obtained. The model parameters are numerically chosen to match empirically derived first order densities which are available in the literature. The empirical data is shown to be in good agreement with that predicted by the model. Finally, implications of such a model for optimal signal detection are discussed.

E2-4 THE CHARACTERIZATION OF NOISE IN COMMUNICATIONS
1550 EARTH TERMINALS:

D.F. Wait, National Bureau of Standards, Boulder, CO 80303

The National Bureau of Standards has made extensive measurements of the noise performance of several communications earth terminals in the last four years. The figure of merit (G/T) is the traditional parameter used to characterize the noise. For this purpose G/T has the disadvantage that it neither characterizes the hardware, nor the hardware plus atmosphere, because the atmospheric effects are excluded from the antenna gain (G) part of G/T, but are included in the system temperature part. Thus for extensive measurements of G/T made at various antenna elevation angle, and at various frequency, the comparative meaning of the results become fuzzy because of the varying temperature and humidity conditions during the measurement. To aid in identifying the validity and self consistency of noise measurement data, we have defined and calculate an alternate noise parameter in our measurements which we call the Noise Equivalent Flux density (NEF). NEF is an analogous to effective input noise temperature for an amplifier. Namely NEF is the noise flux density (w m^{-2} H_z^{-1}) incident normal to the aperture of a noiseless equivalent earth-terminal such that the output noise power equals the output noise power of the actual earth terminal. The advantages of NEF compared to G/T for characterizing the noise in the earth terminal will be discussed.

E2-5
1625 EMPIRICAL MODELS FOR PROBABILITY DISTRIBUTIONS OF SHORT-TERM MEDIAN MAN-MADE RADIO NOISE LEVELS IN THE U.S.: G.H. Hagn, SRI International, 1611 N. Kent Street, Arlington, VA. 22209 and D.B. Sailors, Naval Ocean Systems Center, Code 5321, San Diego, CA 92152

Empirical models have been developed to predict the probability distribution of short-term median values of environmental man-made radio noise levels in the U.S. These models provide predictions for vertically polarized antennas near earth for three specific environmental categories: rural, residential and business. Three models of increasing sophistication are given for each category: simple Gaussian, composite Gaussian, and Chi-square. The models are useful for predicting the distribution of signal-to-noise ratio necessary (but usually not sufficient) for calculating the performance of communications systems. The simple Gaussian model and the Chi-square model are especially useful for analyses when the effects of both noise and undesired signals are considered. The Chi-square model is the best model for skewed distributions and when extrapolation to the tails of the distribution (i.e., beyond the deciles) is needed. The composite (two-sided) Gaussian model is useful when the distribution is skewed, and when undesired signals are not considered. Comparisons are given for each of the models with distributions measured by the Institute for Telecommunication Sciences, Boulder, Colorado; however, these ITS data were used to develop the models. A comparison with other data is desirable, and an independent assessment of the statistical confidence levels is needed.

Commission F Session 5

PROPAGATION ABOVE THE EARTH
Wednesday Afternoon, 8 Nov., UMC East Ballroom
Chairman: J. R. Wait, CIRES, University of Colorado, Boulder, CO

F5-1
1330 EXCITATION OF THE ZENNECK SURFACE WAVE BY A VERTICAL APERTURE: D.A. Hill and J.R. Wait, Institute for Telecommunication Sciences, National Telecommunications and Information Administration, U.S. Department of Commerce, Boulder, CO 80303

The Zenneck surface wave which can be supported by a planar air-ground interface is characterized by a phase velocity greater than that of light and an attenuation in the direction of propagation along the interface. Although the significance of the radial Zenneck wave was debated for several decades, it is now generally accepted that the radial Zenneck wave is not a major contributor to the total field of a vertical electric dipole over a homogeneous conducting earth. The Zenneck wave is generally difficult to excite with a realistic source because it has a rather slow decay with height above the earth's surface. In order to examine the excitation problem quantitatively, we derive the fields of a vertical aperture which is modelled by a magnetic current sheet over a flat, homogeneous conducting earth. A two dimensional model is considered for simplicity, but the results are relevant to the practical three dimensional case.

We first demonstrate that an infinite vertical aperture with a height variation corresponding to that of the Zenneck wave will excite only the Zenneck surface wave with no radiation field. The more practical case of a finite vertical aperture is considered in detail. The resultant solution for the fields involves infinite integrals of the Sommerfeld type, but at large horizontal distances the integrals can be evaluated by the modified saddle point method. Numerical results for frequencies of 1 MHz and 10 MHz are presented to demonstrate the effect of aperture height on the field near the interface. Both land and sea paths are considered.

The fields near the aperture exhibit a Zenneck-like behavior. However, at large distances from a finite aperture, the fields take on the usual ground wave character. The transition region can be described by a simple ray optical picture involving propagation of an inhomogeneous plane wave impinging on the earth at the complex Brewster angle.

F5-2
1400 WAVE TILT AND SURFACE IMPEDANCE ON A TWO LAYERED EARTH WITH VARYING SUBSURFACE IMPEDANCE: Samir F. Mahmoud, Electrical Engineering Department, Cairo University, Giza, Egypt

The problem of a plane electromagnetic wave scattering from a two-layered earth with a periodically varying substrate surface impedance is considered. The aim is to study the effect of a finite lateral extent of an underground conducting layer such as water or oil on the wave tilt and surface impedance which are measurable quantities at the earth's surface. An integral equation for the plane wave spectrum of the reflected waves is derived and an iterative solution is outlined. The special case of a Gaussian profile of the substrate surface impedance is treated in detail and the corresponding wave tilt and impedance at the earth surface are obtained. Another solution of the integral equation which depends on the expansion of the unknown function into the orthogonal Hermite polynomials is presented for the purpose of comparison with the iterative solution. Numerical examples of the wave tilt and surface impedance are presented for frequencies 1 MHz, 150 kHz and 16 kHz representing medium, low and very low frequency plane wave excitation. Preliminary results indicate that for sufficiently fast variations of the substrate surface impedance, the wave tilt and the surface impedance are differently influenced by the subsurface. In this case, the results on the surface impedance are considerably different from those computed on the basis of locally uniform layered earth.

F5-3
1500

DETECTABILITY OF OBJECTS IN THE VICINITY OF TWO-WIRE INTRUSION SENSING SYSTEMS:

S.W. Maley, Electromagnetics Laboratory,
University of Colorado, Boulder, CO 80309

The detection of intrusions into an area on the surface of the earth by electromagnetic sensing can be accomplished by surrounding the area with two leaky coaxial cables spaced a short distance apart and located near the surface of the earth. One of the cables is then excited with an R.F. generator and the other is connected to a receiver. Energy will flow from the excited cable to the other. Any intrusion of an object into the region between the two cables will cause a change in the energy flow. Monitoring the energy flow by means of the receiver thus permits detection of such intrusions.

A key design parameter is the amount by which the flow of energy is changed by an intrusion into the region between the coaxial cables. The problem of determination of the change of receiver input voltage caused by an intrusion can be formulated in a reasonable easy and straightforward manner but the exact solution to the problem seems unattainable for most expected intrusion shapes.

A practical alternative is that of obtaining results for some idealized shapes that have varying degrees of similarity to the actual shapes of interest and that have simplicity permitting an easily usable analytical description. The result of such a study shows that the variation, ΔV, of the receiver input voltage, V, is related to the geometrical cross section, S, of the intrusion by

$$\left|\frac{\Delta V}{V}\right| \simeq \left(\frac{2|\beta|}{\pi}\right)^{\frac{1}{2}} \frac{S}{Lw^{\frac{1}{2}}}$$

where L is the length of the cables, w is the distance between them and $\beta = (k^2 - k_o^2)^{\frac{1}{2}}$ where k is the axial wave number on the coaxial cables and k_o is the wave number for propagation in free space. The earth parameters are absent from this result because of the normalized manner in which it is presented. More specifically the characteristics of the earth influence ΔV by the same factor that they influence V. This result is a rough approximation, but it was obtained for a variety of simple geometrical shapes; so its applicability is felt to be quite general provided the intrusion dimensions are of the order of $\pi/2\beta$ or larger.

F5-4
1530

ELECTROMAGNETIC PROPAGATION IN HORIZONTALLY STRATIFIED TROPOSPHERIC DUCTING ENVIRONMENTS

C. L. Goodhart, Megatek Corporation, San Diego, CA, 92106
R. A. Pappert, Naval Ocean Systems Center, San Diego, CA 92152

Modified refractive index formalism has been used to study waveguide propagation for horizontally stratified but vertically inhomogeneous tropospheric ducting environments. The formalism allows for case studies to be made for a variety of terminal locations as well as for a broad class of refractivity structure which includes the occurrence of multiple layers or ducts. Although most useful in the VHF band the waveguide formalism, depending upon the geometry of the layering and rf terminals can be used into the SHF band. Problems relating to the eigenvalue search will be discussed. Some results relating to the topology of the complex eigenvalue space will be presented as well as some path loss results for multisegmented refractivity profiles. In particular, a case study of beyond-the-horizon propagation which has been previously examined in terms of ducting dueto anelevated layer and in terms of ducting due to an evaporation duct will be re-examined in terms of the simultaneous occurrence of both an elevated layer and an evaporation duct.

IONOSPHERIC IRREGULARITIES
Wednesday Morning, 8 Nov., UMC Forum Room
Chairman: G. Millman, General Electric, Syracuse, NY

G4-1 1330 THE FORMATION, DURATION, AND DECAY OF EQUATORIAL IRREGULARITY PATCHES: THE GROUND SCINTILLATION OBSERVATIONS J. Aarons, H. Whitney, Air Force Geophysics Laboratory, Hanscom AFB, Bedford, MA 01731, E. Martin Mackenzie, Emmanuel College, 400 The Fenway, Boston, MA 02115

In a series of coordinated experiments at equatorial latitudes, intensive measurements have been made of the ionospheric scintillations of synchronous satellite beacon signals. From a study of the timing of the appearance and disappearance of scintillation activity along varying longitudes and through spaced receiver measurements it can be determined if a particular patch is developing (moving westward behind the solar terminator) or is an "old" - developed patch moving eastward.

Several examples have been observed where the irregularity patch unfolds westward, commencing predominantly at about 1940 local time during the equinox observations, shortly after sunset at 300 km. The developing patch comes to an abrupt halt at a particular longitude and then essentially moves as an entity to the east.

The East-West dimensions of the patch range from 50 km to an indeterminate size. The North-South dimensions as measured by airglow observations of depleted ionospheric regions (E. Weber, 1978, personal communication) can extend to over 2000 km. Velocities at Ancon, Peru of post-sunset to midnight irregularity motions ranged in his series of observations from 90-160 meters/sec.

The individual patches maintain their integrity over several hours. The duration of the patch of irregularities across a particular propagation path to a synchronous satellite varies from 15 minutes to several hours; graphs showing the distribution of durations will be given for observations in Peru and in the Ascension Islands.

G4-2
1355

TOTAL ELECTRON CONTENT CHANGES ASSOCIATED WITH EQUATORIAL IRREGULARITY PLUMES

J. A. Klobuchar, J. Aarons, E. Weber, Air Force Geophysics Laboratory, Hanscom AFB, Bedford, MA 01731, L. Lucena, M. Mendillo, Boston University, Boston, MA 02215

During a two week period in late February and early March 1978 Faraday polarization rotation and amplitude scintillation measurements were made at Ascension Island (7.9^{o}S.,14.4^{o}W., -30.4^{o} magnetic dip angle) by monitoring VHF radio waves from the SIRIO geostationary satellite. The purpose of the observations was to measure the simultaneous amplitude scintillations and changes in TEC associated with large equatorial plumes of irregularities which may extend over a several hundred kilometer height range having east-west dimensions of 100-200 kilometers and which move eastward at a velocity of approximately 100m/sec.

Before the onset of strong amplitude scintillation, indicating the arrival of an intense irregularity plume in the ray path, the slope of the TEC background generally showed a large increase. When plumes pass through the ray path the polarization records clearly show depletions in the background TEC; occasionally these depletions are over 20% of the absolute TEC level. On most nights more than one irregularity plume was seen, and on one night, six separate time periods of strong amplitude scintillation were observed. On this night all sky imaging photometer measurements were available which showed that north-south aligned 6300 Å airglow depletions accompany TEC changes and amplitude scintillation. The photometric measurements provide a 2-dimensional description of the size and motion of the irregularity regions.

During the times when the large plumes are observed the Faraday polarization was also seen to fluctuate, with greatest magnitude near the edges of each plume. The polarization fluctuation is tentatively interpreted as evidence for irregularities of an order of magnitude in density having scale sizes of a few tens of kilometers. Thus, the polarization fluctuation occurrence may be useful for extending the upper scale size of irregularities observed from equatorial irregularity plumes.

G4-3
1420 COMPARATIVE MORPHOLOGY OF EQUATORIAL SCINTILLATION IN THE AMERICAN AND PACIFIC SECTORS:

R. C. Livingston, SRI International, Menlo Park, CA 94025

The DNA Wideband Satellite, which is in a sunsynchronous orbit, transmits phase-coherent signals at VHF, UHF, L-band, and S-band. Routine amplitude and phase scintillation observations were made at Ancon, Peru (11°46'S, 77°09'W) from May 1976 through November 1977 and at Kwajalein Atoll (9°24'N, 167°28'E) from October 1976 through October 1977. These data have been processed to determine the seasonal and latitudinal variations of nighttime scintillation occurrence at the two stations.

Periods of high nighttime scintillation occurrence persist for approximately 8 months centered on July at Kwajalein and on December at Ancon. The occurrence statistics show short-term variability but no equinoctial maxima. The occurrence of L-band scintillation is virtually identical at the two stations. However, at Ancon the occurrence of VHF and UHF scintillation is considerably higher than it is at Kwajalein. This is attributed to a somewhat shallower sloped irregularity spectrum at Kwajalein which is verified by the phase scintillation data.

The latitudinal distribution of UHF and VHF scintillation occurrence is asymmetrical about the geomagnetic equator at both stations. During the local spring months the scintillation occurrence apparently peaks beyond 4° south of the magnetic equator. This asymmetry suggests neutral gravity waves as the source of the irregularities. The L-band scintillation, which has a much lower probability of occurrence, is more nearly symmetrically distributed. This suggests a mechanism such as the Rayleigh-Taylor instability, which acts along an entire flux tube.

G4-4
1445

THE STRUCTURE OF EQUATORIAL GIGAHERTZ SCINTILLATION:

C. L. Rino, R. C. Livingston, and J. Owen, SRI International, Menlo Park, CA 94025

Over forty Wideband satellite equatorial passes with various levels of gigahertz scintillation have been carefully processed to determine the structure of the scintillation and its association with large-scale total-electron-content (TEC) variations. The scintillation index, the phase spectral strength and power law index, and the fade coherence time have been measured at VHF, UHF, and L-band.

The gigahertz scintillation is always associated with extremely large TEC variations. Only in a few instances, however, does the TEC structure suggest simple depletion of electron content along some portion of the propagation path. No simple general relationship between TEC structure and gigahertz scintillation has been found.

Theoretical calculations have been performed to convert the measured phase spectral intensity to the corresponding spatial "strength of turbulence." Such a parameterization allows us to make direct comparisons with in-situ data. Preliminary comparisons have been made with AE-E satellite data. The turbulent strength assiciated with the in-situ data can easily account for the gigahertz scintillation levels, although the strongest turbulence appears adjacent to the depletions and not within them as is usually assumed. Finally, we present asymptotic results for strong scattering that accurately predict the measured coherence reduction with increasing perturbation strength.

G4-5 1540 HF AND VHF SCINTILLATIONS NEAR THE MAGNETIC EQUATOR R. A. Rastogi*, J. Aarons, H. E. Whitney, J. P. Mullen Air Force Geophysics Laboratory, Hanscom AFB, MA 01731, J. Pantoja, Geophysical Institute of Peru, Huancayo, Peru

The paper discusses the results of scintillation studies on 41, 140 and 360 MHz radio beacons from ATS-6 satellites received at Huancayo (magnetic dip latitude = 1^{o}N) for the period November 1974-May 1975. Scintillations on 360 MHz were seen only during the nighttime hours with the average value of Scintillation Index (SI) about 20% between 1900-2400 LT. Scintillation Indices on 140 MHz were above 30% between 1900-2400 LT, less than 2% around sunrise and sunset hours. Again a midday peak of about 10% value was seen. Scintillation indices on 41 MHz are above 20% at any of the times with two minima (10-15%) around sunrise and sunset times and two maxima (50-60%) one hour before midday and midnight. The nighttime scintillation on any of the frequency is stronger and more frequent around November-December than around May. The magnitude of day time scintillation on 41 MHz tends toward an equinoxial peak.

Assuming S.I. $\propto f^{-n}$, it is found that the exponent $n \approx 1.3$ so long as S.I. on the lower frequency does not exceed 50%. With increasing scintillation magnitude the exponent decreases and approaches zero during saturated scintillation. It is important to note that the decrease of index n is a fairly smooth function of the S.I. on the higher frequency.

The association of equatorial scintillation during the daytime and nighttime has been studied in relation to the irregularities as inferred from the bottom side ionograms at Huancayo.

*NRC Senior Research Associate, on leave of absence from Physical Research Laboratory, Ahmedabad, India.

G4-6
1605 STATISTICAL DISTRIBUTIONS OF SCINTILLATING TRANSIONOSPHERIC RADIO FREQUENCY SIGNALS:

R. S. K. Cheng and C. H. Liu, Department of Electrical Engineering, University of Illinois at Urbana-Champaign, Urbana, IL. 61801

Ionospheric scintillation phenomenon is studied using the multi-frequency data received from the ATS-6 Radio Beacon Satellite. The statistical distributions of the intensity, phase, in-phase and phase-quadrature components of the complex signal will be investigated through the fitting of the experimental data to several theoretically based distribution models, such as the Generalised Gaussian, the Log Normal, the 2-component model, etc.

The difficulties and complications in data processing prior to the statistical fitting will be discussed. A detrending process is needed to separate the high frequency scintillating signal and the relatively lower frequency component resulting from the variations in TEC. For the 2-component model, further complications result from a second detrending process which is necessary for separating the signal into its focus and scatter components.

The processed data is finally fitted to the theoretical distribution models mentioned above, and the results are compared based on the chi-square fitness test. Such results and their interpretations will be presented. The applicability and validity of the various models to the weak and strong scintillation cases will also be discussed.

G4-7
1630 SPECTRUM AND STATISTICAL PROPERTIES OF THE IONOSPHERIC PHASE SCINTILLATIONS AT 26 MHZ:

Ali Okatan and J. P. Basart, Electrical Engineering Department, Iowa State University, Ames, Iowa 50011

By using a phase stable interferometer, differential phase scintillations due to the ionosphere were observed and analyzed. The observing frequency was 26 MHz at which the ionospheric irregularities pronounce themselves most. A quasi-periodic behavior of the phase scintillations was observed. It was shown that the scintillation process may be modeled as a second order Markov process $\phi(t)$ satisfying the following stochastic matrix equation

$$\frac{d}{dt}\begin{bmatrix}\phi(t)\\ x(t)\end{bmatrix} = \begin{bmatrix}0 & 1\\ -a^2 & -2b\end{bmatrix}\begin{bmatrix}\phi(t)\\ x(t)\end{bmatrix} + \begin{bmatrix}1\\ a-2b\end{bmatrix} w(t)$$

where $x(t)$ is an auxiliary variable, $w(t)$ is a white noise process with zero mean, a and b are coefficients related to the velocity and scale size of electron blobs in the ionosphere. A power-law spectrum of phase fluctuations was observed. The average velocity of the blobs was ranging from 100 m/sec to 200 m/sec and the scale sizes were ranging from 4 km to 20 km. The stochastic and spectrum models give close results for the velocity and scale size of the irregularities. As a result we conclude that time domain models for the phase scintillations can be used quite satisfactorily to obtain information about the structure of the irregularities in the ionosphere. This type of modeling can also be applied to the interplanetary and interstellar plasma.

ELECTROMAGNETIC THEORY
Commission B, Session 8, UMC West Ballroom
Chairman: G. A. Deschamps, University of Illinois, Urbana, IL 61801

B8-1
0830

ROUGH SURFACE SCATTERING - WHAT NEXT:

Rayner K. Rosich, U. S. Department of Commerce, Institute for Telecommunication Sciences, 325 Broadway, Boulder, CO 80303

An analysis reported in Rosich (Ph.D. dissertation, Univ. Colo., Dec. 1977) and in Rosich and Wait (Radio Science, 12, 719-729, Sept-Oct 1977) considered the validity and convergence of perturbation treatments of electromagnetic scattering from rough surfaces by Rayleigh (Proc. Roy. Soc., A79, 399-416, 1907), Rice (in Theory of EM Waves, ed. by M. Kline, Interscience Pub., 351-378, 1951), Barrick (Radio Science, 6, 517-533, 1971), and Wait (Radio Science, 6, 387-391, 1971). The general perturbation solution and numeric results obtained in the analysis are consistent with results of these workers as well as to a more limited extent with the Kirchhoff approximation, and permit explanation of the success of these earlier treatments.

After a very brief overview of the formulation and results of the model developed in this analysis, consideration will be directed to (a) the Rayleigh hypothesis and some of its possible causes and cures, and (b) some suggestions of possible directions for future work. Some remarks on the probable difficulty of several of the latter models will be made.

B8-2
0850

PROBABILISTIC POTENTIAL THEORY (PPT) SOLUTION OF THE VECTOR WAVE EQUATION:*

R. M. Bevensee, Engineering Research Division, Lawrence Livermore Laboratory, P.O. Box 5504, L-156, Livermore, California 94550

The fields of Maxwell's equations can be obtained within a closed region with known sinusoidal-frequency surface excitation from vector magnetic potential $\bar{A}$ and scalar potential ϕ. In the Lorentz gauge both $\bar{A}$ and ϕ derived from it satisfy the homogeneous wave equation within the volume. In cartesian coordinates each spacial component of $\bar{A}$ satisfies the wave equation and is decoupled from the other components. The analogy between the discretized wave equation for $A_i(\bar{r})$ and the equation for random walk of a particle to the surface of known potentials can be exploited to solve non-analytically for the A_i and hence ϕ at any point of interest. The random walk can be performed by Monte Carlo runs or so-called number diffusion (R. M. Bevensee, Proc. IEEE, 61, 423-437, 1973), whichever is most efficient, depending on tolerable error and number of cells in the volume. However the largest dimension of the volume must be $\lesssim$ half wavelength for numerical convergence. The boundary conditions of $\bar{A}_{tan} = \partial A_{normal}/\partial n = 0$ are imposed on perfectly conducting metal walls, and $\bar{A}_{tan} \neq 0$, $\partial A_{normal}/\partial n \neq 0$ may be related to known surface electric current on exciting aperture(s). The PPT method is not as rapid as finite difference techniques but it is easy to program for a computer and apparently does not require unreasonably fine spacial discretization for reasonable numerical accuracy.

*Work performed under the auspices of the U.S. Department of Energy by the Lawrence Livermore Laboratory under contract number W-7405-ENG-48.

B8-3
0910

A STATISTICAL APPROACH TO ELECTROMAGNETIC INTERACTION:

William R. Graham & Charles T.C. Mo, R & D Associates, Marina del Rey, California 90291

When the system interacting with uncontrolled electromagnetic (EM) signals gets very complicated, the deterministic approach of solving the accurate EM boundary value problem for detailed features of the interaction rapidly becomes formidable. Further, not only may the quantitative uncertainties involved in describing the uncontrolled EM signals and in representing the system by a simplified model invalidate the useful application of the detailed features even if they can be obtained; but the very characterization of the interaction by those features in parametrized detail may not be useful or desirable, as with the case of describing the detailed motions of gas molecules in a box. Thus, an alternate approach to the problem acknowledging at the outset the nature of the uncontrolled complications and uncertainties via a statistical formalism may be fruitful. Results of such a statistical approach can be used to estimate and interpret distributions of EM coupling data for large systems, to quantify uncertainty bounds for interaction predictions, and to help characterize degradations of system performances. Specifically in this exploratory paper, we base our approach on the simple hypothesis that elements of the interaction are statistically distributed small dipoles, magnetic and electric. The basic variables being randomized are then the incident EM wave, the sizes and orientations of the dipoles, the lumped load impedances, and the mutual interactions (in the weak and strong limits) produced by the relative random locations of the dipoles. The resulting average enhancement to coupling and its average spread due to the mutual interactions are obtained. Statistical distributions of the induced currents are given for some simple cases. Their major central parts are shown to be insensitive to the modeling detail and approximately lognormal with a standard deviation of $\sim$6 to 7 db, but their extreme percentiles not so. This agrees well with and provides an interesting insight into the general trend of some experimental data, and can also be used as evidence to guard against the latter's misuse.

B8-4
0930

FORWARD SCATTER AND DIFFUSION OF PULSES IN A RANDOM DISTRIBUTION OF SCATTERERS

Akira Ishimaru
Department of Electrical Engineering, University of Washington, Seattle, Washington 98195

When particle sizes are large compared to a wavelength, the forward-scatter theory based on parabolic equations may be applicable. If particle sizes are comparable to or smaller than a wavelength, the forward-scatter theory is applicable only within a short optical distance; the diffusion phenomena then become predominant. Examples are millimeter waves in rain, optical beams in fog or clouds, and optical diffusion in blood. This paper presents a theoretical study of the forward scatter and the diffusion phenomena. A diffusion equation for the incoherent part of the intensity is derived which exhibits a form similar to the wave equation for electromagntic pulses in a conducting medium. The solution is obtained and its approximation shows typical diffusion behavior. The pulse broadening is shown to be approximately proportional to $\tau_s(1-\bar{\mu})$, where τ_s is the scattering distance and $\bar{\mu}$ is the mean cosine of the scattering pattern. It is also shown that in the diffusion region the pulse broadening is generally greater than the transit time, while it is smaller in the forward-scatter approximation. As an example, we used the Henyey-Greenstein scattering pattern and calculated the forward-scatter and the diffusion solutions. This represents many situations for optical beams in fog. The pulse broadening shows clearly the single-scatter region, the forward-scatter region and the diffusion region. We also show the angular broadening and the coherence bandwidth of the medium in each of the three regions as functions of the scattering distance τ_s and the mean cosine $\bar{\mu}$. It is shown that the transition between the forward-scatter and the diffusion regions occurs in the neighborhood of $\tau_s = \bar{\mu}^{\frac{1}{2}}(1-\bar{\mu})^{-1}$ and therefore when the particle sizes are large, $\bar{\mu}$ is close to unity and the forward-scatter region extends to large scattering distances, while for small particle sizes, the diffusion region is predominant.

B8-5
0950

CHIRALITY IN ELECTROMAGNETICS: D. L. Jaggard, Department of Electrical Engineering, The University of Utah, Salt Lake City, Utah 84211; A. R. Mickelson and C. H. Papas, Department of Electrical Engineering, California Institute of Technology, Pasadena, CA 91125

Chirality commonly occurs not only in nature but also in works of art and architecture as well as in manufactured articles [see, e.g., F. M. Jaeger, Lectures on the Principle of Symmetry, Cambridge Univ. Press, London (1917), or H. Weyl, Symmetry, Princeton Univ. Press, Princeton (1952)]. The concept of chirality has played an important role in such diverse areas as chemistry, optics and elementary particle physics. In this presentation we are interested in the interaction of electromagnetic waves with macroscopic metallic chiral objects. We consider both single objects and collections of randomly oriented objects.

An object is said to be chiral if it cannot be brought into congruence with its mirror image through translation or rotation. The mirror image of a chiral object is its enantiomorph. The figure below displays in one column some common chiral objects such as a helix, a Möbius strip, an irregular tetrahedron and a glove. Their enantiomorphs are displayed in the adjacent column. Note that chirality implies the presence of a handedness and a certain lack of symmetry.

CHIRAL OBJECTS AND THEIR ENANTIOMORPHS

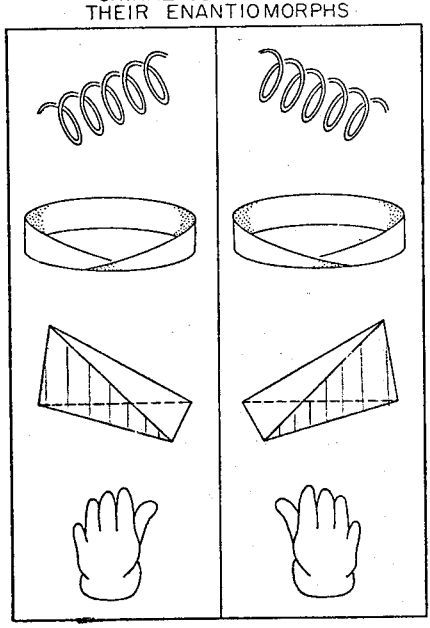

Two conjectures are made here concerning chiral objects. The first involves the optical activity of a collection of chiral objects and the second describes the deformation of chiral objects under electromagnetic forces. The conjectures are made plausible through calculations involving simple chiral objects.

It is anticipated that certain symmetry properties of objects, such as the degree of their chirality, will lead to a deeper understanding of the interaction of electromagnetic waves with these objects.

B8-6
1030

AN ANALYSIS OF THE METHOD OF ALEKSANDROVA AND KHIZHNYAK FOR INVESTIGATING A SOLUTION TO THE PROBLEM OF DIFFRACTION BY A DIELECTRIC WEDGE: I. Sreenivasiah and L. Lewin, Dept. of Electrical Engineering, University of Colorado, Boulder, CO 80309

Recently Aleksandrova and Khizhnyak (Sov.Phys.Tech.Phys., 19, 1385-1389, May 1975) claimed to have obtained a rigorous solution for the problem of plane wave diffraction by a rectangular dielectric wedge and in a later paper (J. Appl. Mech. Tech. Phys., 17, 594-599 , July-Aug. 1976) to diffraction by a dielectric wedge of arbitrary angle. Their method consists of seeking the solution for the fields in the wedge ($-\infty < x < \infty$, $y > 0$, $z > 0$) as a superposition of a plane refracted wave and an unknown wave from the edge,

$$E_x(\bar{r}) = A\, e^{ik_2 y + ik_3 z} + \int_\alpha \frac{\exp[ity + isz]}{s}\, \hat{f}(t)\,dt; \quad s = \sqrt{\epsilon k^2 - t^2} \qquad (1)$$

where the contour of integration α is implicitly defined to go around a part of the branch cut in the t-plane. The assumed form of $E_x(\bar{r})$ in (1) is substituted in Maxwell's equation, in integral form and the spatial integrals involved are carried out by using the plane wave spectral representation of the Hankel function. The remaining ω- and t-integrations are transformed into contour integrals in ξ- and η-planes, respectively, where $\omega = k \cos \xi$ and $\eta = \sqrt{\epsilon} k \cos \eta$. After some contour deformations in the ξ-plane Aleksandrova and Khizhnyak claim to have obtained a well known singular integral equation, of the first kind, for the weighting function [$f(\eta) = \hat{f}(t)$], which they solve using a standard technique. However, for brevity, the authors omit numerous details. While attempting to fill in the details we found that, besides a number of typographical and expository errors, the authors' expression for the incident wave starts with a non-trivial sign error in the exponent. Further, in obtaining the singular integral equation the authors ignore some terms which, if properly accounted for, makes it impossible to use their method to obtain a solution.

After giving a brief account of their method we point out the discrepancies in their evaluation of the integrals and the interpretation of the residues. Starting with the correct expression for the incident wave we present a way of systematically reducing the integrals involved to the desired form and derive the missing terms in their integral equation. We describe a modified approach which was tried by us and consisted of taking the t-integration in (1) to be along the real axis. However, this method will also be shown to fail to give the desired singular integral equation. We conclude that the problem of wave diffraction by a rectangular dielectric wedge has not been solved by the method under review, and that this conclusion must hold also for their later work on arbitrary wedge angles using the identical method;though since no details are given, no detailed analysis can be made.

B8-7
1050

A CRITIQUE OF ZAVADSKII'S METHOD OF SOLUTION TO DIFFRACTION PROBLEMS INVOLVING A RECTANGULAR DIELECTRIC WEDGE:

I. Sreenivasiah and L. Lewin, Dept. of Electrical Engineering, University of Colorado, Boulder, CO 80309

A number of years ago Zavadskii (Sov. Phys.-Acoustics, 12, 170-179, Oct.-Dec. 1966) proposed a method which he claimed would give an exact analytic solution to a class of two-dimensional wedge diffraction problems. His method is an extension of the method used by Malyuzhinets (Sov. Phys.-Acoustics, 1, 152-248, 1955; Sov. Phys.-Doklady, 3, 752-755, 1958) to solve the problem of diffraction by a perfectly conducting wedge or a wedge with impedance faces and involves the representation of the fields as Sommerfeld integrals and reduces the diffraction problem to a set of functional equations for the integrands. Zavadskii obtains a particular solution to these functional equations through a generalized two-sided Laplace transform method.

Zavadskii's method, which is elegant in appearance, seemed to give solutions, with ease, to a class of two-dimensional diffraction problems involving contiguous sectoral media with boundaries separated by rational submultiples of π. However, the solutions obtained by his method contain branch cut integrals which are not evaluated in his paper. Upon examining these branch cut integrals we found them to diverge at infinity in complete violation of the radiation condition. Several attempts were made by us to modify his approach so as to remove this drawback but they did not meet with success except for a trivial case.

After giving a brief summary of Zavadskii's formulation, we discuss the modifications that were tried in an attempt to obtain solutions to electromagnetic plane wave diffraction problems involving a rectangular dielectric wedge ($0 \geq \phi \geq \pi/2$) and i) infinite metal plate along $\phi = \pm\pi/2$, ii) semi-infinite metal plate along $\phi = -\pi/2$, iii) perfect magnetic conductor along $\phi = -\pi/2$ and a semi-infinite metal plate along $\phi = \pi/2$. In all these cases it will be shown that Zavadskii's method, as it is, gives a solution containing branch cut integrals that grow exponentially in the farfield thus violating the radiation condition. For case (i) a simple way of modifying Zavadskii's solution will be given so that the resulting solution conforms with the known exact solution. None of the modifications that were tried to obtain a correct solution to cases (ii) and (iii), proved to be successful. A method involving a secondary solution, with branch cut integrals alone, will be shown to lead to two coupled integral equations. However, it is not clear if a solution to these integral equations exists. Finally, a unique solution will be given to what we call the 'quasi-trivial' problem of illuminating a rectangular dielectric wedge, resting on a semi-infinite metal plate, such that there is no net diffracted wave from the edge.

B8-8
1110

POWER SERIES SOLUTION TO EFIE FOR ELECTRIC FIELD INDUCED IN FINITE CONDUCTING, POLARIZABLE BODIES:

D.P. Nyquist, Department of Electrical Engineering and Systems Science, Michigan State University, East Lansing, MI 48824

Three-dimensional, power-series basis functions are utilized, in conjunction with point matching, to implement a numerical solution to the electric-field integral equation for the $\vec{E}$ field excited by an impressed EM field in a finite conducting, polarizable body of relatively general shape. Simpler alternative basis functions exploited previously fail to provide a general solution because: 1) volumetric pulse-function expansions adequately represent the essentially dipole-type induced field excited by a relatively-uniform impressed electric field, but converge very slowly for the circulatory induced field due to a nearly-uniform impressed magnetic field and 2) expansion in circulatory functions adequately represent the induced field in a rotationally-symetric body with magnetic excitation, but fail to provide a valid representation with electric excitation. The well-known quasi-static solution for the $\vec{E}$ field excited in an electrically-small body by combined electric and magnetic impressed fields is, however, completely represented by the leading terms of the 3-d power-series representation. Retention of additional terms in the series leads to the induced field in larger bodies of relatively general shape (which need not posess rotational symmetry). A 3-d power-series expansion therefore partially overcomes the above limitations, although it may converge slowly for certain combinations of body geometry and excitation. Numerical results for electrically-small bodies are in essential agreement with the quasi-static solution. Extensive numerical results are obtained for the induced field excited in finite bodies of various sizes and shapes for both electric and magnetic impressed fields.

B8-9
1130

COMPUTATION OF SCATTERED FIELD AT LOW TO INTERMEDIATE FREQUENCIES BY OPTIMIZING SIMULATED-IMAGES

Y.L. Chow and M.N. Tutt, Dept. of Elect. Engrg.
C. Charalambous, Dept. of Systems Design
University of Waterloo, Waterloo, Ontario
Canada N2L 3G1

Recently a method was introduced to compute the static field around a charged conducting body by assuming a set of simulated charge images inside (Y.L. Chow and C. Charalambous, USNC/URSI Meeting, Boulder, Colorado, January 9-13, 1978). The strength and locations of the images were determined by minimizing the mean-square-error on the boundary condition through a numerical optimization technique. For smooth conducting bodies, the number of images required was frequently no more than four. Therefore once the images were determined, the field anywhere could be calculated rapidly.

In this paper, the method is extended to calculate the scattered field around a conducting body at low to intermediate (above the Rayleigh region of) frequencies. A simple example of such extension may be the a conducting spheres under an incident plane wave. With only two optimized images, one electric and one magnetic dipole, the back scattering cross-section obtained agrees well with the Mie series result from ka=0 over the first resonant peak to ka$\doteqdot$1.2 (J.J. Bowman et al., "Electromagnetic and Acoustic Scattering by Simple Shapes", North Holland Publishing Co. Amsterdam, 1969, Chapter 10, pp. 401).

The plane wave can be considered to be excited by a distant electric dipole. When the exciting electric dipole is moved closer to the sphere, both the electric and magnetic dipole images move toward the exciting dipole. When the frequency is made to approach zero, the amplitude of the magnetic dipole approaches zero and the amplitude and location of the electric dipole approach the static values given by the regular image method. Like the static counterparts, many examples of arbitrarily shaped conducting bodies under dynamic excitations can be computed. Based on the examples computed, the paper ends on a discussion on the limitations of the optimized image method at different conducting bodies, excitations, near and far fields, at the low to intermediate frequencies.

Commission C Session 6

WAVE RECEPTION AND CHANNEL MODELING
Thursday Morning, 9 Nov., UMC 156
Chairman: V. H. Rumsey, University of California, San Diego, La Jolla, CA 92307

C6-1
0830 STATISTICAL MODEL FITTING OF HANNA UNDERGROUND COAL BURN II, PHASES 2 and 3, INDUCTION SOUNDING DATA: E. A. Quincy, M. M. Rahman, Department of Electrical Engineering, University of Wyoming, Laramie, WY 82071 and J. H. Richmond, Department of Electrical Engineering, The Ohio State University, Columbus, Ohio 43212

Experimentation with techniques of underground coal gasification has presented the challenge for remote delineation and characterization of these conducting burn regions from the surface. Hanna II, Phases 2 and 3 burn, located near Hanna, WY, was conducted on a 30 ft. thick subbituminous coal seam covered with 275 ft. of conducting overburden.
The burn region was sounded (E. A. Quincy, DOE Final Report, Fe-2414-9, July 1978) with a wideband loop-loop induction system employing psuedo-noise and crosscorrelation techniques to produce a transient time response in the field. Frequency response at each system position was obtained by additional processing on a Fourier Analyzer over a passband from 100Hz to 10kHz. Skin depth for this system configuration and site is approximately 5kHz. Consequently model responses (J. H. Richmond, Ohio State University Final Report, 78 4491-5, Febr. 1978) were fitted to the field data at 1kHz for more reliable results. The procedure for fitting the field data is threefold. First, secondary magnitude responses are computed for buried wire grid models for a logical range of parameter values. The second step requires fitting the computed responses to a linear expression by a minimum mean square error (MSE) regression algorithm. The third step requires applying the regression coefficients and the field data to a two-dimensional Bayes minimum MSE estimator algorithm to obtain model parameters. The procedure was repeated for several models and the MSE computed for comparison.
Field measurements taken at three different times during a yearly period are compared showing definite site aging characteristics. These are attributed to temperature changes in the burn region and dispersion of conducting char and ash by the aquifer in the coal seam. Induction responses taken along two perpendicular traverses centered over the gasification wells are fitted to buried conducting box and vertical elliptical cylinder models. Results are also compared to a buried conducting sphere. The shape effect and the effect of vertical pipes at the depth of this coal seam is shown to

be only of secondary importance. Comparison of the induction model fit with a chemical model fit shows that the center of the conducting region may have extended 30m to the left of the well center and spread over a 50 per cent larger horizontal area than estimated chemically. This difference may be due partially to distribution of the conducting material by the aquifer in the coal seam.

C6-2
0900 BANDWIDTH OF LEAKY COAXIAL CABLES IN MINE COMMUNICATIONS: D.A. Hill and J.R. Wait, ITS/NTIA and ERL/NOAA, U.S. Department of Commerce, Boulder, CO 80303

The leaky-feeder technique for mine communications has recently been investigated in several theoretical and experimental studies (e.g. Special Issue of Radio Science, 11, April 1976). Most theoretical studies have concentrated on the attenuation rates of the dominant modes and the coupling loss from the cable to a nearby antenna. In addition to these signal amplitude effects, the bandwidth of leaky-feeder systems is of interest for cases where transmission of wideband signals is desired. Here we analyze an idealized leaky-feeder channel which consists of a uniform leaky coaxial cable located at an arbitrary position within a uniform circular tunnel.

The frequency domain transfer function for the channel is first expanded about the carrier frequency in constant, linear and quadratic terms in both amplitude and phase. Since a distortionless channel is one of constant amplitude and linear phase, the linear and quadratic amplitude terms and the quadratic phase term will cause pulse dispersion and limit the channel bandwidth. In earlier applications of this technique (J.R. Wait, Proc. IEEE, 57, 1784-1785, 1969) to ionospheric pulses, it was not necessary to consider the amplitude distortion as a first order effect. The transmission of a sinusoidal signal with a Gaussian envelope is considered in detail. The transmitted pulse envelope is shown to be stretched in time and the sinusoidal carrier frequency is shifted. The pulse stretching is an inverse function of the channel bandwidth.

Specific numerical results are calculated for attenuation rates, phase and group velocities, and channel bandwidths for frequencies from 1 MHz to 100 MHz. The bifilar mode is of primary interest, but some results are also given for the monofilar mode. The phase and group velocities of the bifilar mode are remarkably frequency-independent and are primarily a function of the cable parameters. This is because the interaction of the leakage fields with the lossy tunnel wall is usually fairly weak. Consequently, the limitations of channel bandwidth due to both phase and amplitude dispersion are not severe.

A more complete transfer function is the mutual impedance between a pair of short dipole antennas located within the tunnel since this includes the antenna-cable coupling (D.A. Hill and J.R. Wait, IEEE Trans. (in press), COM-26, 1978). The resultant channel bandwidth is decreased somewhat due to the introduction of the coupling terms, but it is still typically greater than 10% of the carrier frequency. A more complicated model for the surface transfer impedance of the cable braid which includes spatial dispersion has also been examined.

C6-3
0930 ADAPTIVE ARRAY AND SUPERRESOLUTION OF INTERFERENCE SOURCES: Giorgio V. Borgiotti, Radar Laboratory, Raytheon Missile Systems Div., Hartwell Rd., Bedford, MA 01730

The Adapted Angular Response (AAR) of an adaptive phased array can be defined as the residual power (interference plus thermal) at the output of the adaptive antenna combiner plotted versus the scan direction (for a given interference situation), for each scan condition the processor being allowed to adapt. The plot thus obtained exhibits peaks in the directions of the interference sources, and in fact constitutes an image (or a "map") of their distribution. The most interesting feature of the AAR is its inherent superresolution. By this it is meant that two sources are distinguishable and can be angularly located, even if their separation is a fraction of the aperture 3 db beamwidth. This may be surprising but it does not violate any physical principle. In fact one should suppress the tendency of applying to the AAR the well known Rayleigh criterion on the diffraction limited resolution of an aperture. In its modern formulation the Rayleigh criterion affirms qualitatively that two sources cannot be angularly resolved if they are angularly separated less than approximately a half power beamwidth of the uniformly illuminated aperture, unless the system noise is unrealistically low. This criterion applies to antennas and optical systems working as linear devices. It does not necessarily constitute a valid limitation for the AAR which involves in the generation of each point of the image a highly non linear operation on the correlations among the outputs of the antenna elements.

Only one dimensional array and a one dimensional AAR are here considered, with two interference sources with various separation present. A narrow band system is postulated, that is one whose adaptation bandwidth is small with respect to the inverse of the propagation time corresponding to the antenna aperture maximum dimension. The array is assumed to consist of 21 elements spaced half a wavelength. Different relative angular separations of two sources with various relative levels and ratios of interference to thermal noise have been considered. The results show consistently that a perfect resolution of the two sources greatly beyond the diffraction limit is reachable through the AAR, up to a separation of less than 0.3 times the 3 db beamwidth of the uniformly illuminated aperture.

C6-4
1030

TUNABLE CROSSED-YAGI ANTENNA ARRAYS: A STUDY OF ANTENNA CONCEPTS AND TRADE-OFFS FOR PORTABLE EARTH STATIONS:

W. R. Goddard, L. Shafai, and E. Bridges, Department of Electrical Engineering, University of Manitoba; and S. Thornton-Trump, Department of Mechanical Engineering, University of Manitoba, Winnepeg, Canada R3T 2N2.

In this paper we present the design for a tunable crossed-Yagi antenna array which can be collapsed and carried in a backpack as part of portable communication stations for use with satellite relays (Multipurpose UHF Satellite or MUSAT). The antenna performance requirements include UHF communication channels 274-290 MHz and 370-400 MHz with minimum antenna gains of 13 dBi, circular polarization, and maximum feed mismatch VSWR of 1.5 to 1. It was also necessary to meet weight and environmental conditions which further dictate the practical structure and size of the desired antenna. The Yagi was chosen as a mechanically simple structure with potential to meet the gain requirements in either band upon optimization of element lengths and spacings, and with capacitive tuning in mind. The requirement for a compact system dictated a combined structure for both bands and we met this need by introducing two reflectors, one for each band, and a simple on or off capacitive loading for tuning the common directors. The feed matching was accomplished with a parasitic element near the driven element. For the purposes of optimization needed to obtain the desired electrical performance, we constructed an objective function which included all the factors of gain, bandwidth, and input impedance. The objective function is a weighted sum of the mean decibel gain and its root-mean-square deviation from the mean across each band added to a similar sum for the decibel mismatch loss. Our optimization procedure included variations of the element lengths, spacings, and thicknesses. We have obtained a design for a practical 14 element antenna, 2 metres in length, with a minimum 11.5 dBi gain in the receive band and a 12.3 dBi gain in the transmit band. The desired mismatch loss performance was obtained without the need for a matching network. The mechanical design for this structure gave a system that meets the collapsibility and weight needs, and can withstand 70 km/h wind gusts. The major contribution of our work is to show how a practical, high performance antenna system can be designed with careful selection of approaches to meet performance requirements and tradeoffs between simplicities and complexities in the optimization of the antenna parameters.

C6-5 COMPARISON OF THE ART AND SIRT RECONSTRUCTION
1100 ALGORITHMS IN RADAR TARGET ESTIMATION:

W.-M. Boerner, Communications Laboratory, Info. Eng., UICC, P.O. Box 4348, Chicago, IL 60680;
Y. Das, DRES, Ralston, Alta. TOJ 2NO

The problem of radar target shape estimation has recently been treated as an image reconstruction problem (Y. Das & W.-M. Boerner, IEEE Trans. AP-26(2), 274-279, March 1978) in that the general theory of Radon transforms was applied in order to reconstruct the shape of a three-dimensional radar target. It is known that the cross-sectional area of a target as a function of the distance along the line of sight can be estimated from its backscattered electromagnetic ramp response (E.M. Kennaugh & D.L. Moffatt, Proc. IEEE 53(8), 893-901, 1965), which in turn can be approximately synthesized by using a 10:1 frequency bandwidth in the target's low resonance range (J.D. Young, IEEE Trans. AP-24(3), 276-282, 1976). Thus the determination of the target shape and size using the ramp response signature is reduced to the geometrical problem of reconstructing a body from its cross-sectional areas, which, in essence, is similar to Bojarski's inversion technique (N. Bleistein, J. Acoust. Soc. Am. 60(6), 1249-1255, 1976) as was shown in (Y. Das & W.-M. Boerner, URSI 1978 Spring Mtg., B4-3). The purpose of this paper is to verify the Radon target estimation procedure applying the ART (L.A. Shepp & B.F. Logan, IEEE Trans. NS-21(3), June 1974) and SIRT (P. Gilbert, J. Theor. Biol. 36, 105-117, 1972) algorithms to the shape reconstruction of conducting prolate spheroids. Limitations of these algorithms, which can reconstruct only the widths perpendicular to a single plane and do not account for smoothing across the shadow boundary are discussed and properties of truly three-dimensional reconstruction algorithms are prescribed.

C6-6
1130

THE SELECTION OF OPTIMUM OPERATING WAVELENGTH USING THE GAUSSIAN APPROXIMATION FOR THE FUNDAMENTAL MODE OF GRADED-INDEX FIBERS

R.L. Gallawa,
Institute for Telecommunication Sciences,
Boulder, CO 80303

This paper is addressed to the full utilization of monomode optical waveguides for telecommunications. It considers the question of optimum wavelength and expected pulse spreading when all known dispersion terms are accounted for. Unlike a previous effort in this direction (F.P. Kapron, Electron. Lett., 13, 96-97, 1977), we allow the fiber to have a graded refractive index. This allowance is important since production fibers tend to have refractive index profiles that change smoothly (albeit quickly, in some cases) from the value n_1, at r=o, to n_2 for r≥a, where a is the core radius and n_1 and n_2 are, respectively, refractive indices at r=o, and r≥a. Thus, the so-called profile parameter (denoted by g in this paper) may be large but it is always finite. The graded profile may also be important in operational systems because the critical value of normalized frequency, V_c, above which the fiber is no longer monomode, increases with decreasing value of g; this increase in the value of V_c eases the coupling and splicing problems.

The monomode fiber is easier to analyze than the multimode one because there is no intermodal or monochromatic dispersion. Concentration, then, is on the intramodel or chromatic dispersion and this can be handled by defining an effective refractive index, which accounts for the dispersive terms. Such a tack was used recently to show that the wavelength at which the material dispersion goes to zero is not the optimum wavelength; the waveguide term causes a shift in the wavelength of minimum chromatic dispersion away from the value for the bulk material.

We use the Gaussian approximation of the fundamental mode to describe the effective refractive index. Thus, in principal, all the dispersive terms can be accounted for, even for a graded index fiber.

Commission F (Joint With G) Session 6

REMOTE SENSING OF WIND
Thursday Morning, 9 Nov., UMC Forum Room
Chairman and Organizer: Tom VanZandt, NOAA/ERL/Aeronomy Lab, Boulder, CO

F6-1
0830 THE WAVE PROPAGATION LABORATORY'S PROGRAM FOR REMOTELY SENSING WINDS IN THE LOWER ATMOSPHERE:
R. G. Strauch, R. B. Chadwick, and E. E. Gossard, Meteorological Radar, Wave Propagation Laboratory, Environmental Research Laboratories, National Oceanic & Atmospheric Administration, Boulder, CO 80303

Recent experiments have demonstrated that radars with wavelengths from 0.1 to 10 m can measure atmospheric winds in all weather regimes. In addition to the many research applications for this technology, two operational applications are being pursued: the measurement of winds at airports, particularly along the path of landing and departing aircraft where low-level wind shear has been recognized as a danger to large aircraft, and the measurement of height profiles of horizontal wind from just above the surface to the tropopause, to supply continuous wind data to large-scale numerical models and to local weather forecasters. In the latter application, the radar is one part of a system of remote sensors that might obtain profiles of wind, temperature, and water vapor as well as total cloud liquid water. In addition to mean winds, the radars should be able to provide information on clear air turbulence from the width of the Doppler spectrum. The status of these operational applications of wind-measuring radars will be discussed. The factors that influence choice of wavelength, type of modulation, aperture and power required, etc., will be discussed.

F6-2
0852

WIND MEASUREMENTS USING RADARS AT KWAJALEIN:
G. Weiffenbach, MIT Lincoln Laboratory, Lexington, MA 02173; and R.K. Crane, Environmental Research & Technology, Inc., Concord, MA 01742

The high powered L-band (TRADEX) and UHF (ALTAIR) radars at Kwajalein were used for high spatial and velocity resolution observations of winds in the equatorial troposphere. The pulse compression radars were operated to provide 150m range resolution at L-band and 240m range resolution at UHF. Full Doppler spectra were obtained for each range cell with a 0.1m/s radial velocity resolution. System sensitivities were adequate to detect scattering from clear air turbulence with C_n^2 values greater than 10^{-18} ($m^{-2/3}$) at L-band and 10^{-19} ($m^{-2/3}$) at UHF at a height of 15 km. Preliminary processing of the radar data reveals occurrences of thin turbulent layers with weaker regions of turbulence between the layers. In the weak turbulence regions, the radial velocity measurements reveal single line spectra with Doppler spreads of less than 1m/s. These lines are in good agreement with the expected radial component of the wind calculated from radiosonde or Jimsphere observations. In regions of strong turbulence, multiple lines are observed. These lines represent the turbulent mixing of air across a thin stable layer with high wind shear. Lines may be identified with the motion of the air above and below the thin layer and intermediate velocity values corresponding to the discrete nature of the larger scale mixing across the thin layer.

F6-3
0914 HIGH RESOLUTION STRATOSPHERIC OBSERVATIONS AT THE ARECIBO OBSERVATORY: R.F. Woodman, Arecibo Observatory, Arecibo, PR 00612

Recent instrumental developments and modifications have allowed us to perform stratospheric scatter observations with 30m resolution using the S-band planetary radar (5300 MHz) and with 150m resolution using the 430 MHz radar. For the latter the pulses are coded with a complementary code. Decoding and coherent integration are performed digitally, and spectral analysis of each of 256 altitude ranges is performed on-line. Preliminary results will be presented showing the occurrence of turbulence layers 200 to 1000m thick, separated by as much as a few kilometers in the 25 to 32 km region and by less than a kilometer down to the resolution of the instrument in lower altitudes.

F6-4
0936 RADAR OBSERVATIONS OF THE STRATOSPHERE OVER JICAMARCA: D.A. Fleisch and W.E. Gordon, Rice University, Houston, Texas 77001

A series of 48-hour experiments using the Jicamarca 50 MHz radar to study the atmosphere in the 15-30 km region was conducted quarterly in 1977. The antenna was phased to produce one vertical and two off-vertical beams, to allow three dimensional wind determination. Real and quadrature components of the receiver outputs were coherently integrated for 1/4 s and recorded on magnetic tape. Analysis has yielded signal-to-noise, Doppler shift, and spectral width information with a height resolution of 3 km and time resolution of one minute. Horizontal wind vectors derived from mean Doppler shift agree closely with daily radiosonde data from the Lima airport. Vertical velocities are typically $\pm$ 20 cm/s with zero mean. Fluctuations in wind speed are found to occur with periods of 5 minutes to 24 hours. The signal-to-noise ratio for the vertical beam is consistently $\sim$ 10 dB greater than the value for the off-vertical beam which indicates a specular contribution to the scattering process.

F6-5
1032 PRECISION OF TROPOSPHERIC-STRATOSPHERIC WIND MEASUREMENTS: N.J.F. Chang, SRI International, Menlo Park, CA 94025, W.E. Ecklund and B.B. Balsley, Aeronomy Laboratory, National Oceanic and Atmospheric Admin., Boulder, CO 80303

The results of detailed comparisons of radar-derived wind profiles using the Chatanika radar with a series of 12 rawinsonde launches at approximately 45-minute intervals during 6 April 1978 at Poker Flat, AK, are presented. Radar-derived wind profiles are generally in good agreement with rawinsonde-derived wind profiles, but significant differences are found occasionally. The significance of these differences and the precision of the radar measurements are discussed. Particular attention is given to the propagation of errors from the radar line-of-sight measurements to resolved velocities.

F6-6
1054 RECENT RESULTS FROM THE SUNSET RADAR: J.L. Green, K.S. Gage, and T.E. VanZandt, Aeronomy Laboratory, National Oceanic and Atmospheric Admin., Boulder, CO 80303

One of the main interests of mesosphere-stratosphere-troposphere (MST) radar groups is the structure of the refractive index irregularities that reflect the radio waves. Understanding these structures is important not only in order to understand the MST experiment itself, but also because of the information they give on processes in the atmosphere. It appears that these structures can be categorized into either turbulent irregularities or laminar structures that give rise to quasi-specular echoes, although intermediate structures must also exist.

It has been shown that the quasi-specular echoes are associated with stable atmospheric layers, are observed only with a vertically pointed antenna, and are as much as 30 dB stronger than echoes observed from the same altitude and within a few minutes with an antenna inclined from the vertical. Recent studies have shown that these echoes can occur at any altitude between 4 and 27 km, endure as long as a day, and often exhibit positive or negative vertical velocities. The specularity of these echoes was found to be within a few degrees, by comparing the radar reflectivity from a vertically pointed antenna with that from an antenna pointed 7° from the zenith, but with a deep null in the vertical direction.

As regards turbulent structures, we have extended our previous model for calculating vertical profiles of the refractivity turbulence structure constant C_n^2 from background meteorological parameters by including the fluctuations of atmospheric stability as well as of vertical shear. Further comparisons between the model and observations will be shown.

F6-7
1116 COHERENT VHF BACKSCATTER FROM THE MESOSPHERE OVER URBANA, ILLINOIS AND JICAMARCA, PERU: S.A. Bowhill, I.D. Countryman, K.P. Gibbs, and K.L. Miller, Aeronomy Laboratory, Department of Electrical Engineering, University of Illinois, Urbana-Champaign

About 20 days of mesospheric data have been obtained using the VHF radar system of the University of Illinois at Urbana, with a new vertically pointing antenna array. Superposed on the normal level of scalar scatter are bursts of intense scatter, the scattering cross section per unit volume being apparently enhanced by a factor of up to 1000. These regions of enhanced scatter are interpreted as intermittent bursts of intense turbulence, producing ionization irregularities for which we propose the name "whitecaps." They appear to be associated with the dissipation of strong, vertical coherent gravity waves from the mesosphere below them. The properties of the whitecaps observed at Urbana are contrasted with the intermittent bursts of mesospheric scalar scatter observed at Jicamarca, Peru.

F6-8
1138 A NEW MST RADAR FACILITY AT POKER FLAT, ALASKA: B. B. Balsley, W. L. Ecklund, and D. A. Carter, Aeronomy Laboratory, National Oceanic and Atmospheric Admin., Boulder, CO 80303

General concepts, basic parameters and preliminary design details of NOAA's new MST (mesosphere-stratosphere-troposphere) radar in Alaska will be discussed. This system, when completed, will operate at 49.92 MHz, will have a peak pulse power of 6.4 MW, and an average power of 128 kW divided equally into a dual beam antenna array having a physical area of 4×10^4 m^2.

PROPAGATION WITHIN THE EARTH
Thursday Morning, 9 Nov., UMC East Ballroom
Chairman: D.C. Chang, Electrical Engineering Dept., University of Colorado, Boulder, CO

F7-1
0830 GUIDED WAVES ALONG AN AXIAL CONDUCTOR IN A CIRCULAR TUNNEL WITH LAYERED WALLS: J.R. Wait, D.B. Seidel and P.C. Orum, Cooperative Institute for Research in Environmental Sciences, University of Colorado, Boulder, CO 80309

An analysis is presented for the electromagnetic modes in a uniform tunnel structure that is a model for radio wave propagation in an underground passage. The tunnel crossection is circular and the external medium can be concentrically layered to allow one to examine the influence of inhomogeneities in the rock. An axial conductor is located anywhere within the tunnel but its radius must be small compared with other significant dimensions. Following early approaches (e.g. J.R. Wait and D.A. Hill, IEEE Trans. AP-22, 627-630, 1974), an exact mode equation is developed for the structure. This involves the rather complicated coupling of the T.E. and T.M. waves. Fortunately, a great simplification is possible when the quasi-static approximation is invoked (J.R. Wait, IEEE Trans. AP-25, 441-442, 1977). The mode equation then reduces to an explicit, albeit complicated, form to determine the axial propagation constant of the dominant mode.
The numerical results show that the attenuation rates depend in a rather complicated manner on the conductivity, permittivity and layering of the tunnel wall. Nevertheless, it may be feasible to use this dependence as a remote sensing tool. It has the advantage of being an in-situ measurement of the undisturbed rock. Also, of course, the effective parameters so deduced are directly useful for predicting the performance of leaky feeder communication systems that use transmission modes in such environments.

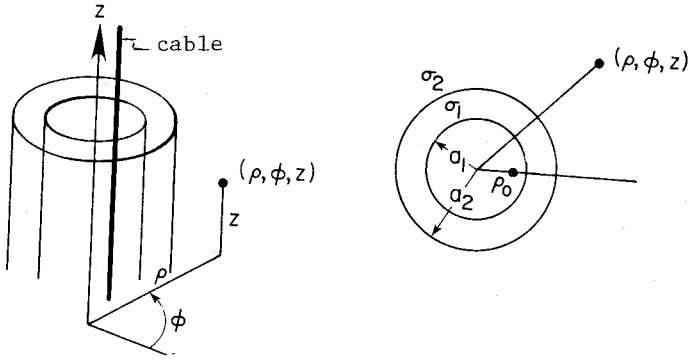

Layered tunnel model showing axial conductor.

F7-2 0850 THEORY OF TRANSMISSION OF ELECTROMAGNETIC WAVES ALONG A DRILL ROD IN CONDUCTING ROCK: J.R. Wait and D.A. Hill, Cooperative Institute for Research in Environmental Sciences, University of Colorado/ NOAA, Boulder, CO 80309

The possibility exists that electromagnetic signals can be transmitted along a drill stem or metal rod in a conducting host rock. The idea is that the lower portion of the vertical rod is to be excited inductively in such a fashion that axial currents will propagate to the surface where they may be detected. Because the rod is in contact with the surrounding conducting medium, we expect that the attenuation rate will be fairly high even in the best of circumstances. Nevertheless, it is important to establish the theoretical limits of this type of transmission as a mechanism for transmitting information. This is the purpose of the present study.

An initial examination of the problem suggested that the metal rod be excited by a coaxial solenoid that could be fed with alternating current. This configuration is sometimes employed in non-destructive testing of cables. However, some consideration indicated that this scheme would not excite axial currents on the rod of any substantial magnitude. A more promising configuration that suggests itself is a toroidal coil that encircles the rod. Electromagnetically, such a coil, when energized by an A.C. source, is equivalent to a circumferential magnetic current. If the inner radius of this toroid were allowed to coincide with the outer surface of the rod, we would, in effect, be exciting the rod by a voltage generator. Of course, this would be most effective in driving currents along the rod. It is not necessary, however, to require that the toroid be tightly wound about the rod. Thus, in our analysis, we will consider the toroid to have a mean radius somewhat greater than the radius of the rod. Another important practical consideration is that the rod will be of finite length. At the bottom end, the axially induced current will vanish so this will be a boundary condition that must be imposed. At the surface, the rod could be terminated in various ways. However, we feel that the optimum situation would be a simulated metal ground plane. Thus, for this study, such is assumed.

Admittedly, the model we have employed is highly idealized. However, the assumption in the calculations that the rod is perfectly conducting can be easily relaxed by using an appropriate value for the series impedance Z_s. Actually, it appears that, to within graphical accuracy, the results would not be changed. A more important limitation would be the imperfect contact between sections of the rod if it were not continuous throughout its length. In such cases, the axial current flow could be inhibited with an effective increase of the total signal loss.

F7-3
0910

ATTENUATION AND PROPAGATION OF RADIO WAVES IN A SLAB TUNNEL IN THE PRESENCE OF A CONDUCTING CABLE AT MEDIUM FREQUENCIES:

David C. Chang, CIRES and Electromagnetics Laboratory, University of Colorado, Boulder, CO 80309

The question of the attenuation of radio signals at medium frequencies in a mine tunnel is duscussed. In the absence of any long conducting rails or cables, it is well known that the propagation and attenuation characteristics of the fundamental mode depends strongly upon the size of the tunnel compared with the skin-depth of the surrounding medium. Specifically, the complex phase factor Γ_s for a wave of the form $\exp(i\omega t - i\Gamma_s z)$ is given approximately by

$$\frac{\Gamma_s}{k_1} = \left(1 - i\,\frac{2}{k_2 h}\right)^{\frac{1}{2}}$$

where k_1 and k_2 is respectively the wave number of air and the surrounding medium (rock or slate); h is the height of the tunnel. If, however, a long conductor of small cross-section is present, the field distribution inside the tunnel is now more influenced by the radius of the conductor, a, as well as the distance ℓ away from upper boundary. Provided that both $|k_2 h|$ and radius of the conductor are sufficiently small, i.e., $|k_2 h|^2 \ll 1$ and $(2\ell/a)^2 \gg 1$, the complex phase factor in this case can be shown to be

$$\frac{\Gamma_c}{k_1} = \left[1 - \frac{\ell n\, i 2 k_2 \ell_e}{\ell n\left(\frac{2\ell_e}{d}\right)}\right]^{\frac{1}{2}} \quad ; \quad \ell_e = \ell e^{-\pi^2 h^2/6\ell^2}$$

For parameters pertinent to practical application, one may conclude that the attenuation almost always decreases in the presence of the conductor.

F7-4
0930

LOW-FREQUENCY BEHAVIOR OF THE PROPAGATION CONSTANT ALONG A THIN WIRE IN AN ARBITRARILY-SHAPED MINE TUNNEL:

E. F. Kuester, Electromagnetics Laboratory, Department of Electrical Engineering, University of Colorado, Boulder, CO 80309
D.B. Seidel, Cooperative Institute for Research in Environmental Sciences, University of Colorado/NOAA, Boulder, CO 80309

Seidel and Wait (1978) have investigated the complex propagation constant (phase and attenuation coefficients) of the fundamental mode of propagation for radio waves along a thin wire or cable located in an elliptical mine tunnel, and found that the attenuation rate for low frequency is insensitive to the shape of the ellipse if the cable-wall distance and cross-sectional area are kept constant. We consider here tunnels of more general cross section, and obtain a characteristic equation for the propagation constant , valid for sufficiently low frequency, by means of a variational formulation of an integral equation. The characteristic equation involves only the electrical parameters of the tunnel walls, the radius of the wire, and the capacitance per unit length that the wire would have if the tunnel walls were perfectly conducting. Agreement with exact calculations for several geometries is found to be excellent below about 100 KHz, and acceptable even up to 1 MHz or more, for typical tunnel parameters. Since the wire capacitance can be shown to depend most importantly on its distance from the wall and on the area of the tunnel, the conclusion of Seidel and Wait can be made more precise and extended to tunnels of arbitrary cross-section.

F7-5
1010 MODES IN BRAIDED COAXIAL CABLES IN CIRCULAR AND ELLIPTICAL TUNNELS: D.B. Seidel and J.R. Wait, Cooperative Institute for Research in Environmental Sciences, University of Colorado/NOAA, Boulder, CO 80309

Radio frequency transmission in circular and semi-circular tunnels each containing a braided coaxial cable is considered. The general formulation accounts for both the ohmic losses in the tunnel wall and a thin lossy film layer on the outer surface of the dielectric jacket of the cable. Using a quasi-static approximation, it is found that the propagation constants of the low-frequency transmission line modes are obtained through the solution of a cubic equation. However, for the special case when the conductivity thickness product of the lossy film layer vanishes, this cubic equation reduces to a quadratic. The spatially dispersive form of the braid transfer impedance is also accounted for. It is shown that the quasi-static theory is well justified for frequencies as high as 100 MHz for typical tunnel geometries. Finally, these techniques are extended to a tunnel of elliptical cross-section. We find that, for frequencies up to 20 MHz, that the attenuation rate is relatively insensitive to the ellipticity if the cable-to-wall separation and the cross-sectional area are kept constant.

F7-6
1030 A MICROWAVE COAL THICKNESS SENSOR: K.C. Roe, Electromagnetic Fields Division, National Bureau of Standards, Boulder, CO 80303

A microwave coal thickness sensor has been developed for use in underground coal mines to determine the top coal layer thickness where the coal has been mined. The amount of top coal left after mining affects coal mine safety (root strength) and maximum coal recovery (profit).
The sensor is a low power radar system operating from 1 to 4 GHz. Distances are displayed in numerical digits showing both antenna to coal distance and coal thickness (cm or inches.)
The intended use is to mount such a system on an underground mining machine so that the machine operator can monitor his cutting height without having to drill holes in the roof. This type of sensor may also be adapted to automatic mining machines that are controlled from computers or microprocessors.

F7-7
1050

CALCULATED EFFECT OF A BURIED CABLE ON EARTH RESISTIVITY MEASUREMENTS: J.R. Wait and K.R. Umashankar, CIRES, University of Colorado/ NOAA, Boulder, Colorado 80309

There is a surprising lack of quantitative information on the influence of buried cables or metal pipes on the measurement of earth resistivity using probe techniques. A potential theory formulation for the fields of a point source of current in the presence of an infinitely long cable is quite straightforward. The extension to allow for the effect of ground stratification has also been worked out (J.R. Wait, Quarterly of the Colorado School of Mines, 73, 1-21, Jan. 1978). The situation for a homogeneous half-space is illustrated in the top figure and the cable is characterized by an axial impedance per unit length. The geometry for the two layer earth model is also shown. The apparent resistivity, as a function of electrode spacing, is shown for a typical example (computed for $\sigma_2/\sigma_1 = \rho_1/\rho_2 = 0.1$). Similar curves have been prepared for the four electrode or Wenner array.

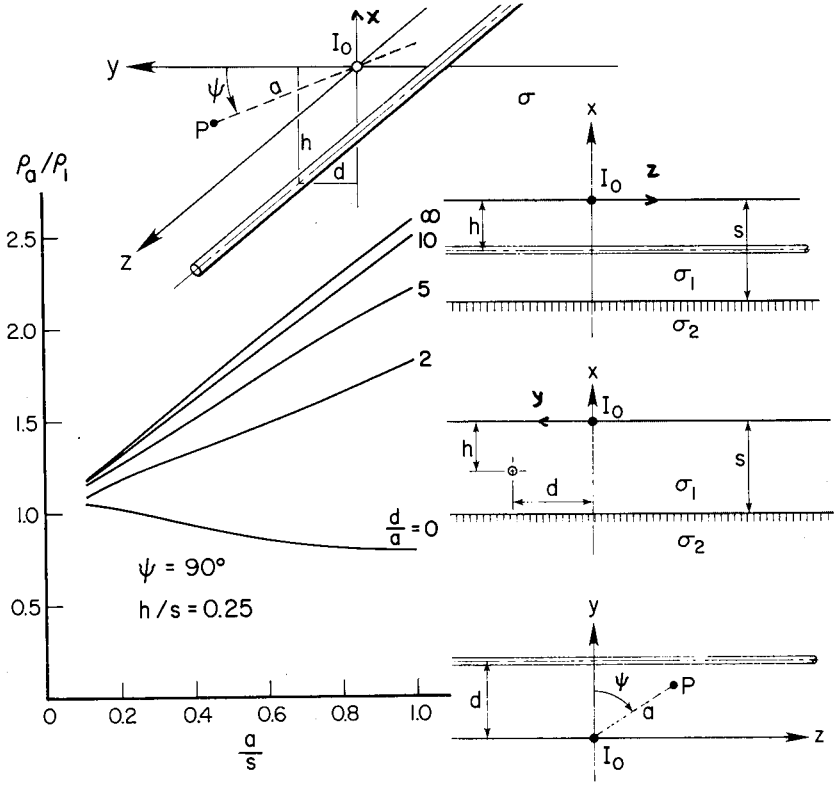

F7-8
1110 ON THE THEORY OF AN ELECTROMAGNETIC CRACK DETECTOR IN HOT DRY ROCK GOETHERMAL APPLICATIONS:

A. Q. Howard, Jr., Associate Professor, Department of Electrical Engineering, University of Arizona, Tucson, Arizona 85721

A two coil bore hole instrument has been proposed to map the orientation and location of the heat exchange surface relative to a bore hole. Because both the transmitter and receiver loops are in the immediate vicinity of each other and of the bore hole environment, the secondary currents set up in the crack cannot be easily observed. A parameter estimation procedure is proposed which involves many measurements in which the coils angular orientations are varied. In order to recover the magnetic dipole moment of the eddy currents in the crack, the dipole moment of the bore hole currents in the cavity environment needs to be understood. The major part of paper is therefore devoted to a three dimensional quasi-static mode matching calculation of the bore hole dipole fields in the absence of the crack. A computationally improved form of the Green's function is derived which converges exponentially in the axial coordinate. As is characteristic of modal solutions, the interior field convergence is exponential rather than algebraic as with typical point matching schemes. Some numerical results of the model are given which suggest that a simple approximation for the received magnetic fields are accurate to within about 10% of the formal numerical solution.

FUTURE MEETINGS SPONSORED BY USNC/URSI:

The following is the schedule for future meetings sponsored by USNC/URSI, with names of local arrangements and/or technical program committee chairmen:

1979 National Radio Science (some commissions only), IEEE Ap-S and Bioelectromagnetics Society Joint Meetings, Seattle WA, 18-21 June (A. Ishimaru, Department of Electrical Engineering , FT-10, University of Washington, Seattle, WA 98195).

1979 National Radio Science Annual Meeting, Boulder, CO, 5-8 November (S.W. Maley, Department of Electrical Engineering, University of Colorado, Boulder, CO 80309, and T.B.A. Senior, Department of Electrical and Computer Engineering, University of Michigan, Ann Arbor, MI 48109).

1980 Canadian/American Radio Science and IEEE AP-S Joint Meetings, Quebec City, Canada, 2-6 June (J.A. Cummins, Université Laval, Dept. de Genie Electrique, Faculté des Sciences, Cité Universitaire, Quebec G1K 7P4, Canada, and Professor G.L. Yip, Department of Electrical Engineering, McGill University, Montreal, Quebec H3C 3G1, Canada).

As indicated, some of the meetings are being held jointly with those of other organizations.

1715-1800 continued

Commission J Business Meeting	UMC 157

1800-2400

IEEE AP-S AdCom Meeting	UMC 215

2030

Very Long Baseline Interferometry Network Users' Group	UMC 158

WEDNESDAY, 8 NOVEMBER

0830-1200

B-5	Guided Waves	UMC 158
B-6	Scattering - II	UMC West Ballroom
C-4	Communication Theory and Systems	UMC 156
E-1	Interference and Its Suppression	UMC 159
F-4	Propagation Through Random Media With Applications to Remote Sensing	UMC East Ballroom
G-3	Ionospheric Effects of Solar Power Satellites	UMC Forum Room
J-3	Long-Length Radio Astronomy	UMC 157

1330-1700

A-3	Recent Advances in Microwave, Millimeterwave Measurements	UMC 158
B-7	Poster Session	UMC West Ballroom
C-5	Circuits and Systems	UMC 156
E-2	The Characterization and Modeling of Noise and Interference	UMC 159
F-5	Propagation Above the Earth	UMC East Ballroom
G-4	Ionospheric Irregularities	UMC Forum Room

1715-1800

Commission B Business Meeting	UMC West Ballroom
Commission E Business Meeting	UMC 159
Commission G Business Meeting	UMC Forum Room

1800-2200

IEEE Antenna Standards Committee Meeting	UMC 217
IEEE Wave Propagation Standards Committee	UMC 215

2000

USNC/URSI Executive Committee Meeting plus Commission Chairmen and Vice Chairmen	UMC 159
Electromagnetics Society Meeting	UMC 157B

THURSDAY, 9 NOVEMBER

B-8	Electromagnetic Theory	UMC West Ballroom
C-6	Wave Reception and Channel Modeling	UMC 156
F-6/G	Remote Sensing of Wind	UMC Forum Room
F-7/B	Propagation Within the Earth	UMC East Ballroom